Bob,

I had Ed write this for your + Franks information

R

Good - I recommend a discussion on this point with appropriate [redacted] personnel, Could it be I do? [illegible]

25X1

Declass Review by NGA.

NPIC/TDS/D-1134-67
8 December 1967

MEMORANDUM FOR: Chief, Exploitation Systems Branch, DS

25X1 SUBJECT : [redacted] Report "Display Size and Position"

1. The subject report outlines various criteria to be considered in the development of rear projection displays. This memorandum considers the conclusions reached relative to the [redacted] Rear Projection Viewer. 25X1

25X1 2. The [redacted] Viewer has an on-axis resolution capability at the screen of 10 lp/mm/Mag. Power @ 3X and 6 lp/mm/Mag. Power @ 70X. The subject report states that "display resolutions less than 9.23 l/mm should be compensated for with larger displays and greater viewing distances (greater than 14 inches)." If a person's resolving capability is directly proportional to the viewing distance, then his eyes can be positioned 21.6 inches from a screen to resolve 6 lp/mm. At this position, the slant range to the edge of a 30 inch screen will be 26.1 inches which will allow a resolving capability of 4.95 lp/mm--the viewer will only project 4.8 lp/mm at the screen edge at 70X. At the viewing distance of 21.6 inches, a 34° field-of-view is required to see a 30 inch wide screen and this is only 4° greater than the report recommends. The report places rather strong emphasis on the fact that "major head and neck movements occur for lateral eye rotations greater than 30°"; however, the [redacted] Zoom 70 has a 40° field-of-view and this instrument is used in a scanning mode on a routine and daily basis. Although this use does not mean that this large a viewing angle is comfortable, there have never been complaints of discomfort over years of use; therefore, it is reasonable to suggest that the 30° limit on the field-of-view should be re-examined relative to the photo interpretation function.

25X1

3. In any analysis of the type described above strict reliance on a specific viewing distance can be rather misleading--unless the head is restrained relative to the screen. In reality, an operator will not keep his head rigidly fixed in a specified position over long periods of time thus making the data less pertinent than it might first appear.

4. Other considerations and recommendations found in the report such as viewing angle seem to be valid and if possible--within the restraints imposed by the contract and the current physical optical/mechanical design--these criteria will be incorporated into t[redacted] 25X1

Distribution:
Orig & 1 - Addressee
2 - ESB Files

1. ASSUMES NO HEAD MOVEMENT
[illegible] SCANS
HEAD MOVEMENT (NOT RIGID POSITION)
2. ASSUME 14" VIEWING DIST.

ENCLOSURE to
DK-214

DISPLAY SIZE AND POSITION

Display size is most properly established by information content requirements. While this approach has been sucessfully applied with alphanumeric displays, it is extremely difficult with photographic displays because of the problems of specifying content requirements such as scale, field of view, resolution, etc. Furthermore, in image display situations, display size can be traded with film movement, and size must be established by "instantaneous" information requirements.

A more fruitful approach appears to lie in the examination of the film movement vs eye movement trade. Within limits, the use of eye rather than film movements is highly desirable; mechanical requirements are simplified, maximum speed and flexibility are achieved. The limits, however, of ease and comfort of eye movements impose restrictions on display size.

Anthropometric considerations limit the visual angle within which eye movements can be made comfortably and effectively.

Ideally, minimum fatigue results when movements are limited to eye rotation alone. Although some head movement accompanies nearly all eye movements, major head and neck movements occur for lateral eye rotations greater than 30° (Spiro, 1961). Eye elevation, above the horizontal, is especially fatiguing (Weston, 1953). The normal resting eye position, because of natural body slouch and the tendency for the eye to assume a downward cast is about 15 degrees below the horizontal (Morgan, et al, 1963). These considerations lead to the preferred viewing angles shown in Figure 1. It should be noted that for situations requiring maximum speed and accuracy of eye fixations (e.g., dynamic display or critical scan time constraints), the recommended angles should be halved.

These recommended angles define a specific display size once the viewing distance is selected. Viewing distance should be consistant with displayed resolution within the constraints of visual comfort. Data for resolution of sine wave targets by Lowry and DePalma (1962) indicate that maximum usable display resolution at a 14-inch viewing distance is 9.23 l/mm on the display. Unless the resolution is less than 9.23 l/mm, therefore,

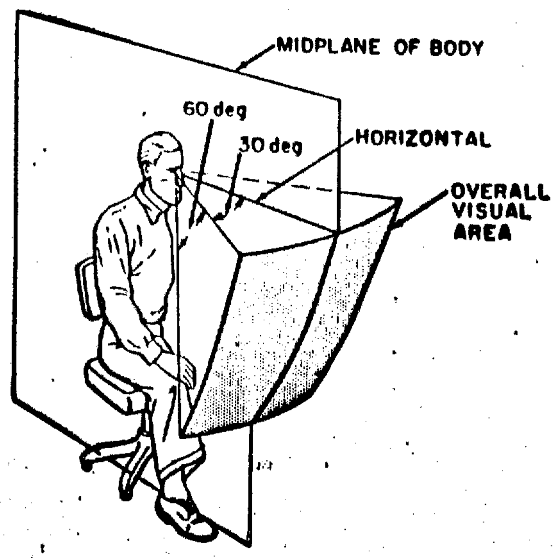

FIGURE 1: RECOMMENDED VIEWING ANGLES

(from Morgan, et al., 1963)

the viewing distance should be 14 inches. At greater distances or higher resolution levels the eye becomes the limiting factor in resolution. Prolonged viewing at distances less than 14 inches produces fatigue. Display resolutions less than 9.23 l/mm should be compensated for with larger displays and greater viewing distances.

At a 14-inch viewing distance, the recommended viewing angles define a suggested display size of about 16 inches. Larger display areas can be used to assist the interpreter in locating desired areas and moving them to the center of the display but detailed viewing or systematic scan of areas outside the recommended display size should not be required.

Nominal viewing distance is defined as the distance from the eye to the display along a line normal to the display surface. Because of body movement restrictions the viewing distance will increase for other areas of the display (assuming a flat display surface). The amount of the increase will depend on the distance and direction from the center of the display, the placement of the display, and the restrictions on interpreter body movement.

In addition, rear projection screens show degradations in brightness as the viewing angle becomes less perpendicular with the screen surface. Table 1 shows the effects of these factors for three screen tilt angles. The following data and assumptions were used to develop the values in the table.

1) Screen size is 16 inches.
2) Nominal viewing distance is 14 inches.
3) Entire display is located in recommended visual areas shown in Figure 1.
4) Line-of-sight at the screen tilt angle is normal to screen surface.
5) Eye position as a function of viewing angle from Brues (1946). Assumes shoulders fixed.
6) Resolution limits at 20 ft-L (assumed maximum display illumination) from Lowry and Depalma (1962).
7) Effect of brightness tentatively extrapolated based on Moon and Spencer (1944).
8) Screen gain data for Polacoat LS-60C.

	TILT (degrees)		
	0°	15°	30°
Max Resolution Degradation due to Viewing Distance	18.5%	6.5%	13.0%
Max Brightness Degradation	76.0%	71.0%	57.0%
Max Resolution Degradation due to Brightness	12.2%	10.7%	6.3%
Total Degradation	28.5%	16.5%	18.5%

TABLE 1: DISPLAY TILT EVALUATION

Contrast degradation will also occur as a function of viewing angle. This factor could not be evaluated but will be a maximum for 0 degree tilt and a minimum for 30° tilt. It should be noted that only 3 specific positions were evaluated and that these evaluations are primarily analytical. No experimental data directly applicable to this problem is known to exist. The results should be validated.

The recommended display size of 16 inches is appropriate only if such a display can provide the required information content. Figure 2, based on the work of Steedman and Baker (1960), helps to evaluate this factor. These data are based on the finding that a target size subtending 12 minutes of visual arc is necessary for form recognition. If greater information content (e.g., greater ground coverage for a given target) is required, then the recommended display size must be compromised unless image motion can be used to compensate for the restricted field-of-view.

K+E LOGARITHMIC 359-125G KEUFFEL & ESSER CO. MADE IN U.S.A.

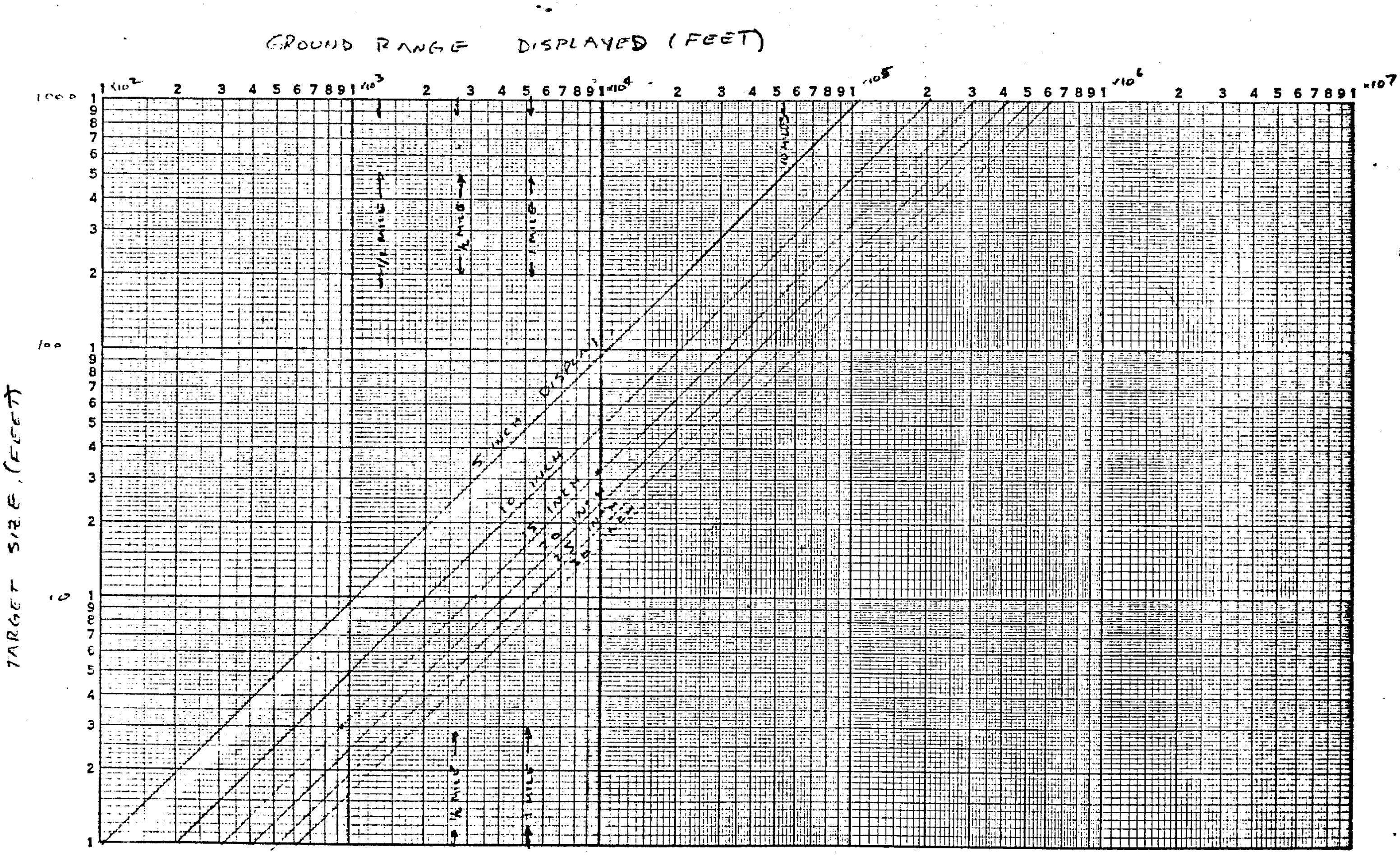

FIG 2

14 INCH VIEWING DISTANCE, 12 MINUTE TARGET SIZE

REFERENCES

Brues, A., "Movement of the head and eye in sighting," in Human Body Size in Military Aircraft and Personal Equipment, AF-TR-5501, Aero-Med Lab, WADC, 1946.

Lowry, E. M. and DePalma, J. J., "Sine-wave response of the visual system," J. Opt. Soc. Amer., Vol 52, pp 328-335, March 1962.

Moon, P., and Spencer, D., "Visual data applied to lighting design," J. Opt. Soc. Amer., Vol 34, pp 605-617, October 1944.

Morgan, C. T., Cook, J. S., Chapanis, A., and Lund, M. W., Human Engineering Guide to Equipment Design, McGraw-Hill Book Co., New York, 1963.

Spiro, I. J., "Eye location for a wide-field large-exit-pupil otical system," J. Opt. Soc. Amer., Vol 51, pp 103-104, January 1961.

Weston, H. C., "Visual fatigue, with special reference to lighting," in Symposium on Fatigue, Med Res Council, London, 1952.

increasing the level of performance, without in any way affecting the kind of performance.

The empirically derived index of spatial summation, $p=0.57$, for flicker in the central fovea is higher than might be expected on the basis of threshold measurements, accepting Pieron's law[4] that threshold intensity is inversely proportional to the 0.3 power of area for targets between 1 and 40 min. in diameter in the fovea, as being a reasonable approximation. However, Weale[3] derived an index $p=0.64$ from the flicker data of Kugelmass and Landis[6] which is very close to the value reported here. The slight discrepancy may be due to the fact that their largest target was 14.60° in diameter. One might expect the extrafoveal component to show slightly more interaction, and inspection of their data shows that $dN_c/d\log A$ is not completely independent of area at the higher values.

The conclusion seems reasonable that the degree of areal summation for flicker in the fovea is different from that for threshold discrimination.

[4] H. Pieron, Année psychol. 30, 87–105 (1929).

[6] S. Kugelmass and C. Landis, Am. J. Psychol. 68, 1–19 (1955)

JOURNAL OF THE OPTICAL SOCIETY OF AMERICA VOLUME 51, NUMBER 7 JULY, 1961

Sine-Wave Response of the Visual System. I. The Mach Phenomenon*

E. M. Lowry and J. J. DePalma
Research Laboratories, Eastman Kodak Company, Rochester, New York

(Received December 17, 1960)

In order to develop a complete specification for the appraisal of the quality of a photographic system by the use of sine-wave response functions, the sine-wave response of the complete visual system must also be known. A method has been worked out for determining the above-mentioned response of the eye. Whenever the eye views a diffuse luminous boundary in which a sudden change of luminance gradient occurs, a bright line appears at the junction of the gradient and the higher luminance, and a dark line at the junction of the gradient and the lower luminance. This phenomenon is a purely subjective one, because physical measurements of the luminances involved show no luminance higher or lower than the two between which the gradient exists.

A visual slit photometer has been built with which the subjective intensity distribution may be evaluated directly. By application of Fourier analysis, the objective and subjective intensity distributions have been combined to yield the sine-wave response of the visual system.

INTRODUCTION

If progress is to be made toward an understanding of how useful the sine-wave response is as a method of appraising image quality in photographic reproduction, the response characteristics of the visual system must be *accurately known and properly applied* as one element in the cascaded system. It should be emphasized that, while the transfer functions for lenses and emulsions are entirely physical, in the case of the visual system these functions are psychophysical and, consequently, factors are operative which are absent in a strictly physical analysis.

From the image of a test object formed on the retina by the lens of the eye, a number of investigators, including Flamant,[1] DeMott,[2] and Stultz and Zweig,[3] have attempted to obtain or interpret information pertaining to the visual spread-function or transfer function. Such data do not include the response of the nervous system associated with the eye, and therefore cannot be applied immediately to the problem of appraising the quality of an image as seen by an observer, since they are primarily objective measures rather than subjective ones.

Several authors, among them Schade,[4] Selwyn,[5] Rosenbruch,[6] and Ooue,[7] have made use of the contrast sensitivity of the eye for different spatial frequencies, as the measure of importance for the visual response to sinusoidal intensity waves. In this connection, contrast sensitivity is defined as the contrast necessary, in a sine-wave test object of known spatial frequency, for threshold perceptibility. When this *threshold object contrast* is plotted as a function of the frequency, or visual angle, of the sinusoid, it is called the "sine-wave contrast sensitivity" of the eye. First Schade,[4] and later Ooue,[7] have taken the reciprocal contrast sensitivity and called it the "sine-wave response." Although, in either form, this is a very important and useful function, it has not yet been proved, so far as the authors are aware, to be truly the sine-wave response function. This is evidenced by the fact that sine-wave response is the ratio of *image-to-object contrast* at each frequency, and the idea

* Communication No. 2135 from the Kodak Research Laboratories.

[1] F. Flamant, Rev. opt. 34, 433 (1954).

[2] D. DeMott, J. Opt. Soc. Am. 49, 571 (1959).

[3] K. F. Stultz and H. J. Zweig, J. Opt. Soc. Am. 49, 693 (1959).

[4] O. H. Schade, J. Opt. Soc. Am. 46, 721 (1956).

[5] E. W. H. Selwyn, Phot. J., B88, 6 (1948).

[6] K. J. Rosenbruch, Optik 16, 135 (1959).

[7] S. Ooue, J. Appl. Phys. (Japan) 28, 531 (1959).

of response in this connotation is suprathreshold and not threshold. There may be some simple relation between reciprocal contrast sensitivity versus frequency and the sine-wave response of the eye. However, for such a relationship to exist, the method of reciprocal contrast sensitivity must measure the response, or at least the equivalence of the response, and not just some function of the signal.

Under most normal viewing conditions, the eye is operating in a region where both luminance and detail size are well above threshold. The method proposed in this paper assumes linearity between signal and response, but over only a narrow suprathreshold range, and furthermore does not rely on the as-yet-unknown relationship between threshold and suprathreshold response.

NEW APPROACH TO THE DETERMINATION OF THE SINE-WAVE RESPONSE OF THE EYE

Apparatus and Experimental Technique

A phenomenon, which was first reported by Mach[8] in 1865 and which has since been the subject of study by a number of investigators, seemed to lend itself to the determination of the subjective response of the eye to an objective energy distribution, at well above the threshold for either size or brightness. Mach discovered that whenever the eye views a diffuse luminous boundary in which a sudden change of luminance gradient occurs, a white line is visible where there is a rapid decrease in gradient and a dark line where there is a rapid increase. As shown in Fig. 1, the luminance gradient between the light and dark lines, as seen by the eye, departs from the linearity which exists in the physical gradient and for the edges studied approximates an S shape. Edges with other than linear gradients have not been examined quantitatively as yet, although their investigation is planned.

The phenomenon just described and known as the Mach bands is purely subjective because physical measurement of the intensities involved shows no intensity higher or lower than the two between which the gradient exists.

In order to determine the sine-wave response function of the visual system, it is necessary in some way to evaluate a transfer which is psychophysical rather than a purely physical one such as that involving a lens or a photographic emulsion. For this purpose, the Mach bands appeared ideal, because here we have a physical stimulus which is rather easily measured and at the same time a visual response to the stimulus which may be evaluated by psychophysical methods.

An evident mathematical formulation which has been used by workers in this field[9–11] is that the distribution

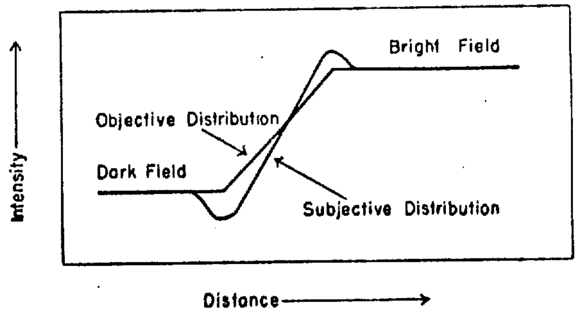

FIG. 1. Diagrammatic representation of the Mach phenomenon.

of energy in the image space $I(x')$ of an object intensity function $O(x)$ transmitted through an image-forming element, the characteristics of which are known from its line spread function $A(x)$, can be found by convoluting the object distribution with the line spread function:

$$I(x')=\int_{-\infty}^{\infty} A(x'-x)O(x)dx.$$

This expression will be more fully discussed later in this paper but is introduced here since it is the determination of the image function $I(x')$ with which we are here concerned. Fiorentini,[12] and Fiorentini and Toraldo di Francia,[13] and also Hartwig,[14] McCollough,[15] and Kühl,[16] have studied the luminance distribution as seen by the eye when looking at a penumbral shadow or diffuse edge. These observers were interested primarily in the effect of illumination gradients on the sensation of brightness. The present study goes a step further and applies such measurements of apparent luminance distribution to the determination of the visual transfer function or sine-wave response.

In our investigation of the subjective impression received from a physically linear luminance gradient, diffuse edges of various widths, having the required intensity distributions, were obtained by wrapping strips of white and gray paper spirally around a cylinder. The cylinder, with its paper strips, was then illuminated and rotated at high speed. The luminances of the white and gray strips were photometered with a modified Macbeth illuminometer and the limits of the gradient established. These were found to be approximately 20 and 3 ft-L, respectively. The surround was kept constant at about that of the lower luminance. Because the edges of the paper strips wrapped around the drum were straight, the spatial distribution of luminance was linear when the drum was rotated. Since neither physical photometry, luminance photometry, nor photography

[8] E. Mach, *The Analysis of Sensations* (Jena, 1886), pp. 216-21.
[9] R. V. Shack, J. Research Natl. Bur. Standards 56, 246 (1956).
[10] E. Ingelstam, E. Djurle, and B. Sjögren, J. Opt. Soc. Am. 46, 707 (1956).
[11] P. B. Fellgett and E. H. Linfoot, Phil. Trans. Roy. Soc. London A247, 369 (1955).

[12] A. Fiorentini, "Problems in contemporary optics" (Proc. Florence Meeting, September 10-15, 1954) (Ist. Naz. di Ottica, Firenze, 1956), p. 600.
[13] A. Fiorentini and G. Toraldo di Francia, Optica Acta 1, 192 (1955).
[14] E. Hartwig, Optik 15, 414 (1958).
[15] C. McCollough, J. Exptl. Psychol. 49, 141 (1955).
[16] A. Kühl, Physik. Z. 29, 1 (1928).

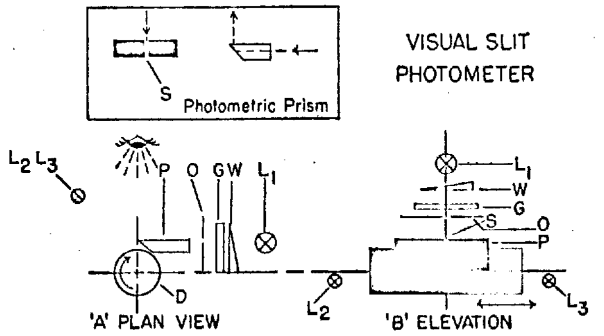

FIG. 2. Schematic of visual slit photometer.

showed any luminance higher or lower than those of the paper strips, it must be concluded that the light and dark lines which were observed, as well as the apparent departure from linearity of the gradient, were entirely subjective.

In order to measure the apparent luminance distribution corresponding to the subjective brightness of diffuse edges, a visual slit photometer was developed. With this instrument the eye sees a two-part field in which one part consists of a uniformly illuminated slit $\frac{1}{2}$ mm wide at the center of a dark field, and the other part is formed by the face of the rotating cylinder on which the diffuse edge appears. The slit is illuminated from the rear by a diffusing screen and light source with a neutral wedge between the source and the screen to modulate the illuminance. Figure 2 shows diagrammatically the arrangement of the component parts. At A and B are plan views of the apparatus. The drum D is illuminated by the two sources L_2 and L_3. Light from L_1 passes through the wedge W, diffusing screen G and diaphragm O into the prism P, where it is reflected to the eye of the observer by the silvered strip S on the blackened hypotenuse face of the prism.

As the observer views the rotating drum covered with the paper strips, he sees the diffuse edge bounded at its lighter side by a bright line and at its darker side by a dark line. By adjusting the position of the drum, which is movable back and forth along its axis, and by proper modulation of the light source with a neutral wedge, the experimenter is able to match the brightness of the slit with that of the juxtaposed portion of the edge under examination. Any possible visual effect of nonuniformity in the test field is ruled out, since the end point is at a brightness match between the slit and the portion of the field adjacent to the slit. Consequently, there is no apparent discontinuity at balance. From the luminance calibration of the slit, the luminance at the condition of photometric balance is determined. A series of such readings, made at different points across the diffuse edge, permits plotting the subjective luminance impression versus distance across the edge. When both objective and subjective luminances for a given edge are plotted on the same graph, the resulting pair of curves depict the actual linear distribution of luminance and the apparent distribution seen by the eye. The phenomenon represented by the curve of apparent luminance distribution has been a matter of common observation by anyone who has looked at a penumbral shadow or a diffuse edge.

The values of subjective luminance obtained from a series of measurements showed an average deviation from the mean of approximately ±10%. Figures 3, 4, and 5 represent the results for several linear gradients. The edges having these gradients were 7.5, 2.5 mm, and a reflected edge, of which each side was 4.8 mm wide. Although not shown in these curves, each distribution was cut off to zero luminance at the ends of the drum, which was out of the effective field of view. Examination of Figs. 3 and 4 demonstrates that for a given luminance difference, the width of the bright and dark bands becomes less, the steeper the gradient. As the width of the edge approaches zero, the width of the bright and dark lines or bands also approaches zero, until for a really sharp edge the eye may be unable to distinguish any lines differing in apparent luminance from those luminances which form the edge itself, and the subjective impression of luminance matches that produced by the stimulus. That is to say, under such conditions there may be no luminance apparent which is either higher or lower than those of the adjoining fields.

Theory and Method

The quality criterion of an optical system no longer tends to be characterized by the limit of resolution, which gives little information about suprathreshold response, but rather by the newer concept of the transfer function. The transfer function, more commonly called the sine-wave response function, tells us how the amplitudes (contrast) of a series of sinusoidal waves change

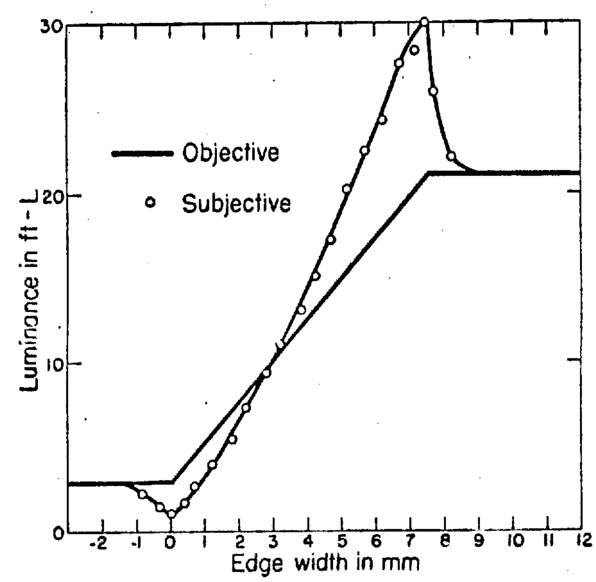

FIG. 3. Luminance distribution for edge No. 11: solid line, objective distribution; open circles, subjective distribution.

as they are transferred through the system. More explicitly, it is defined as the Fourier transform of $A(x)$, the line spread function:

$$A^{\#}(\nu)=|A^{\#}(\nu)|e^{i\theta(\nu)}=\int_{-\infty}^{\infty}A(x)\exp[-2\pi i\nu x]dx, \quad (1)$$

where x is a spatial coordinate, (ν) is the spatial frequency of the component wave in lines or sine cycles per millimeter, θ is the phase shift in radians of the component wave from its geometric image position, and the symbol # denotes a transform operation. The expression (1) is called the complex transfer function because it includes a phase function $\theta(\nu)$ as well as the amplitude function $|A^{\#}(\nu)|$.[17] The phase shift occurs when the spread function is asymmetrical. When the spread function is symmetrical, as for example in photographic emulsions,[18] $\theta(\nu)=0$ and Eq. (1) reduces to the Fourier cosine transform, $A^{\#c}(\nu)$,

$$A^{\#c}(\nu)=|A^{\#c}(\nu)|=\int_{-\infty}^{\infty}A(x)\cos 2\pi\nu x dx. \quad (2)$$

Although the sine-wave response function is basically a fundamental measure of the fidelity of an optical system, it has not yet attained the inherent uniqueness which it has been assumed to possess, mainly because the interpretation and application of such functions to practical imaging problems have not progressed as rapidly as have the development of theory and accurate measuring techniques. Although the transfer function tells how well different spatial frequencies are transmitted through the system, it has yet to be determined how closely the sine-wave response function correlates with the quality of images which have little resemblance to a periodic pattern, especially as evaluated visually. Wolfe[19] has encountered this problem in his study of the relationship between the spread function of photographic emulsions and picture definition. Until such time as the correct interpretation of such functions is explicitly determined, analysis of image quality by sine-wave response may lead to erroneous conclusions. However, this is but a temporary objection and should not overshadow the real importance of sine-wave analysis to optical imagery. Its significance is evident in the particular case of the assessment of a system acting in concert, e.g., the visual evaluation of a photographic reproduction which has been produced by imaging a detailed object through a lens system onto an emulsion. Here the sine-wave approach becomes especially useful because if the response of each component in the system is known, the final response is simply the product of all the component responses, provided, of course, that the transfers are linear. Thus, it becomes possible to design and control, to some degree at least, the individual components of the system to achieve a particular over-all result.

As was stated in the introduction, in order to make use of such Fourier methods, the sine-wave response of each component must be accurately known and properly applied. The transfer function has been quite

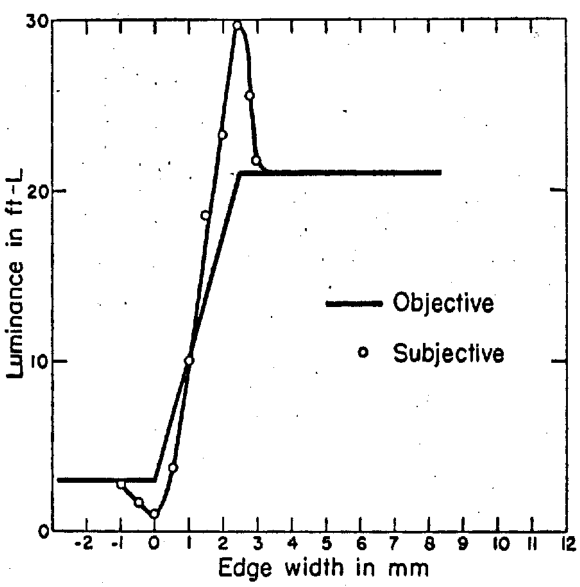

FIG. 4. Luminance distribution for edge No. 12: solid line, objective distribution; open circles, subjective distribution.

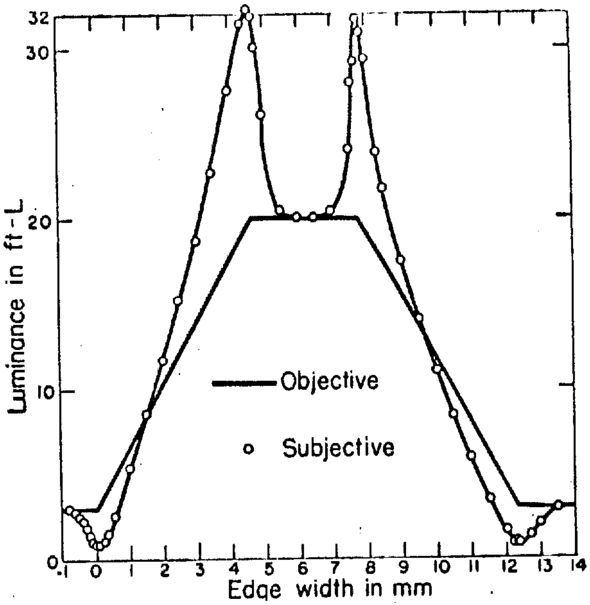

FIG. 5. Luminance distribution for edge No. 16: solid line, objective distribution; open circles, subjective distribution.

[17] The amplitude function $|A^{\#}(\nu)|$ is sometimes called the "modulus" and the phase function, the "argument."
[18] R. L. Lamberts, J. Opt. Soc. Am. 49, 425 (1959).
[19] R. N. Wolfe, J. Opt. Soc. Am. 49, 1133(A) (1959); 50, 1140(A) (1960).

thoroughly investigated for lens systems[10,20-22] and for the photographic emulsion.[10,18,23] However, so far as the authors are aware, the sine-wave response has not been determined for the complete visual system. Using the above-mentioned cascade principle and the data obtained by means of the Mach phenomenon, a method is proposed to determine this function. In order to use this method, it must be assumed that the visual transfer is linear over a narrow suprathreshold range. To explain how the derivation of the sine-wave response was accomplished, we must start with the fundamental definition for the modern treatment of optical imagery, that is, convolution:

$$I(x')=\int_{-\infty}^{\infty} A(x'-x)O(x)dx, \tag{3}$$

where $I(x')$ and $O(x)$ are the one-dimensional luminance distributions in image and object space, respectively, x is the projected object coordinate, x' is the image coordinate, and again $A(x)$ is the line spread function. It should be noted that the spread function is a characteristic of the optical system only and is assumed to be independent of the object distribution. Whereas this point is quite obvious when reference is made to purely physical systems, it is not so obvious when the psychophysical system of the eye is considered. This will be discussed in a later section.

The convolution theorem, from which Eq. (1) is easily derived,[21] shows how the illuminance at any point x' in image space can be found from the luminance of the contributing points in object space which have been modified by the spread function. The important fact to be deduced from the convolution theorem in the present problem is that it is possible to derive mathematically the spread function of the visual system by inversion of the integral in Eq. (3), provided, of course, that the appropriate object and image distributions are known. As has been explained previously, by making use of the Mach phenomenon, these two functions, both of which are assumed to be proper and consistent with the definition of convolution, were measured—$O(x)$ was measured with a standard type of visual photometer and $I(x')$ was measured with the special photometer described in this paper. A simpler and more useful determination of the inversion of Eq. (3) for the purposes of obtaining the sine-wave response directly is based on the well-known Fourier integral theorem,[22,24] by which the convoluted spatial distributions reduce to the product of their Fourier spectra:

$$I^{\#}(\nu)=A^{\#}(\nu)\cdot O^{\#}(\nu), \tag{4}$$

$$A^{\#}(\nu)=\frac{I^{\#}(\nu)}{O^{\#}(\nu)}=\frac{|I^{\#}(\nu)|}{|O^{\#}(\nu)|}\exp\{i[\theta_I(\nu)-\theta_O(\nu)]\}. \tag{5}$$

Here, each function from Eq. (3) is transformed to the spatial frequency domain ν; that is, $I^{\#}(\nu)$ and $O^{\#}(\nu)$ are the complex Fourier transforms of the image and object distributions, respectively:

$$I^{\#}(\nu)=|I^{\#}(\nu)|\exp[i\theta_I(\nu)]=\int_{-\infty}^{\infty} I(x)\exp[-2\pi i\nu x]dx, \tag{6}$$

$$O^{\#}(\nu)=|O^{\#}(\nu)|\exp[i\theta_O(\nu)]=\int_{-\infty}^{\infty} O(x)\exp[-2\pi i\nu x]dx; \tag{7}$$

and $A^{\#}(\nu)$ is the sine-wave response of the visual system as has been explained and can be seen from Eq. (1). The phase function $\theta_O(\nu)$ for the object and $\theta_I(\nu)$ for the image must be included because of the asymmetrical nature of all of the distributions used, except for the object curve of edge No. 16 (see Fig. 5). It can be seen that Eq. (4) is the quantitative basis for the important cascading procedure mentioned.

It now becomes clear why Flamant's spread function used in Eq. (1) would not yield the correct sine-wave response of the eye. This would give the sine-wave response of the eye lens, ocular media, and retina only; that is, the physical response, and not the complete response we are seeking. The sine-wave response, Eq. (5), was computed for the edges shown in Figs. 3, 4, and 5. This was accomplished by first taking the Fourier transform of the object and image distributions (taking into account the cutoff to zero luminance as mentioned earlier), Eqs. (6) and (7), then substituting into Eq. (5) and performing the division for the various appropriate spatial frequencies. Since the viewing distance was maintained constant for each edge (14 in.), the three separate determinations of the transfer function should be approximately the same. This is based on the provision that the spread function is dependent solely on accommodation and pupil diameter and is independent of the object distribution. When the viewing distance is constant and the adaptation level does not vary greatly, it is felt that the visual spread-function is invariant, as it indeed must be for the convolution to have any real meaning. The reasonableness of this assumption will be evident later in the discussion of Fig. 8.

There were several methods available for determining the Fourier transforms of the spatial distributions needed for Eq. (5). Perhaps the most direct is to first express the experimentally determined distributions

[20] E. H. Linfoot, J. Opt. Soc. Am. 46, 721 (1956).
[21] P. Lindberg, Optica Acta 1, 80 (1954).
[22] P. M. Duffieux, *L'Integral de Fourier et ses applications à l'optique* (Soc. anon. Oberthur, Rennes, France, 1946).
[23] J. A. Eyer, J. Opt. Soc. Am. 48, 938 (1958); L. O. Hendeberg, Arkiv Fysik 16, 417 (1960).
[24] In N. Wiener, *The Fourier Integral and Certain of its Applications* (Dover Publications, New York, 1933).

analytically. In t
objective distrib
matical form an
distributions and
termined or easil
The transform
known approxim
proach might be
tions, since such
and their ratio w
wave response in
Although some
using all of the a
to be somewhat
difficulty of adju
data to such met
The method
transforms, and
satisfactory, was
high-precision h
puter was easily
and afforded gr
reduction was gr
The harmonic
coefficients of a
function as bein
analyzes the inte
of harmonic wav
multiples n of the

However, for Eqs.
the Fourier int
aperiodic and of i
for the Fourier in
distribution rathe
to J. S. Chandler
method whereby
the analyzer. A

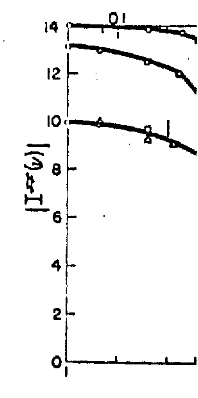

FIG. 6. Fourier tr
curves: curve 1, edg
edge No. 16.

analytically. In this case, the Fourier transforms of the objective distributions are accessible in closed mathematical form and are of the type $(\sin x)/x$. The image distributions and their transforms are not readily determined or easily handled analytically, however.

The transforms could also be determined by well-known approximate integration methods. Another approach might be through the derivatives of the functions, since such derivatives are Fourier-transformable and their ratio would be sufficient for finding the sine-wave response in Eq. (5).

Although some preliminary determinations were made using all of the above-mentioned methods, each proved to be somewhat unsatisfactory, mainly because of the difficulty of adjusting and applying the experimental data to such methods.

The method employed to determine the Fourier transforms, and that which proved to be the most satisfactory, was that of analog computation using a high-precision harmonic analyzer. This analog computer was easily adaptable to our experimental data, and afforded great flexibility and speed, and data reduction was greatly simplified.

The harmonic analyzer is intended to determine the coefficients of a Fourier series, that is, it treats the function as being periodic and of finite period. It analyzes the intensity distribution into a discrete set of harmonic waves whose spatial frequencies are all multiples n of the reciprocal of the period p,

$$\nu = n/p. \tag{8}$$

However, for Eqs. (4) and (5) to be valid, we must use the Fourier integral where the function must be aperiodic and of infinite period. The frequency analysis for the Fourier integral then is in terms of a continuous distribution rather than a discrete one. We are indebted to J. S. Chandler of these Laboratories for suggesting a method whereby the proper analysis could be made on the analyzer. A series of curves of increasing period

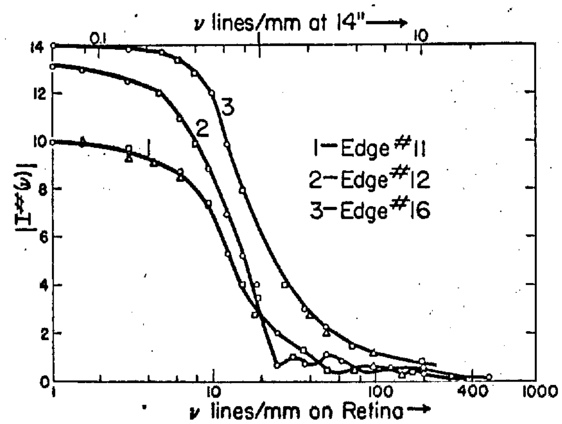

FIG. 6. Fourier transforms of subjective image distribution curves: curve 1, edge No. 11; curve 2, edge No. 12; curve 3, edge No. 16.

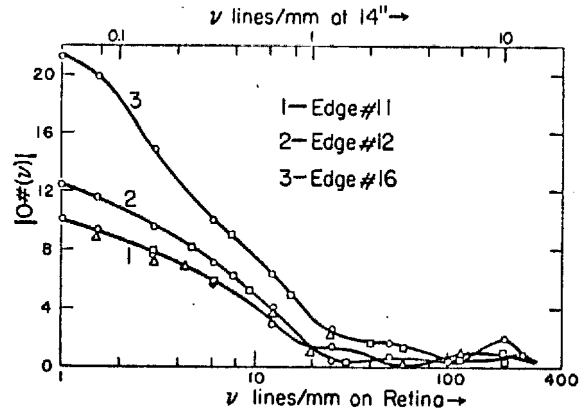

FIG. 7. Fourier transforms of object distribution curves: curve 1, edge No. 11; curve 2, edge No. 12; curve 3, edge No. 16.

were made of each of the edges and a harmonic analysis was performed on each. Although the analysis was necessarily different for each curve in the series because the periods were different, nevertheless, within the range of the function itself, the different analyses of the same curve are equivalent.[25] In the limit of such a process we approach the Fourier integral,[26] and the experimental results show excellent agreement between the different harmonic analyses of the same function. This can be seen from the transforms shown in Figs. 6 and 7. Figure 6 shows the Fourier transforms of the image of each edge obtained in this way, and Fig. 7 shows the transforms of the respective object curves. The corresponding image and object transforms were then used in Eq. (5) to determine $|A^*(\nu)|$, the amplitude function of the sine-wave response. These curves are shown in Fig. 8. It can be seen that all of the object and image transform curves approach zero at the higher

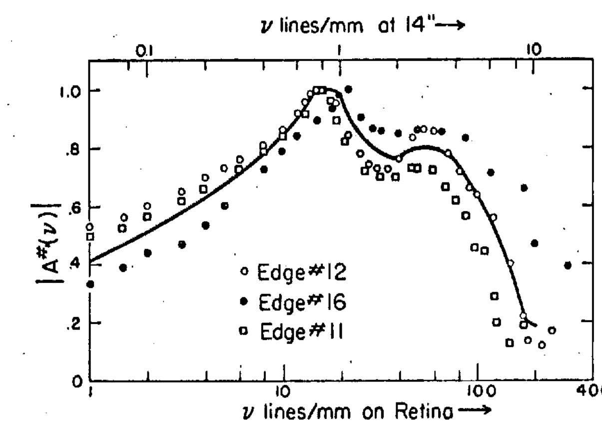

FIG. 8. Sine-wave response of the complete visual system: squares, edge No. 11; open circles, edge No. 12; solid circles, edge No. 16.

[25] R. W. Ditchburn, *Light* (Interscience Publishers, Inc., New York, 1953) p. 88.
[26] C. R. Wylie, *Advanced Engineering Mathematics* (McGraw-Hill Book Company, Inc., New York, 1951), pp. 138–139.

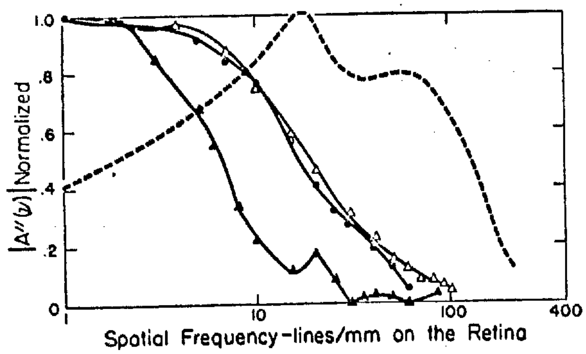

FIG. 9. Comparison of sine-wave response of complete visual system (from present study) with those calculated from other data for the optical system of the eye: open circles, present study; solid triangle, from DeMott's spread function for an excised steer eye; solid circles, from Flamant's spread function; open triangles, from Stultz and Zweig.

frequencies. Consequently, the sine-wave response data in this frequency range are subject to some uncertainty and therefore where the response approaches zero are difficult to determine.

DISCUSSION

The phenomenon reported by Mach shows great promise as a means for establishing more definitely the sine-wave response of the visual system, as well as for evaluating other visual phenomena. The data reported here are illustrative of the results which have been obtained with linear gradients, constant luminance difference, and a fixed viewing distance. It is shown by the curves of Fig. 8 that the sine-wave response decreases at low frequencies, that is, below approximately 1 line/mm in object space (at 14 in.) or 16 lines/mm on the retina. This is generally verified if a series of sine-wave test objects in this frequency range are viewed. It is found that the response goes down as zero frequency is approached.

The differences between the sine-wave response curves for the three edges used are probably due to errors in the difficult photometric measurements. Because of these inherent errors, it is felt that the degree of coincidence of the three sine-wave response curves indicates that the spread function is approximately invariant when the viewing distance is constant and adaptation does not vary greatly. It is hoped that further investigation will verify this relationship.

The data reported here do not agree with the sine-wave response as calculated from the spread functions determined by Flamant, by DeMott (for an excised steer eye), and by Stultz and Zweig (see Fig. 9). It seems quite evident that the difference in results, especially at the low frequencies, is due to the fact that the purely physical approach disregards the physiological response. Also, the information derived from the sine-wave response curve, determined by the method reported here, agrees well with other data, e.g., that the resolving power of the visual system lies in the frequency range of from 150 to 200 lines/mm on the retina.

Preliminary calculations of the phase function $[\theta_I(\nu)-\theta_C(\nu)]$ in Eq. (5) show that apparently the asymmetry of the visual spread-function is small. Data concerning phase will be included and discussed in a later paper on the determination of the spread function of the visual system from the sine-wave response curve of Fig. 8. When this has been done it should be possible to determine the contributions of both the physical and physiological spread functions to the spread function of the entire visual system. In this connection, it appears likely that the physiological spread function acts in somewhat the same fashion that an unsharp mask does or that development effects do in the photographic process.

It should be noted [Eq. (5)] that the complete specification of sine-wave response requires a determination of any possible phase shift. This may be additional evidence that the reciprocal contrast sensitivity mentioned earlier is not truly sine-wave response because the phase cannot be readily determined from measurements of contrast sensitivity.

ACKNOWLEDGMENTS

We are grateful to F. Kottler, E. Marchand, and J. Chandler of these Laboratories for their interest and advice regarding the mathematical procedures and the harmonic analysis used in obtaining the results reported.

Coefficients of distortion ellipsoid:

$$\gamma_{11}=0.9565 \quad \gamma_{12}=-0.0256$$
$$\gamma_{22}=1.0826 \quad \gamma_{13}=0.0037$$
$$\gamma_{33}=1.0892 \quad \gamma_{23}=-0.0018$$

The sphere in $X_1X_2X_3$ space (for source "C") and the two distortion ellipsoids in $X_4X_5X_6$ space for source "A" and source "M", respectively, are illustrated in Figs. 8 to 10 by a few contour lines. In these figures the tristimulus values are renotated by more familiar symbols, that is, $X_1\equiv Y$, $X_2\equiv X$, $X_3\equiv Z$ and $X_4\equiv Y'$, $X_5\equiv X'$, $X_6\equiv Z'$. As was to be expected, the distortion of the reference sphere caused by changing from source "C" to source "A" is considerably more evident than that caused by changing from source "C" to source "M".

JOURNAL OF THE OPTICAL SOCIETY OF AMERICA VOLUME 52, NUMBER 3 MARCH, 1962

Sine-Wave Response of the Visual System. II. Sine-Wave and Square-Wave Contrast Sensitivity*†

J. J. DePalma and E. M. Lowry
Research Laboratories, Eastman Kodak Company, Rochester, New York

(Received August 28, 1961)

Part I of this series described a method which yielded the sine-wave response of the complete visual system by assuming that the Mach phenomenon is the result of a convolution, in the optical sense, of the object luminance distribution with the effective spread-function of the visual system. This second paper is concerned with measuring the response of the visual system to sine-wave and square-wave spatial distributions using the threshold criterion of contrast sensitivity. Particular emphasis is placed on the low spatial frequencies, a region which is believed to be critically important in the mechanism of visual contrast phenomena. Results strongly imply interaction of two basic mechanisms in the visual system. These mechanisms may be characterized individually as a low-pass filter component (optical) and a high-pass filter component (neural, chemical, electrical, etc.).

INTRODUCTION

THERE are several parameters which affect the imaging characteristics and performance of the visual system. Some of these parameters are easily measured and evaluated directly. Others, because of their inaccessibility or complexity, must be evaluated indirectly by empirical methods. With the advent of the sine-wave response function as a relatively new tool in the assessment of optical systems and its rather elegant mathematical techniques for data transformation and extraction, it was felt that this new approach, if successfully applied, might yield quantitative information about the visual system hitherto unavailable.

Part I of this series[1] described a method which is believed to yield the sine-wave response of the complete visual system by assuming that the luminance distribution perceived when viewing a diffuse-edge object (Mach phenomenon) is the result of a convolution, in the optical sense, of the object-luminance distribution with the effective spread function of the complete visual system. A specially designed, visual-slit photometer was used to measure the perceived luminance distribution. By application of Fourier analysis, this distribution and the easily measured, object-luminance distribution were used to determine the sine-wave response.

The sine-wave response function is based on suprathreshold information, i.e., it is the normalized ratio of the image to object modulation of component sinusoidal intensity waves as a function of the spatial frequency of the sine waves. Most data collected for the visual system have, of necessity, been determined by object-threshold techniques. Several investigators have implied that it may be possible, by such threshold measurements of sine-wave patterns, to determine the sine-wave response.

This second paper in this series is concerned with measuring the response of the visual system to sine waves and square waves by threshold techniques under the same viewing conditions used in the earlier Mach experiments. Particular emphasis is placed on the very low spatial frequencies, a region which, in Part I, was shown to be extremely important in the visual process

* Communication No. 2220 from the Kodak Research Laboratories. Based in part on a paper given at the Pittsburgh Meeting of the Optical Society of America, in March, 1961.

† A note on p. 1441 in the December 1961 issue of the J. Opt. Soc. Am., announced the decision of the ICO subcommittee for Image Assessment Problems to change "what is at present known under a variety of names, e.g., sine-wave response, frequency response, contrast transfer, etc.," to "optical transfer function" when the complex function (i.e., including phase) is intended, as it was in Part I of this series. The agreement also provides the term "modulation transfer function" for use when phase is not pertinent. When these nomenclature recommendations were adopted, this paper was already in press. The new nomenclature will be adhered to in any future papers.

[1] E. M. Lowry and J. J. DePalma, J. Opt. Soc. Am. 51, 740 (1961).

and from which a more complete understanding of the imaging characteristics of the visual system may be possible.

PROCEDURE

Several investigators[2–6] have determined, in one form or another, the sensitivity of the visual system to spatial sine waves. Kelly[7] has recently determined the time correlate of this function.

As usually defined, contrast sensitivity is the contrast in the test object necessary for threshold perceptibility. In order to expand the classical definition of contrast sensitivity to include periodicity in the test object, use will be made of the following quantities:

C_T = threshold contrast of test object,
B_{max} = maximum luminance in test object at threshold,
B_{min} = minimum luminance in test object at threshold,
T_1 = maximum transmittance in test object,
T_2 = minimum transmittance in test object,
B_0 = sphere luminance (illuminance of test object),
$B_1 = B_0 T_1$,
$B_2 = B_0 T_2$,
B_{VL} = veiling luminance,
ν_0 = spatial frequency of test object (cycles/mm or lines/mm),
ν_r = spatial frequency on the retina (cycles/mm or lines/mm),
M = magnification,
P_0 = object distance,
P_I = effective image distance.

The defining equation for contrast sensitivity is

$$C_T=\frac{B_{max}-B_{min}}{B_{max}+B_{min}}. \qquad (1)$$

When a sine-wave or square-wave test object is used instead of the usual two-part juxtaposed photometric field, these functions will then be called the sine-wave and square-wave contrast sensitivity, respectively.

A number of variables govern the results obtained for these functions, among the most important of which are: the test object itself; the luminance of the object; the condition of visual adaptation; the viewing distance or accommodation; and the visual angle subtended by the test field. In order to determine the effect of each of these parameters, therefore, great care must be exercised to maintain control over as many of them as possible. Since in much of the work on sine-wave contrast sensitivity which has been reported in the literature complete evaluation of the individual contribution of these parameters was not attempted, as, for example, in determining the change in sine-wave contrast sensitivity with accommodation, it seemed advisable to make a further and more complete investigation of this function. Also, since results of the earlier investigation of the sine-wave response indicated that so far as the visual mechanism is concerned the region of very low spatial frequencies is of considerable importance, it was concluded that measurements in this region should be stressed.

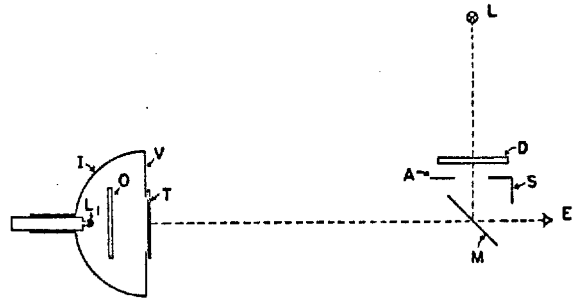

Fig. 1. Schematic of instrument for measuring contrast sensitivity for both sine-wave and square-wave test objects.

For the present experiments, a series of large test objects were prepared by R. L. Lamberts, of these Laboratories, in which the spatial frequencies (ν_0) varied from 0.05 to 9.0 cycles or lines/mm. These test objects consisted of two series. In one, the patterns were sinusoidal and in the other, the light to dark transitions were at a maximum, i.e., square wave. In both of these patterns, the transmittance (and, consequently, the luminance) varied in only one direction.

In investigating the effect of the above-mentioned parameters, the sine-wave and square-wave contrast sensitivity is most usefully expressed as a function of the spatial frequency on the retina, ν_r. The spatial frequency on the retina is computed from the spatial frequency in the test object by the following simple relationship:

$$\nu_r=\nu_0\cdot 1/M=\nu_0\cdot P_0/P_I. \qquad (2)$$

In calculating ν_r for each test object and for each viewing situation, the usually accepted value[8] of 17 mm was used as the effective image distance P_I, that is, the distance from the second nodal point of the eye lens to the retina.

EXPERIMENTAL METHOD

The test objects were mounted in front of an integrating hemisphere, Fig. 1, designed so that they could be uniformly illuminated over a wide range of luminances and viewed at distances of up to 56 in. Light

[2] E. W. H. Selwyn, Phot. J. B88, 6 (1948).
[3] O. H. Schade, J. Opt. Soc. Am. 46, 721 (1956).
[4] K. J. Rosenbruch, Optik 16, 135, (1959).
[5] G. Westheimer, J. Physiol. 152, 67 (1960).
[6] S. Ooue, J. Appl. Phys. (Japan) 28, 531 (1959).
[7] D. H. Kelly, J. Opt. Soc. Am. 51, 422 (1961).

[8] It is recognized that P_I, the distance from the second nodal point of the eye lens to the retina, changes slightly with accommodation (see Helmholtz's *Physiological Optics*, Vol. 1, Opt. Soc. Am., p. 152; Gullstrand, loc. cit., p. 351, or *Text-Book of Ophthalmology*, Duke-Elder, Vol. 1, Chap. XVII), but since this relationship is not known explicitly the authors have used 17 mm as has been recommended (see Committee on Colorimetry, Optical Society of America, *The Science of Color* (Thomas Y. Crowell Company, New York, 1953), p. 74.

TABLE I. Contrast sensitivity for sine-wave test object, constant luminance, 20 ft-L; visual angle, 6°. ν_0=frequency in cycles or lines/mm in object space. ν_r=frequency in cycles or lines/mm on retina.

Obj. space ν_0	10-in. viewing distance Retina ν_r	C_T	14-in. viewing distance Retina ν_r	C_T	35-in. viewing distance Retina ν_r	C_T	56-in. viewing distance Retina ν_r	C_T	10-ft viewing distance Retina ν_r	C_T
0.05	0.747	0.01120	1.046	0.0091	2.615	0.0041	4.184	0.0043	8.965	0.0053
0.075	1.120	0.00682	1.569	0.0067	3.922	0.0027	6.275	0.0027	13.45	0.0040
0.15	2.241	0.00356	3.138	0.0036	7.844	0.0019	12.55	0.0025	26.89	0.0050
0.25	3.735	0.00308	5.229	0.0026	13.07	0.0019	20.92	0.0037	44.82	0.0096
0.50	7.471	0.00202	10.46	0.0034	26.15	0.0041	41.84	0.0096	89.65	0.0310
0.60	8.965	0.00289	12.55	0.0036	31.38	0.0066	50.20	0.0130	107.6	0.0550
0.80	11.95	0.00566	16.73	0.0038	41.84	0.0100	66.94	0.0230	143.4	0.1790
1.00	14.94	0.00906	20.92	0.0034	52.29	0.0130	83.67	0.0410	179.3	0.2740
1.20	17.93	0.01090	25.10	0.0047	62.75	0.0210	100.4	0.0600	...	...
1.60	23.91	0.01500	33.47	0.0083	83.67	0.0400	133.9	0.1120	...	...
1.80	26.89	0.01520	37.65	0.0100	94.13	0.0500	150.6	0.1590	...	...
2.40	35.86	0.02110	50.20	0.0180	125.5	0.1790	200.8	0.8410	...	...
2.80	41.84	0.02330	58.57	0.0240	146.4	0.3050	...	...	...	...
3.60	53.79	0.04570	75.30	0.0390	...	...	...	...	...	...
4.00	59.76	0.05470	83.67	0.0500	...	...	...	...	...	...
5.00	74.71	0.06450	104.6	0.1080	...	...	...	...	...	...
6.00	89.65	0.10900	125.5	0.1920	...	...	...	...	...	...
7.00	104.6	0.21600	146.4	0.2830	...	...	...	...	...	...

(2850°K) from the lamp L_1, which is mounted on the end of an adjustable sleeve, illuminates the white interior of the hemisphere I, and a sheet of fine-ground, pot-opal glass O. The opal glass forms the uniformly luminous background against which the test object T is viewed by the observer E. At V is a variable square diaphragm by means of which the visual angle subtended at the eye of the observer by the test object is controlled. The observer views the test object through a veiling luminance provided by the lamp L (2850°K), the diffusing screen D, and the partially transmitting mirror M. The purpose of the veiling luminance is to control the luminance of the test field at a fixed level for each series of test objects and provide a means by which contrast can be varied. A diaphragm at A and the screen S shield the observer's eyes from direct light from the diffusing screen and from any stray light which might interfere with adaptation. No artificial pupils were used and other optics were purposely omitted so that the observer looked directly at the test object. In making an observation for threshold, the veiling-luminance source is adjusted so that the luminance of the diffusing screen D, as reflected from the mirror M, is approximately 20 ft-L. With the sphere I illuminated and the test object T in place, neutral-density filters are inserted over the aperture in the sphere to reduce the luminance until the test object is reduced to threshold detectibility, as reported by the observer. The observer then completes the luminance adjustment of the sphere by making the necessary fine variations of the voltage on the lamp L_1 until threshold is reached. A check on the total luminance is then made to ensure a value of 20 ft-L. A running control of all luminances throughout the sequence of operations is kept with a modified Macbeth illuminometer. At this point, lamp L is moved toward or away from the diffusing screen D, as required to maintain a total luminance of 20 ft-L, and the observer readjusts the voltage on lamp L_1 for threshold. When a setting for threshold, i.e., disappearance of the pattern, has been completed, illuminometer readings are made of both the veiling luminance B_{VL}, and the sphere luminance B_0.

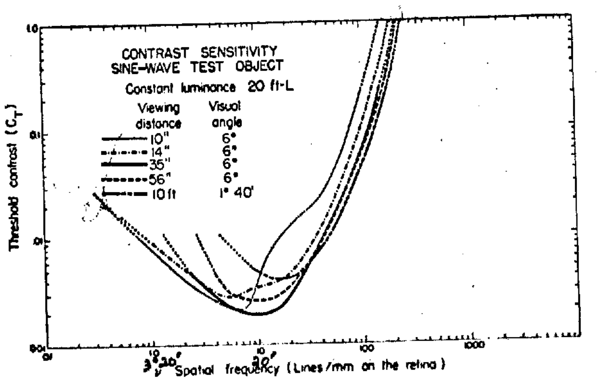

FIG. 2. Contrast sensitivity for sine-wave test objects as a function of the retinal spatial frequency of the sine wave.

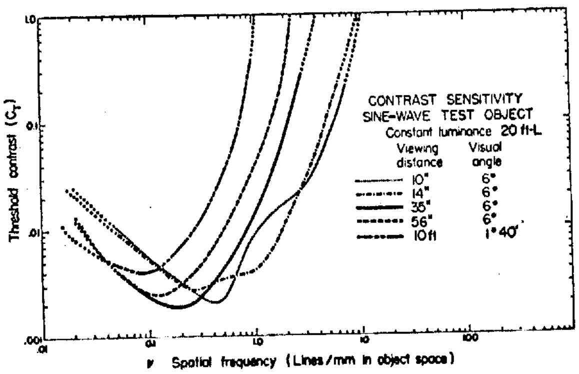

FIG. 3. Contrast sensitivity for sine-wave test objects as a function of the spatial frequency of the sine wave in object space.

TABLE II. Contrast sensitivity for square-wave test object, constant luminance, 20 ft-L; visual angle, 6°. ν_0=frequency in cycles or lines/mm in object space. ν_r=frequency in cycles or lines/mm on retina.

Obj. space ν_0	10-in. viewing distance Retina ν_r	C_T	14-in. viewing distance Retina ν_r	C_T	35-in. viewing distance Retina ν_r	C_T	56-in. viewing distance Retina ν_r	C_T
0.05	0.747	0.0026	1.046	0.0029	2.615	0.0025	4.184	0.0019
0.075	1.120	0.0028	1.569	0.0023	3.922	0.0024	6.275	0.0017
0.10	...	...	2.092	0.0020	5.229	0.0021	8.367	0.0015
0.125	...	...	...	...	6.537	0.0021	10.46	0.0015
0.15	2.241	0.0017	3.138	0.0018	7.844	0.0017	12.55	0.0015
0.175	...	...	...	...	9.151	0.0021	14.64	0.0023
0.20	...	...	...	...	...	...	16.73	0.0022
0.25	3.735	0.0019	5.229	0.0016	13.07	0.0024	20.92	0.0031
0.30	...	...	...	...	15.69	0.0027	25.10	0.0035
0.375	...	...	7.844	0.0018	...	...	...	...
0.50	7.471	0.0019	10.46	0.0019	26.15	0.0037	...	...
0.625	9.338	0.0028	13.07	0.0023	32.68	0.0056	...	...
0.75	11.21	0.0026	15.69	0.0033	...	...	...	...
0.875	...	...	...	...	45.76	0.0110	...	...
1.00	14.94	0.0030	20.92	0.0041	52.29	0.0140	...	...
1.25	18.68	0.0095	26.15	0.0080	65.37	0.0230	...	...
1.50	22.41	0.0130	31.38	0.0086	78.44	0.0310	...	...
2.50	37.40	0.0230	52.29	0.0340	130.7	0.1620	...	...
3.00	44.80	0.0480	62.75	0.0550	...	...	...	...
4.00	59.76	0.0770	83.67	0.1140	...	...	...	...
5.00	74.71	0.1680	104.6	0.2340	...	...	...	...
6.00	89.65	0.2680	125.5	0.5060	...	...	...	...
7.00	...	...	146.4	0.9320	...	...	...	...
8.00	119.5	0.5500	...	...	...	...	...	...
9.00	134.5	0.7350	...	...	...	...	...	...

By using the data previously obtained from microdensitometer measurements of the maximum transmittance T_1 and minimum transmittance T_2 of the sine-wave and square-wave test objects, as well as the sphere luminance B_0 at threshold, with the test objects removed, the values B_1 and B_2 are easily calculated. These values, together with the veiling luminance B_{VL}, were then used to determine the threshold contrast by substituting into Eq. (1):

$$C_T=\frac{B_{\max}-B_{\min}}{B_{\max}+B_{\min}}=\frac{(B_1+B_{VL})-(B_2+B_{VL})}{(B_1+B_{VL})+(B_2+B_{VL})} \quad (3)$$

$$=\frac{B_1-B_2}{B_1+B_2+2B_{VL}}. \quad (4)$$

Table I contains the data on contrast sensitivity so obtained for sine-wave test objects viewed at distances of 10, 14, 35, and 56 in., respectively, with a constant visual angle of 6° and a constant field luminance of 20 ft-L. A slight modification of the apparatus in Fig. 1 increased the viewing distance to 10 ft, although because of the size of available test objects the visual angle subtended at the eye by the test object in this case was reduced to 1° 40′.

The data in Table I are shown in Fig. 2, in which the threshold contrast is plotted as a function of the spatial frequency of the sine wave on the retina (ν_r). Figure 3 also presents data from Table I, but in this graph threshold contrast is plotted as a function of the object spatial frequency ν_0.

Table II contains the data on contrast sensitivity for square-wave test objects and Figs. 4 and 5 are graphs of these data in which the threshold contrast has been plotted as a function of ν_r and ν_0, respectively.

RESULTS AND DISCUSSION

Inspection of the curves in Fig. 2 reveals that for all viewing distances maximum contrast sensitivity occurs at frequencies in the neighborhood of 10 lines/mm on the retina and that contrast sensitivity decreases (higher threshold) for both lower and higher spatial frequencies. It is also seen that as the viewing distance is increased the threshold contrast, in general, decreases for any spatial frequency higher than the minimum. Perhaps of more significance is that just the reverse

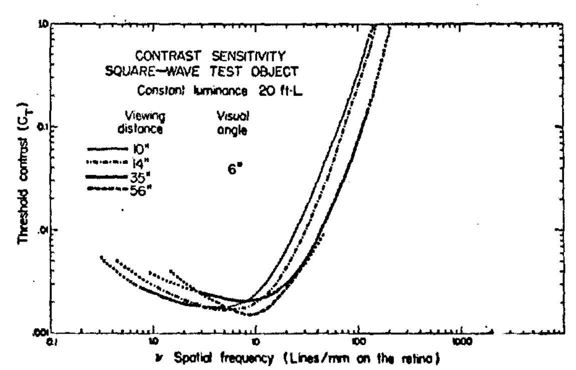

FIG. 4. Contrast sensitivity for square-wave test objects as a function of the retinal spatial frequency of the square wave.

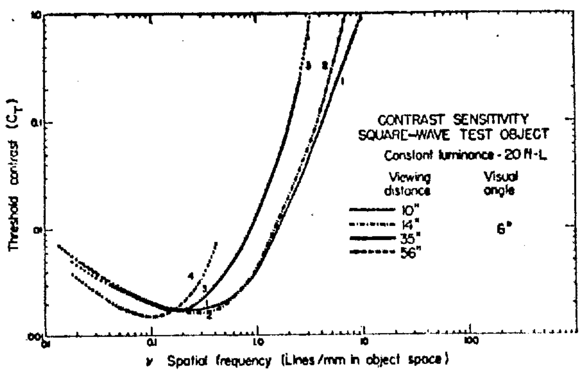

FIG. 5. Contrast sensitivity for square-wave test objects as a function of the spatial frequency of the square wave in object space.

is true as zero frequency is approached from the minimum. This result is also in basic agreement with the data reported in Part I of this series,[1] that is, that the sine-wave response of the visual system decreases at the lower frequencies as well as at the higher frequencies. The maximum response to sine waves, as determined by using the Mach phenomenon method, was shown to be around 15 lines/mm on the retina, with a similar decrease in response at both higher and lower frequencies.

It is interesting to observe in some of the curves of these figures the rather unusual behavior of contrast sensitivity (C_T) in the middle-frequency range. Whether these humps are artifacts caused by something in the experimental technique or are real cannot be ascertained at present. However, since they correspond more or less to the dip in the sine-wave response curve obtained by the Mach phenomenon, they may possibly be attributed to some factor in the visual system which is critically operative when the eye is accommodated for reasonably near vision. It is hoped that further experimental data will verify the existence of this deviation from the smooth curve.

Figure 3 also presents data from Table I, but in this case the threshold contrast is plotted as a function of the spatial frequency in object space, ν_0. When plotted in this system of coordinates, the order of arrangement of the curves is seen to be reversed from that of Fig. 1 since, regardless of the viewing distance, the frequency in object space, of course, remains constant. For example, if the sine-wave test object of frequency 1 cycle/mm is viewed, the threshold contrast required is highest for a viewing distance of 10 ft and lower for each of the other distances in descending order, except for the 10-in. distance. The hump in the curve for 10 in. is more exaggerated than in the one for 14 in. and, accordingly, reverses the order of threshold contrast over a limited frequency range. In other respects, the curves portray the same facts as those of Fig. 2, that is, that contrast sensitivity decreases for both high and low frequencies with the minimum required contrast (maximum sensitivity) in the frequency range of from 0.1 to about 0.6 cycle or line/mm.

As was the case for the sine-wave test objects, Figs. 4 and 5 show that the square-wave contrast-sensitivity curves also demonstrate a decrease in sensitivity at both high and low frequencies. However, in the case of square-wave test objects, the contrasts necessary for perceptibility in the low-frequency range are much lower than for the sine waves. Close examination of the curves for sine-wave and square-wave test objects reveals a very interesting result. In using this threshold criterion, it is found that while the visibility of very coarse square waves is better than that of sine waves of the same coarseness, just the reverse is true in the high-frequency region. This effect is illustrated for the 14-in. viewing distance in Fig. 6. In this figure it is seen that the limit of resolution for the square wave is about 150 lines or cycles/mm, whereas that for the sine wave is about 200 lines or cycles/mm. A possible explanation of this effect is that, in the threshold criterion for detectibility of the periodic pattern, the judgment of the very coarse patterns is influenced by the effect of the spatial contour of the test objects on their apparent contrast, whereas the judgment of the very fine pattern tends to be made on the basis of the separation of the lines and spaces, that is, resolution. There is ample evidence that this process is involved when one looks at these test objects. For a very fine pattern, say, 8 lines or cycles/mm ($\nu_r = 167$), the line-space ratio for the sine wave is much greater than the line-space ratio of a square wave. As seen visually, the line-space ratio of the square wave is nearly 1.0, while that for the sine wave is about 2.0. This certainly suggests that a higher-frequency sine wave will be visible, and this is borne out by the data in Fig. 6.

Throughout this general study of the sine-wave response and contrast sensitivity of the visual system, we have stressed the point that these functions are dependent on several parameters. Although to most workers in this field this statement is obvious, nevertheless there are numerous examples in the literature where

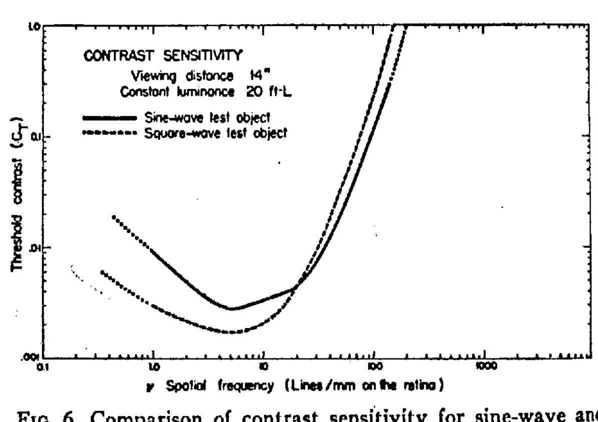

FIG. 6. Comparison of contrast sensitivity for sine-wave and square-wave spatial distributions taken for the same viewing conditions.

this important fa
must be emphasiz
appearance of a p
by means of expe
acteristics of the v
the various obj
viewing distance,
for which the vis
to say, the viewin
and controlled in
human observer
sults are to be ob
that the visual fu
are viewed at dif
literature visual
of illumination h
derived under a c
appearance of o
discriminately as
obtained with an
ments have led i
Many investigat
the visual syst
(usually thresho
ration of two o
visual angle (an
seen that this fu
of contrasts ma
visual angle, dep
object is viewed
parameter must

A further defe
in the data of T
of Fig. 7. Here
shown for two
namely, 20 and
visibility of th
from about ν_r=
for the higher l
spatial frequenc

TABLE III. Cont
ing distance, 35 in
lines/mm in object
retina.

Obj. space ν_0
0.05
0.075
0.15
0.25
0.50
0.60
0.80
1.00
1.20
1.60
1.80
2.40

this important fact has been neglected. Therefore, it must be emphasized that in evaluating or assessing the appearance of a particular object-intensity distribution by means of experimentally determined response characteristics of the visual system, care must be taken that the various object parameters, such as luminance, viewing distance, visual angle, etc., correspond to those for which the visual function was determined. That is to say, the viewing situation must be accurately known and controlled in any particular evaluation where the human observer is an integral part, if meaningful results are to be obtained. It has been noted, for example, that the visual function changes when the test objects are viewed at different distances. In many cases in the literature visual evaluations of objects under one level of illumination have been made with a visual function derived under a different level of illumination. Also, the appearance of objects viewed naturally are often indiscriminately assessed by means of a visual function obtained with an artificial pupil. Results of such experiments have led in some cases to erroneous conclusions. Many investigations of the response characteristics of the visual system specify the dependent variable (usually threshold contrast) as a function of the separation of two object elements expressed in terms of visual angle (analog of spatial frequency ν_0). We have seen that this function is not unique because a variety of contrasts may be obtained for any one particular visual angle, depending on the distance from which the object is viewed. In such cases, the accommodation parameter must be controlled and specified.

A further defense of this point of view may be found in the data of Table III, shown plotted in the curves of Fig. 7. Here the sine-wave contrast sensitivity is shown for two different test-object luminance levels, namely, 20 and 300 ft-L. The curves indicate that visibility of the sine waves in the frequency range from about $\nu_r = 8-260$ lines or cycles/mm is greater for the higher luminance level, whereas it is lower for spatial frequencies less than 8 lines or cycles/mm. The

TABLE III. Contrast sensitivity for sine-wave test object, viewing distance, 35 in.; visual angle, 6°. ν_0 = frequency in cycles or lines/mm in object space. ν_r = frequency in cycles or lines/mm on retina.

Obj. space ν_0	Retina ν_r	C_T 20 ft-L	C_T 300 ft-L
0.05	2.615	0.0041	0.00477
0.075	3.922	0.0027	0.00289
0.15	7.844	0.0019	0.00173
0.25	13.07	0.0019	0.00156
0.50	26.15	0.0041	0.00193
0.60	31.38	0.0066	0.00275
0.80	41.84	0.0100	0.00395
1.00	52.29	0.0130	0.00522
1.20	62.75	0.0210	0.00627
1.60	83.67	0.0400	0.01240
1.80	94.13	0.0500	0.02300
2.40	125.5	0.1790	0.03530

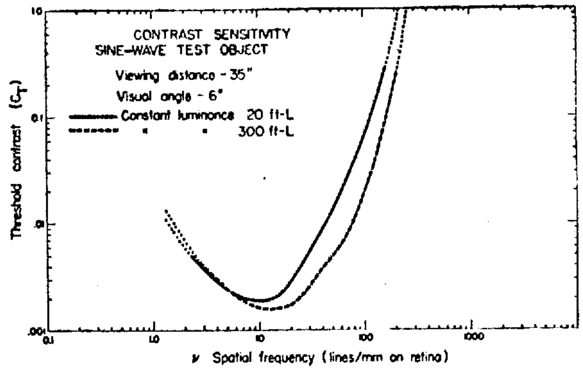

FIG. 7. Contrast sensitivity for sine-wave test objects taken at two luminance levels.

most likely explanation for the decrease in threshold contrast at the higher frequencies for the 300-ft-L condition may probably be deduced from the optics of the eye. The pupil diameter for 300 ft-L has been found to be approximately 2.3 mm,[9] while that for the 20 ft-L is 3.3 mm. The former condition will be less subject to image degradation than the latter, owing to reduction in the aberrations and an increase in depth of focus.[10] Hence, the sine waves should be imaged with greater fidelity at the higher luminance. No such simple explanation for those frequencies below 8 lines or cycles/mm seems possible as yet, no doubt because the answer involves the higher-order perceptual mechanisms of the human observer.

It will be noticed from an inspection of all of the curves in which threshold contrast is plotted as a function of spatial frequency that maximum sensitivity is somewhat higher (lower threshold contrast) than that normally quoted and recognized for the least-perceptible difference in luminance. For example, the minimum required contrast for either sine-wave or square-wave test objects is of the order of 0.002, which is lower than the value of 0.01 to 0.015 usually accepted for sensitivity to luminance differences. Several factors in the present situation contribute to the lower threshold. The most obvious factor is the difference in the definition of contrast sensitivity or luminance discrimination which is usually specified as $\Delta B/B$, where ΔB is the increment in luminance which is just perceptible at the luminance level B, and B is equal to the mean luminance of the two contrasting fields at threshold, i.e.,

$$B = \frac{B_{max} + B_{min}}{2}. \tag{5}$$

Thus:

$$\frac{\Delta B}{B} = \frac{B_{max} - B_{min}}{\frac{B_{max} + B_{min}}{2}} = 2C_T. \tag{6}$$

[9] J. W. T. Walsh, *Photometry* (Constable and Company Ltd., London, 1953), p. 54.
[10] P. W. Cobb, Am. J. Physiol. 36, 335 (1915).

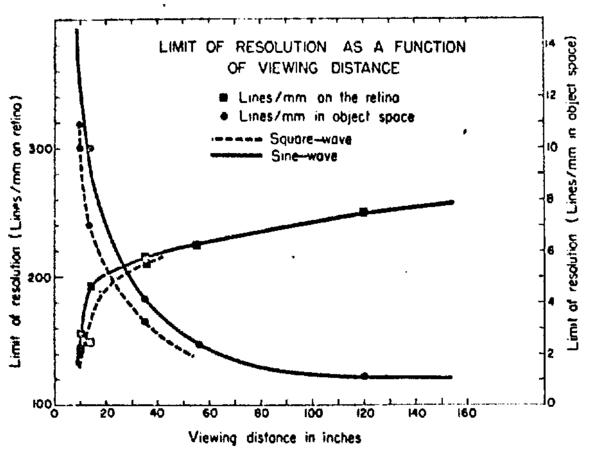

FIG. 8. Limit of resolution of the visual system as a function of viewing distance for both square-wave and sine-wave test objects. (Luminance, 20 ft-L.)

Therefore, the classical method of determining contrast sensitivity introduces a factor of 2, which itself gives a value twice as great as the one we find. Both Schade[3] and Ooue[6] have used Eq. (6) as their defining equation for sine-wave contrast sensitivity. Another factor contributing to the lower threshold value which we report is our use of a large test-field angle, namely, 6°, whereas most luminance-discrimination data[11] are taken for much smaller field angles. It has been shown by Crozier and Holway[12] that the percent error of luminance matching decreases as field size increases.

Perhaps the most important factor contributing to the lower threshold is related to the criterion of the photometric threshold measurement. In the present case, judgments are based on the disappearance of any contrasting pattern in the visual field as opposed to the usual equality of brightness criterion adopted for most photometric work which uses a bipartite field. As long ago as 1889, Lummer and Brodhun[13] advocated the use of *equality of brightness contrast* rather than *equality of brightness* for photometry, and they published data to show that the precision of measurement so obtained could be greatly increased. Later, Pfund[14] developed a contrast type of photometric prism with which he obtained a sensitivity of 0.0048 compared to that of 0.019 for an equality-of-brightness method.

Most evaluations of the response characteristics of the visual system have in the past been based on the limit of resolution, which itself of course is a threshold measurement. It is evident that the limit of resolution or resolving power of the visual system is just one point on the sine-wave or square-wave contrast-sensitivity curve. Again, we see that the limit of resolution (with no artificial pupils and no interposed optics) is a function of the viewing distance and luminance level. The limit of resolution as used here refers to that spatial frequency in lines or cycles/mm which is just imperceptible at the maximum object contrast, namely, 1.0. When the curves of Figs. 2–5 are extrapolated slightly, as shown by the dotted lines, it is possible not only to obtain the values of the limit of resolution of the visual system in cycles or lines/mm on the retina or in object space but also to determine how the resolution limit changes with viewing distance. Table IV shows the limit of resolution determined in this manner for different viewing distances for both sine-wave and square-wave test objects, when the luminance is maintained constant at 20 ft-L. These data are plotted and shown in Fig. 8. It is at once evident from the curves that the limit of resolution of the visual system falls at higher retinal frequencies as the viewing distance is increased, regardless of the type of test object used. This seems to be in basic agreement with some of the work reported by Freeman,[15] by Luckiesh and Moss,[16] and by others, that visual acuity increases with stimulus distance. Most of their work involved the bar type of test object with no periodicity, although in some of the experiments by Luckiesh and Moss periodic bar patterns were used. These workers attributed part of this change of acuity with viewing distance to the fact that the pupil is changing with accommodation. Other factors which have been suggested as possible reasons for this change seem to be minor compared to the factor of accommodation itself. Contrast diminution and object distortion would of course be expected to be higher for an eye lens broadened for near vision than the thinner lens for distant vision.

TABLE IV. Effect of viewing distance on the limit of resolution, constant luminance, 20 ft-L.

Viewing distance (inches)	Limit of resolution, cycles or lines/mm for: Sine-wave test object, On the retina ν_r	Sine-wave test object, In object space ν_0	Square-wave test object, On the retina ν_r	Square-wave test object, In object space ν_0
10	155	10.4	145	9.71
14	193	9.23	150	7.17
35	215	4.11	210	4.02
56	225	2.69	...	...
120	250	1.39	...	...

It is seen also from the curves of Fig. 8 that for the viewing conditions of this experiment the limit of resolution as a function of viewing distance is higher for sine-wave test objects than for square-wave test objects, a partial explanation for which was given earlier.

[11] E. M. Lowry, J. Soc. Motion Picture Television Engrs. 57, 187 (1951).
[12] W. J. Crozier and A. H. Holway, J. Gen. Physiol. 23, 101 (1939–40).
[13] O. Lummer and E. Brodhun, Instrumentenkunde 9, 461 (1889).
[14] A. H. Pfund, Phys. Rev. 4, 477 (1914).
[15] E. Freeman, J. Opt. Soc. Am. 22, 285 (1932).
[16] M. Luckiesh and F. K. Moss, J. Opt. Soc. Am. 23, 25 (1933).

CONCLUSIONS

It has been shown that, using the criterion of C_T, the contrast sensitivity of the visual system to sine waves is a function of the spatial frequency of the sine wave and has a maximum sensitivity at about $\nu_r = 7-15$ cycles or lines/mm, depending on the viewing condition. From this maximum (minimum C_T), the sensitivity to sine waves decreases for spatial frequencies both higher and lower than this. The same general relationships hold for the contrast sensitivity of the visual system to square waves, although there are some important differences of degree as explained previously.

As has been mentioned earlier in this paper and also in Part I, other determinations have been made of C_T. In the earlier work reported in the literature in which a pattern of multiple bars or of just two or three bars was used, there seems to be no indication of the decrease in contrast sensitivity at low frequencies or large separation of the bars. So far as the authors have been able to ascertain, the first concerted determination of the threshold contrast using sine-wave distributions was conducted by Selwyn,[2] and the first hint of the decrease in sine-wave contrast sensitivity at the low frequencies can be seen in Fig. 5 of his paper on visual resolving power. Rosenbruch[4] made an extensive study of both sine-wave and square-wave contrast sensitivity, but none of his data show this low-frequency decrease. Schade[3] and Ooue[6] (who followed the lead of Schade) do show this decrease for the sine-wave distributions and the data reported in our study are in quite good agreement with theirs. Westheimer[5] has followed a similar approach but has not obtained the decrease at the low frequencies.

In several of the determinations mentioned, two or three of the parameters affecting the threshold were allowed to vary. In some, artificial pupils were used to obtain the "perfect lens" condition. In others, the accommodation parameter was not evaluated.

In conclusion, there seems to be little doubt from the results of Part I and from those of this study that any analysis of the imaging and image-transfer mechanism of the complete visual system must have as its basis both a high-pass and a low-pass filter component, somehow acting in concert. The maximum response to sine waves at retinal frequencies of about 7–15 lines or cycles/mm and the subsequent decline in response for higher and lower frequencies strongly suggest the interaction of two basic mechanisms. The simplest and most logical explanation seems to be that the low-pass component is associated with the optics of the eye, which includes eye lens, ocular media, pupil diameter, and retinal diffusion. For one specific visual condition, Flamant[17] has experimentally determined this component. Evaluation of its sine-wave response characteristics[1] show it to behave as one would expect any simple optical system to behave, i.e., maximum response at zero frequency and gradual decline in response as the spatial frequency increases. The high-pass component of the visual system, which is presumably responsible for the Mach phenomenon and other visual-contrast phenomena, appears to be intimately related to the inhibitory processes taking place from the retina back to the brain and is no doubt composed of a complexity of interrelated mechanisms—neural, chemical, electrical, and psychological.

[17] F. Flamant, Rev. opt. 34, 433 (1954).

02157

6 December 1968

SCHEDULE OF EVENTS

12/8	to 12/22	△1	Scale 3X to 30X zoom lens design to 3X to 45X or 50X, maintaining a good resolution at 3X.
12/23	to 1/2		Vacation
1/3	to 1/13	△2	Optimization of 3X to 50X lens design.
1/13	to 1/20	1	Lens evaluation.
1/20	to 2/3	△3	Correct back focal distance of lens design.
2/3	to 2/17	2	Light source and optical design of illuminator condensing lens design.
2/17	to 3/15	△4	Package and mechanical layout of zoom lens and illuminator assemblies into the present NOD/100 Viewer.
3/15	to 4/1	3	Cost estimate to complete the design and manufacturing of the new optical systems and modify and test the present NOD/100 Viewer.
2/17	to 4/1		Revise the present NOD/120 Viewer requirements to be compatible with the modified NOD/100 Viewer performance.

△ Critical milestone which must be met in order for the program to proceed.

25X1

9 DEC

UPGRADING THE SCV 3-30X 5" FORMAT

FINISHED IT IN ABOUT AUG INCLUDING CONDENSOR

3X→45X SCALEING UP 8 LP/MM/MAG POW ACROSS FIELD

Zenon Hg AC device can get by with less power supply
dc is straight zenon

Potential Problem of illumination pattern. "Newtons ring effect"

300hr tube will probably be reduced to 200hrs if used on its side.

Concern over film cooling presently at border-line
3X-41X PROBABLY VERY GOOD.

NASA Houston Texas.

25X1

12 10 Comparator + DataLogger.

Approved For Release 2005/05/02 : CIA-RDP78B04770A001900020032-6

25X1

File 02157
MISC.

50-130 3400 - DUPE ON 5427 (ESTAR 2420) 3.6 (0.76)

SO 102 (4401) 3401 -

SO-380 (OTB), SO132 3404 - DUPE ON 8430 (2430) USING D-76 (HIGHEST RES) DMIN .28 DMAX = 1.8 ABOB 1.6

EK 100 FT-CANDLES @ VIEWING [illegible]
ROOM <10% AMBIENT LEVEL
5500°K 4100°K
MACBETH 3800°K @ 200 FT-CANDLES

Approved For Release 2005/05/02 : CIA-RDP78B04770A001900020032-6

[redacted] 68Y92

STATUS REPORT # 2

for

MOD 110 LOW MAGNIFICATION ZOOM LENS DESIGN

and

ILLUMINATION SYSTEM
STEP I

April 12, 1968

[redacted]

Engineering Specialist

Approved by

 [redacted]

Supervisor,
Intelligence Equipment

[redacted]

In January of 1968, a status report [redacted]8Y12) was submitted which defined the characteristics of the two NOD-110 zoom lenses. This report indicated that the predicted performance of the high magnification lens (24X to 70X) would essentially meet the resolution requirements. 25X1

The low magnification (3X to 30X) lens predicted performance showed that it too would meet the axial resolution requirement. However, the predicted performance at the screen edge was considerably below that required. Since good resolution at the screen edge at low magnification is needed for operational acceptance, further work had to be done.

After reviewing the prior effort and analyzing the results in detail, it was determined that the first order solution would have to be modified. The modified first order solution included the addition of a positive auxiliary element. Also, in the optimization, greater emphasis was placed on the low magnification off-axis imagery. The initial results proved to be encouraging as substantial off-axis improvement was made. Despite the emphasis on the low magnification/off-axis imagery, both the on-axis and higher magnification imagery remained excellent. There was only one problem. The physical size of the lens, both diameter and length, was excessively large. This would preclude housing the lens within the specified NOD-110 envelope and also leave no space for the high magnification lens.

Based on a system analysis, it was concluded that if the lens could be scaled down to 0.85 of its size, it would meet the physical size requirement. This was done and continued optimization of the scaled-down lens showed further improvement.

Further optimization was continued until the design appeared to meet the total requirements. At this point an evaluation run was conducted. The results of the evaluation are included in this report. Predicted resolution is shown in Figures 1 and 2. Modulation transfer function curves are shown in Figures 3 through 12. Phase data are also included in Figures 13 through 17. Both monochromatic data (at $\lambda = 5461$ Å) and heterchromatic data (the summation of four wavelengths, ($\lambda_1 = 5461$ Å, $\lambda_2 = 5876$Å, $\lambda_3 = 4861$ Å and $\lambda_4 = 6563$ Å) are plotted for each magnification.

The negative auxiliary lens was not included in the evaluation. Experience on this program, as well as the NOD-100 and others, has shown that a well corrected negative auxiliary lens produces very little, if any, degradation. It will, however, be included in the final system.

The enclosed MTF curves are, of course, theoretical. In actual practice both the effects of minor imperfections, as well as the degradation caused by other system elements (such as screen) must be considered. As the resolution is increased the MTF of each of the system elements becomes more critical. It is anticipated that the final system performance will equal, or slightly exceed, that depicted in the data presented by [redacted] 25X1
25X1 [redacted] in a meeting on 19 March 1968.

Screen Brightness

A preliminary analysis of the NOD-110 screen brightness has been made to determine the amount of screen brightness, both on axis and edge of field, that will be provided.

The axial screen brightness in foot lamberts is determined from the expressions:

$$B_s = \frac{\pi \, BtG}{4(F/NO)^2 \, M^2}$$

10MM → 4mm ARC LENGTH

Where B_s = Screen brightness in foot lamberts

B = Source brightness in candles/foot^2

t = Transmittance of optical system

G = Screen gain

M = Magnification of projection optical system

F/NO = Effective F-number of projection system

The following numerical values were used to determine the screen brightness:

B = 13×10^6 candles/foot^2

t = 0.015 including the 1.5 neutral density filter

G = 2.0 NOD LS-G 60 GAIN=5 OF NOD 100

The value for source brightness of 13×10^6 candles/foot^2 is for a Hanovia DL-5064-000 custom made 2500 watt Xenon lamp made by Osram. The transmittance of 0.015 includes a 1.5 neutral density filter in the film gate, and the screen gain of 2.0 is for the Polacoat LS 60 screen material. The predicted axial screen brightness, using these numerical values, will be as plotted in Figure 18.* Included also is a family of screen brightness curves for different density filters between 1.0 and 1.5.

In the design of a Köhler type condenser lens system for a projection lens, the image of the source should fill the projection lens entrance pupil for maximum condenser lens efficiency. The condenser lens must also be large enough to illuminate the film format completely. It becomes considerably more complicated to design a condenser lens for a zoom projection lens where the entrance pupil varies in both location and diameter with magnification. In addition, the physical dimensions of the radiating source are critical. If the source is small, the magnification of the condenser lens must be large, requiring a large condenser lens numerical aperture. This is especially true at low magnifications when the entire film format must be illuminated.

* These predictions are accurate to ± 20%.

Until considerable progress on the design of the NOD-110 condenser lens has been made, the screen brightness predictions are being made using the long arc custom made Osram lamp to ensure that the lens entrance pupils are filled at all magnifications. Consideration of higher wattage Xenon lamps, which have greater brightness as well as larger arc lengths, will also be made.

In the calculations for screen brightness, consideration was made for high efficiency coatings for all air-glass surfaces, including the condenser lens surfaces. High efficiency reflectance for mirrors was also considered, resulting in an overall optical transmittance of 50 percent (without the neutral density filter).

The screen brightness will not vary more than ten percent when measured along an axis which is always pointing to the pupil of the projection lens. ** Any deviation from this axis will reduce the brightness by an amount which is characteristic of the screen material, where the gain varies with the bend angle. In the case of Polacoat LS 60, the gain varies from 2.0 at zero bend angle to a gain of 1.0 at approximately 25 degrees bend angle. Thus, the brightness will be reduced by one-half at a bend angle of 25 degrees.

The attached page from the SMPTE Journal is included to illustrate the effects of off-axis brightness.

** It should be understood that at low magnification there will be vignetting at the corners.

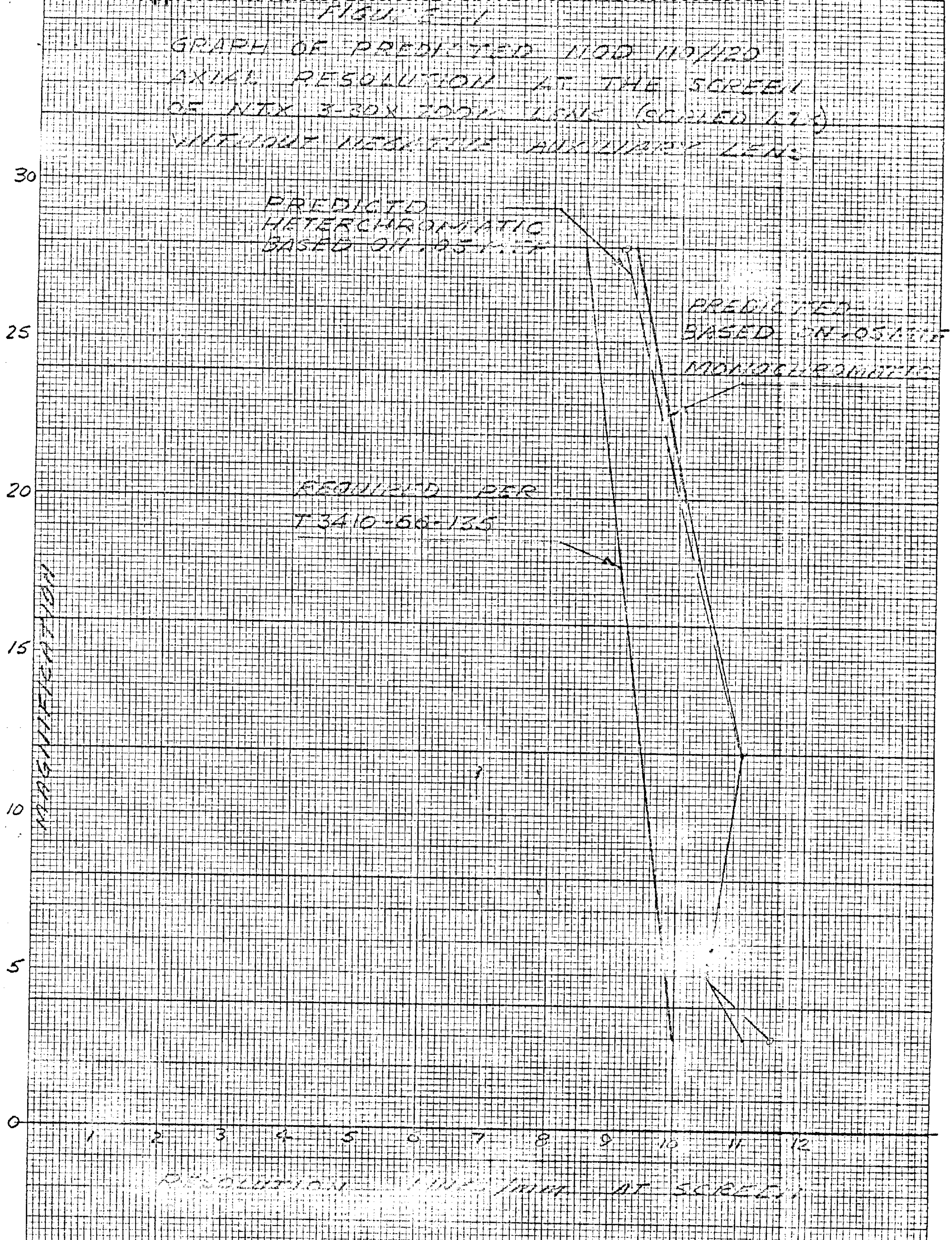
GRAPH OF PREDICTED MOD 110/120
AXIAL RESOLUTION AT THE SCREEN
OF NTX 3-30X ZOOM LENS
AUXILIARY LENS
PREDICTED
HETERCHROMATIC
PREDICTED
BASED ON
REQUIRED PER
T3410-56-135
MAGNIFICATION
30
25
20
15
10
5
0
1
2
3
4
5
6
7
8
9
10
11
12
AT SCREEN

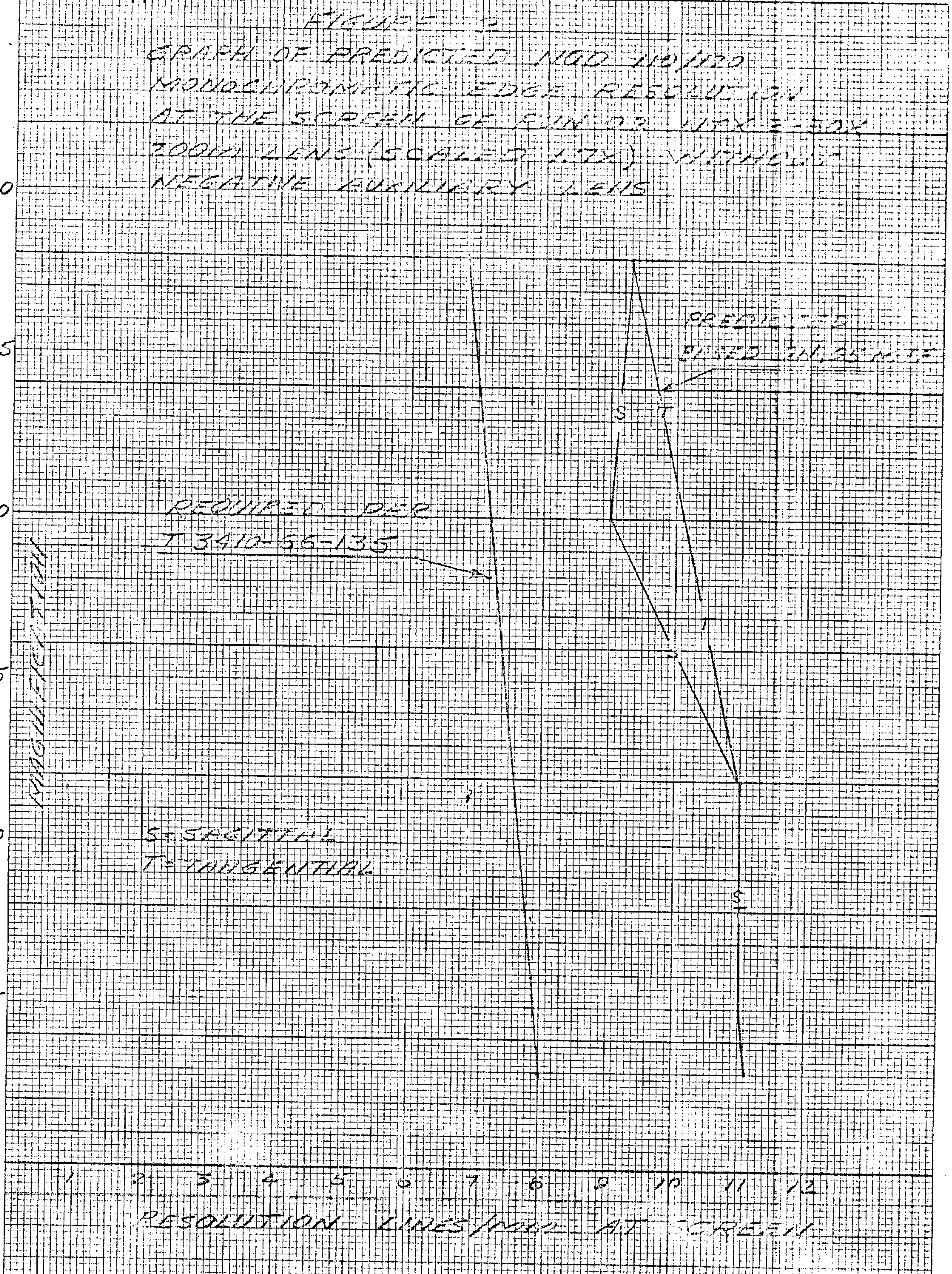
GRAPH OF PREDICTED MOD 110/120
MONOCHROMATIC EDGE RESOLUTION
AT THE SCREEN OF RUN 02 WTX 3-30X
ZOOM LENS (SCALED 1.7X) WITHOUT
NEGATIVE AUXILIARY LENS
REQUIRED PER
T 3410-56-135
S
T
S-SAGITTAL
T-TANGENTIAL
MAGNIFICATION
30
25
20
15
10
5
1
2
3
4
5
6
7
8
9
10
11
12
RESOLUTION LINES/MM AT SCREEN

4-11-6

FIGURE 2A
GRAPH OF PREDICTED MOD 110/120
EDGE HETEROCHROMATIC RESOLUTION
AT THE SCREEN OF RUN 22 NTX 3-30X
ZOOM LENS (SCALED 1.7X) WITHOUT
NEGATIVE AUXILIARY LENS

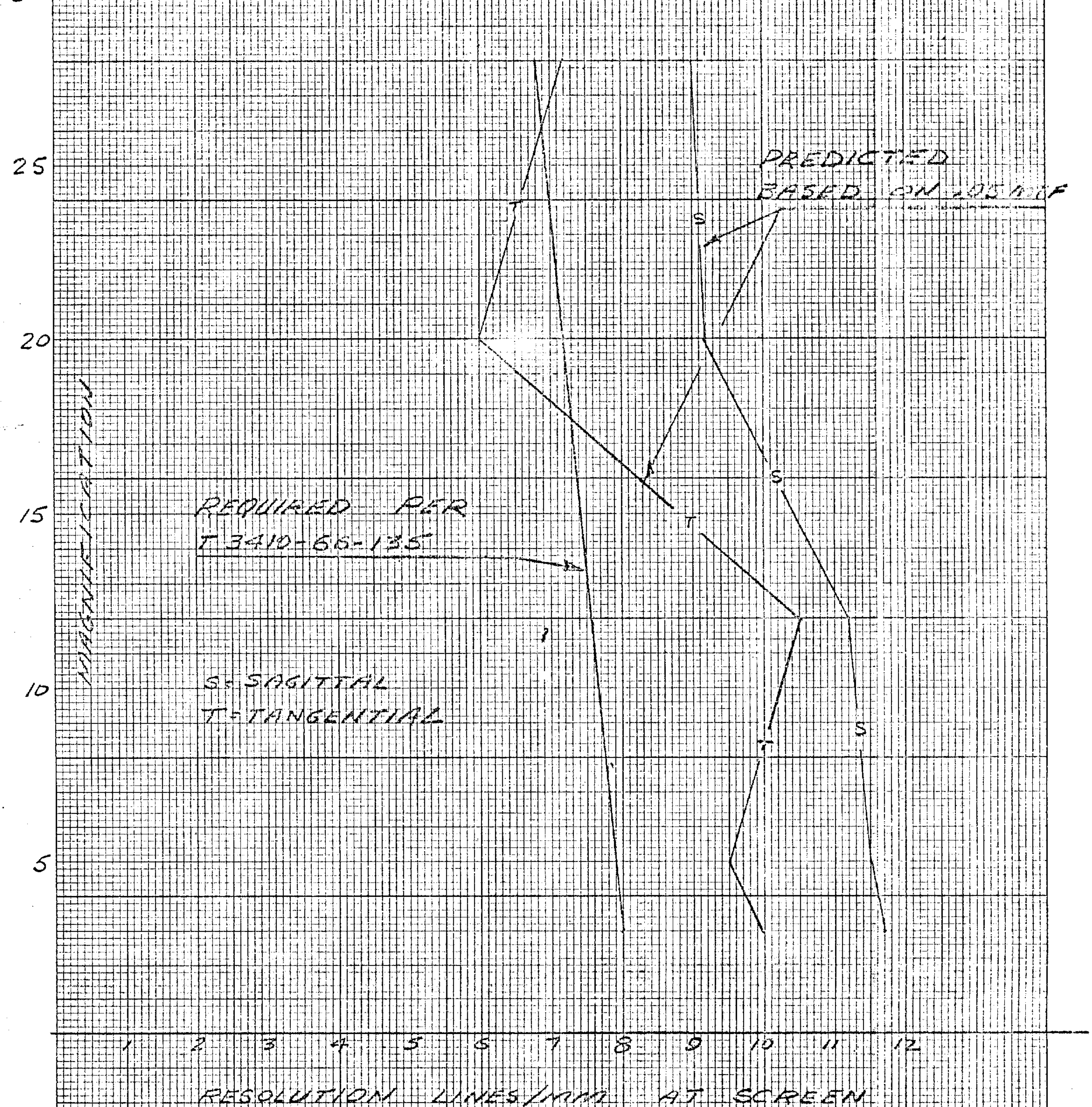

4-11-68

FREDERICK POST COMPANY
301TR20 CROSS SECTION 20 X 20 PER INCH

NSS 3-30 SCALED 1.7X
28X

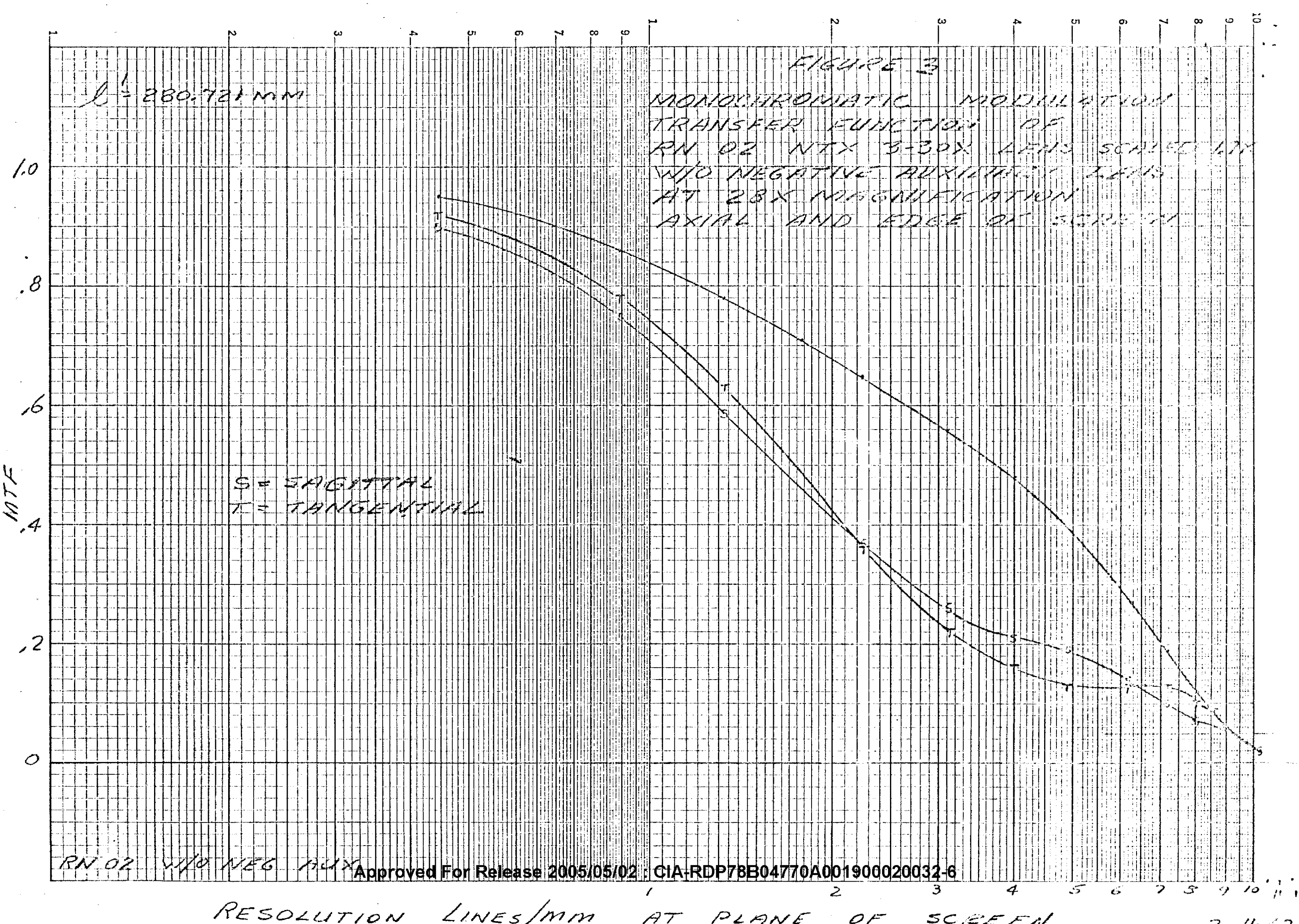

K+E SEMI-LOGARITHMIC 46 4973
2 CYCLES X 70 DIVISIONS MADE IN U.S.A.

NSS 3-30 SCALED 1.7X

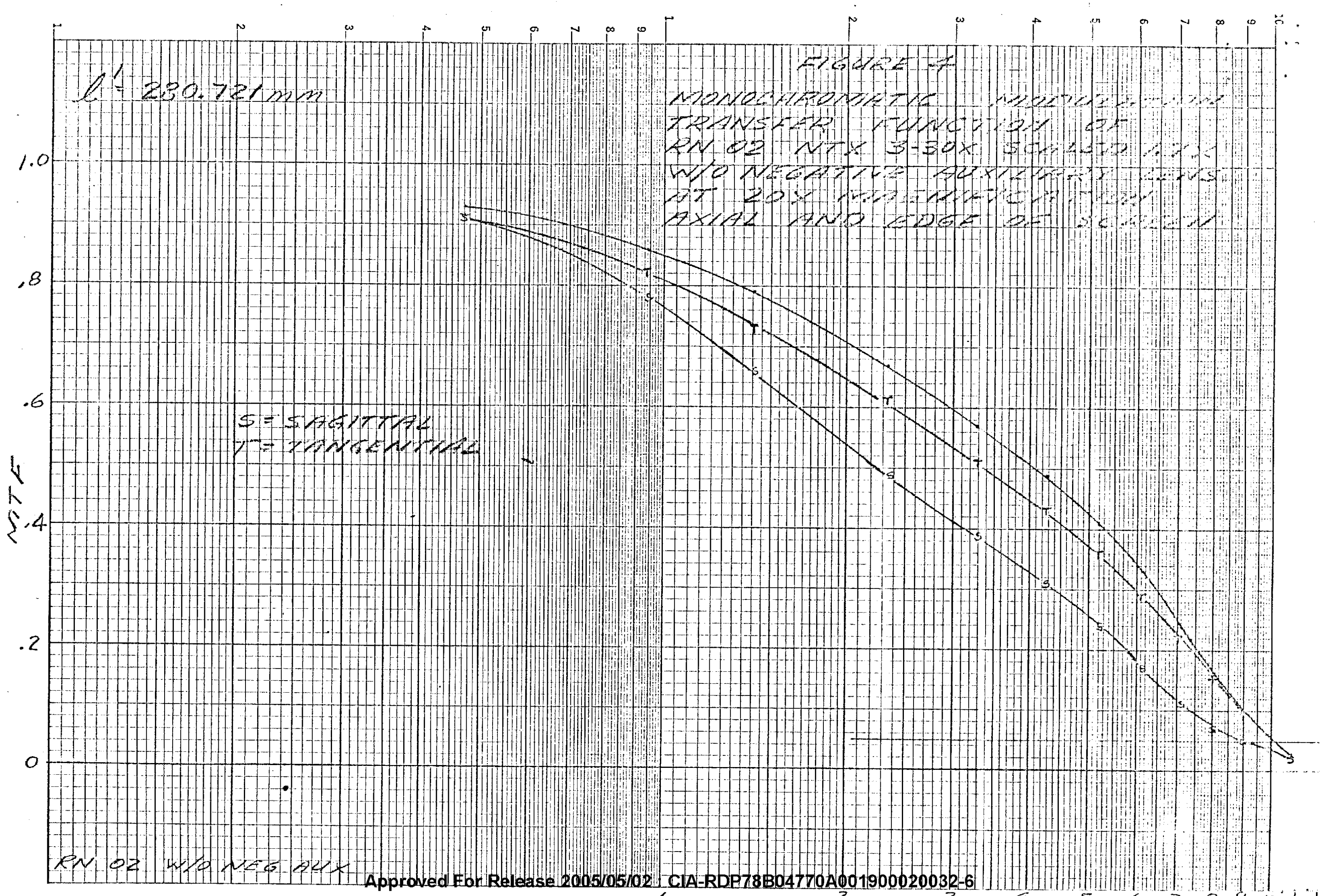

Approved For Release 2005/05/02 : CIA-RDP78B04770A001900020032-6

RESOLUTION LINES/mm AT PLANE OF SCREEN

NSS 3-30 SCALED 1.7x
12X

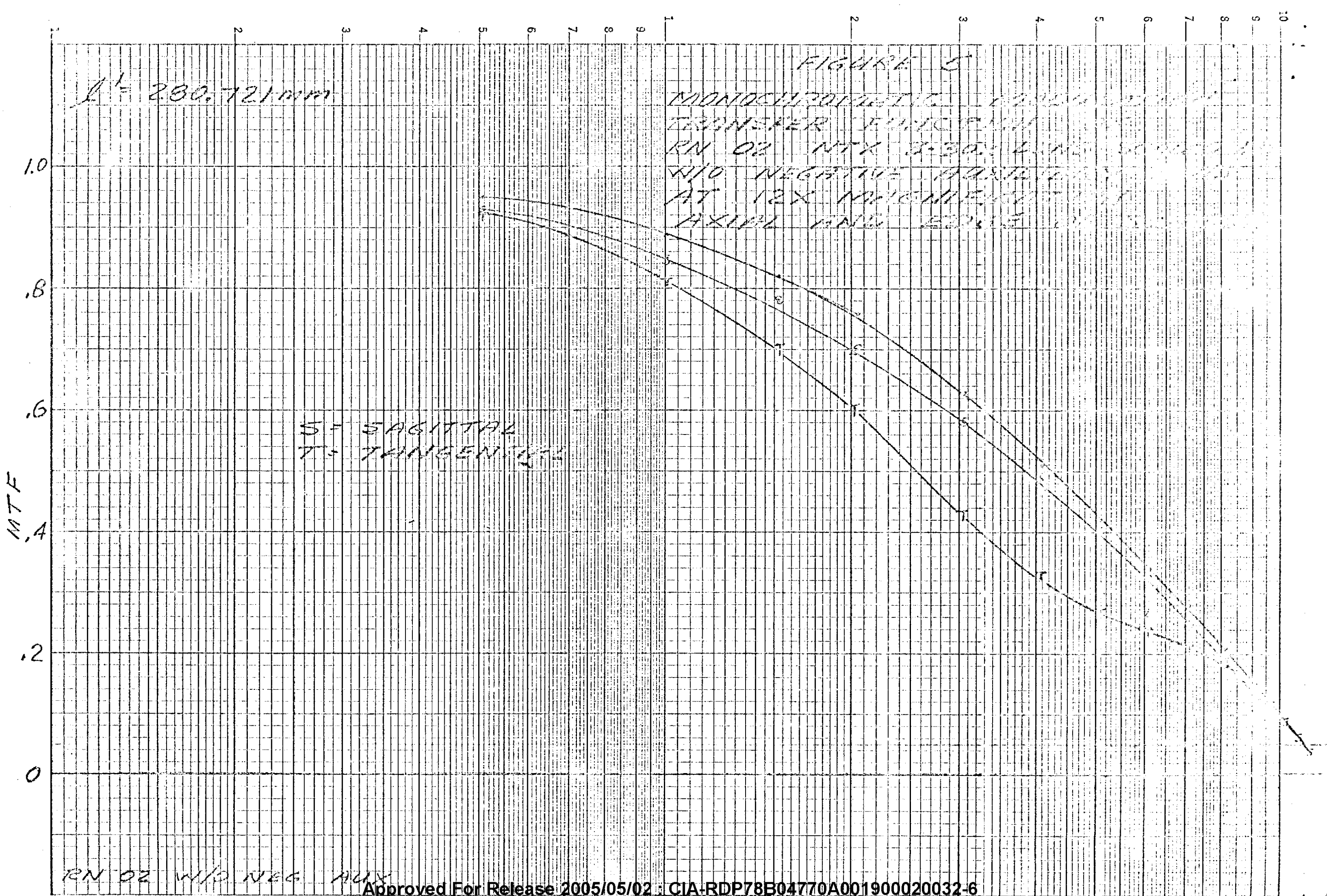

Approved For Release 2005/05/02 : CIA-RDP78B04770A001900020032-6

RESOLUTION LINES/MM AT PLANE OF SCREEN

K+E SEMI-LOGARITHMIC 46 4973
2 CYCLES X 70 DIVISIONS MADE IN U.S.A.

NSS 3-30 SCALED 1.7X

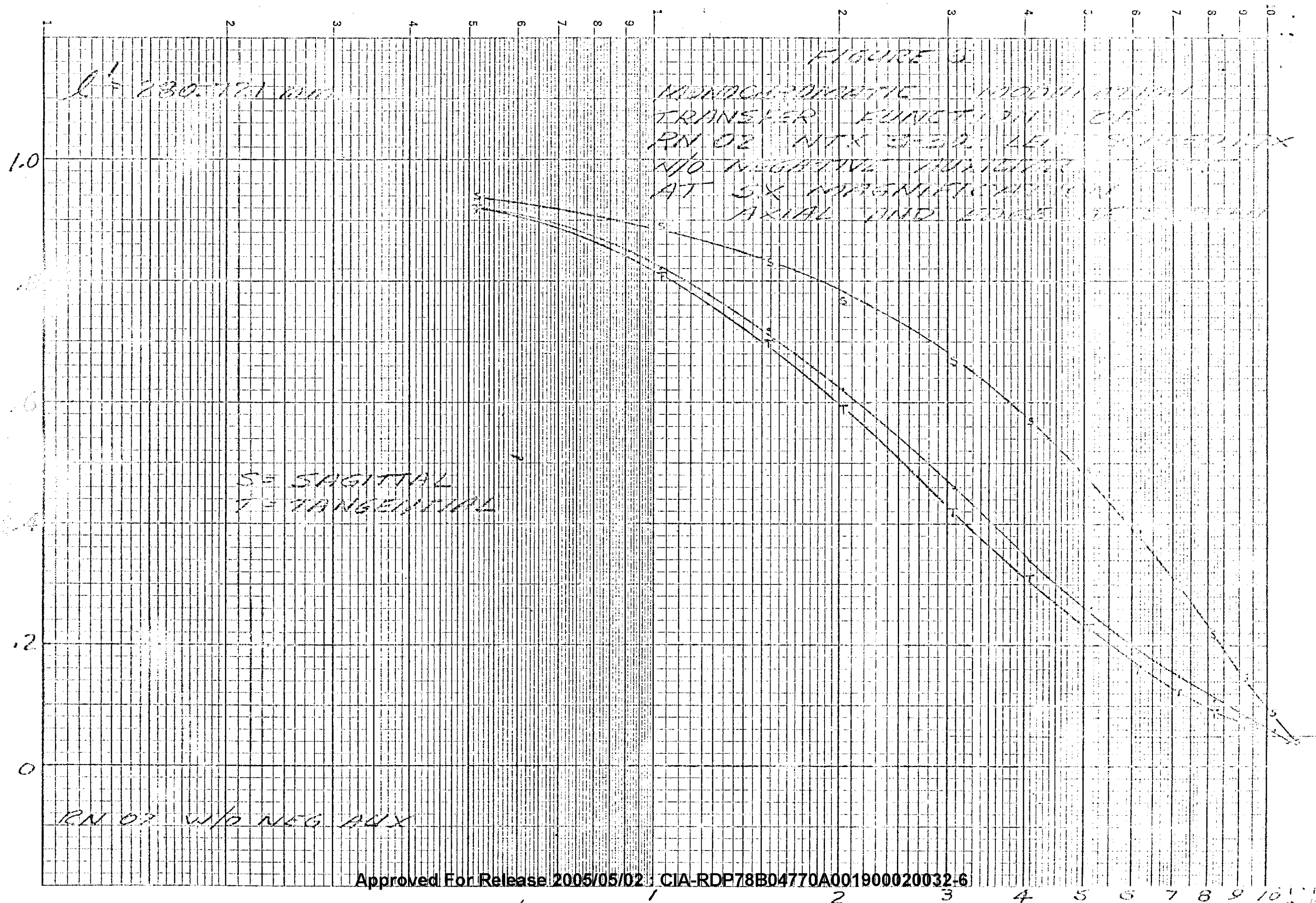

RESOLUTION LINES/MM AT PLANE OF SCREEN

K&E SEMI-LOGARITHMIC 46 4973
2 CYCLES X 70 DIVISIONS MADE IN U.S.A.

NSS 3-30 SCALED 1.7x

3X

Approved For Release 2005/05/02 : CIA-RDP78B04770A001900020032-6

RESOLUTION LINES/MM AT PLANE OF SCREEN 3-16-6

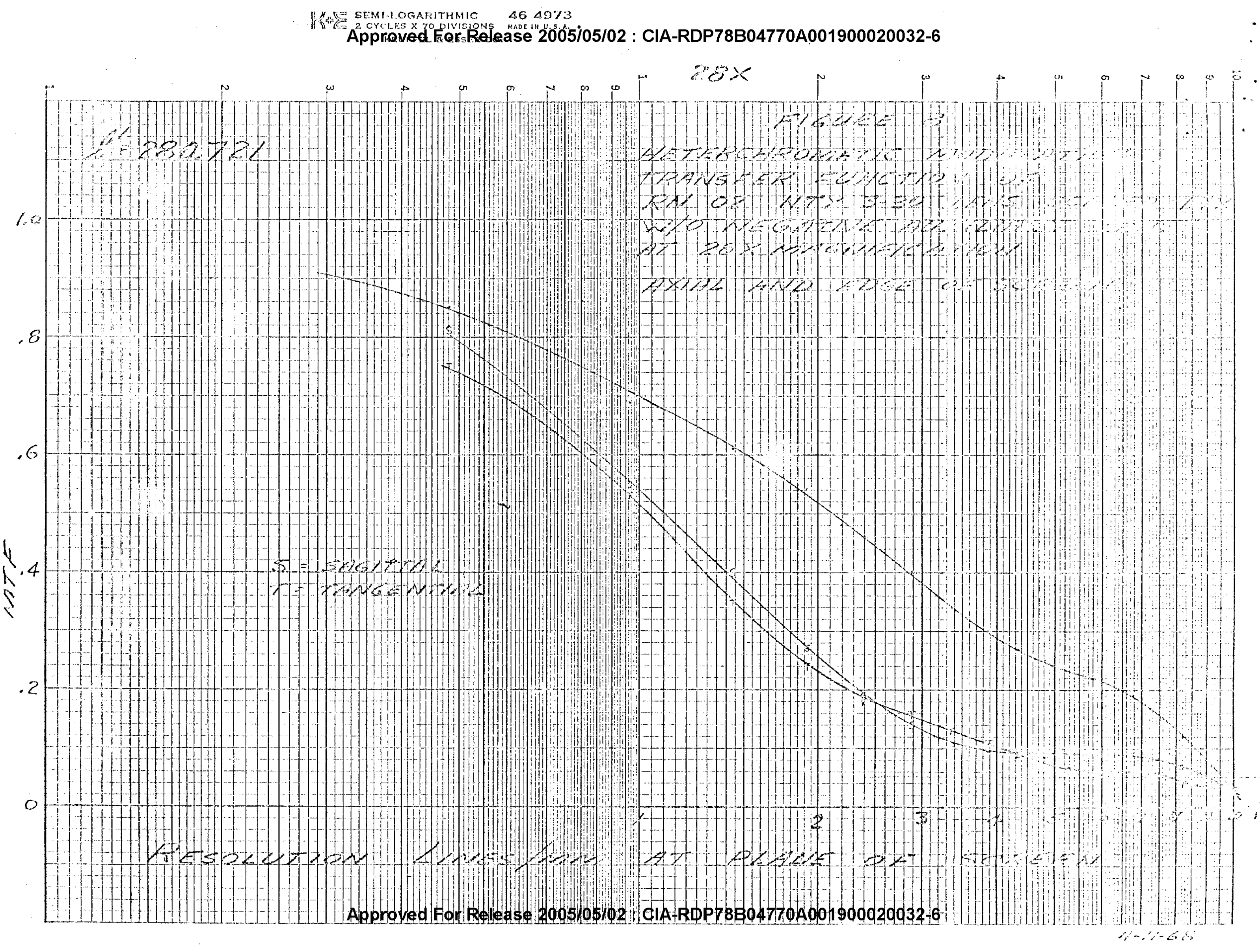
K+E SEMI-LOGARITHMIC 46 4973
2 CYCLES X 70 DIVISIONS MADE IN U.S.A.
28X
FIGURE 8
S = SAGITTAL
T = TANGENTIAL
MTF
RESOLUTION LINES/MM AT PLANE OF

K+E SEMI-LOGARITHMIC 46 4973
2 CYCLES X 70 DIVISIONS MADE IN U.S.A.

20X

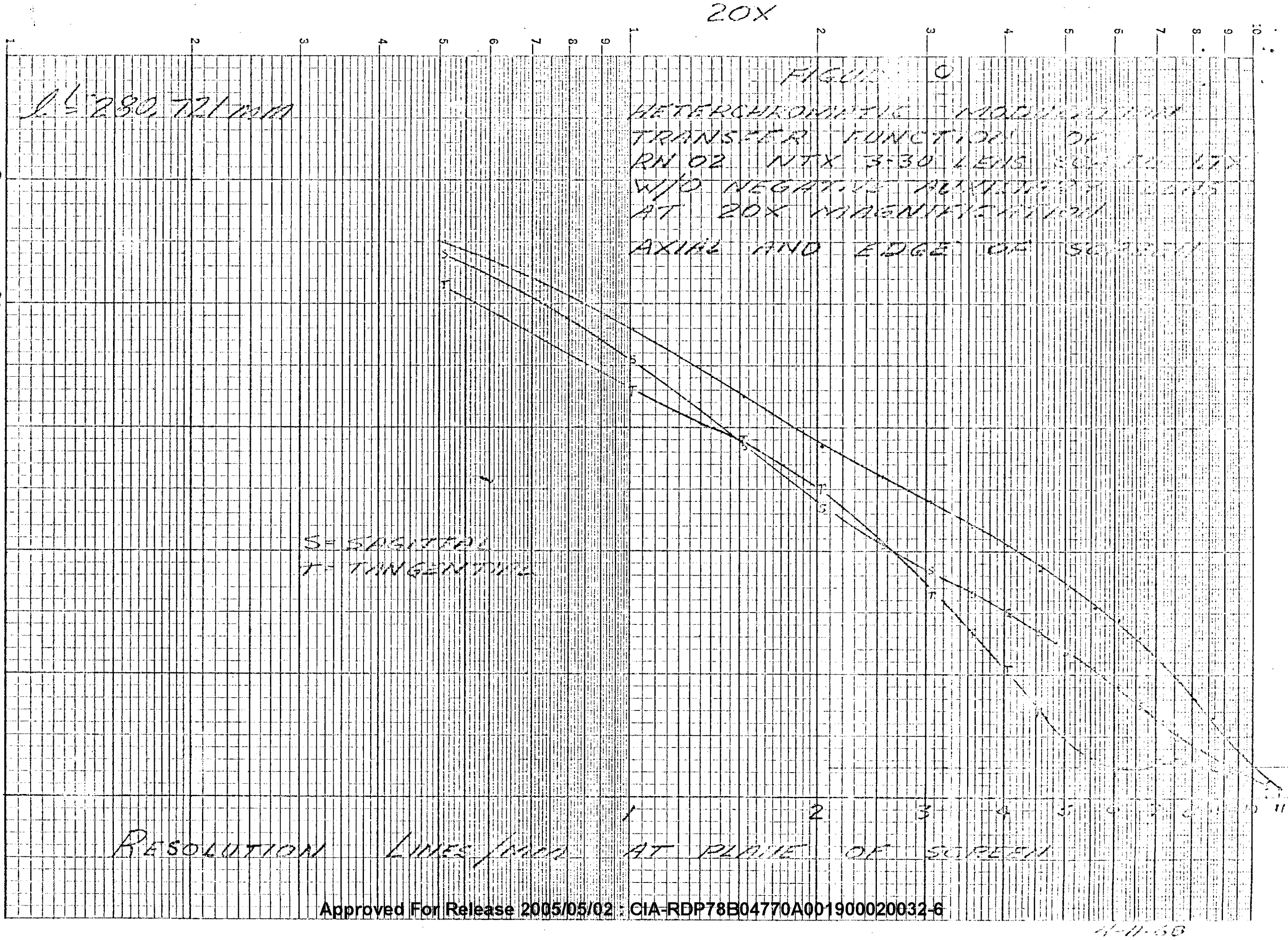

Approved For Release 2005/05/02 : CIA-RDP78B04770A001900020032-6

4-11-68

K+E SEMI-LOGARITHMIC 46 4973
2 CYCLES X 70 DIVISIONS MADE IN U.S.A.

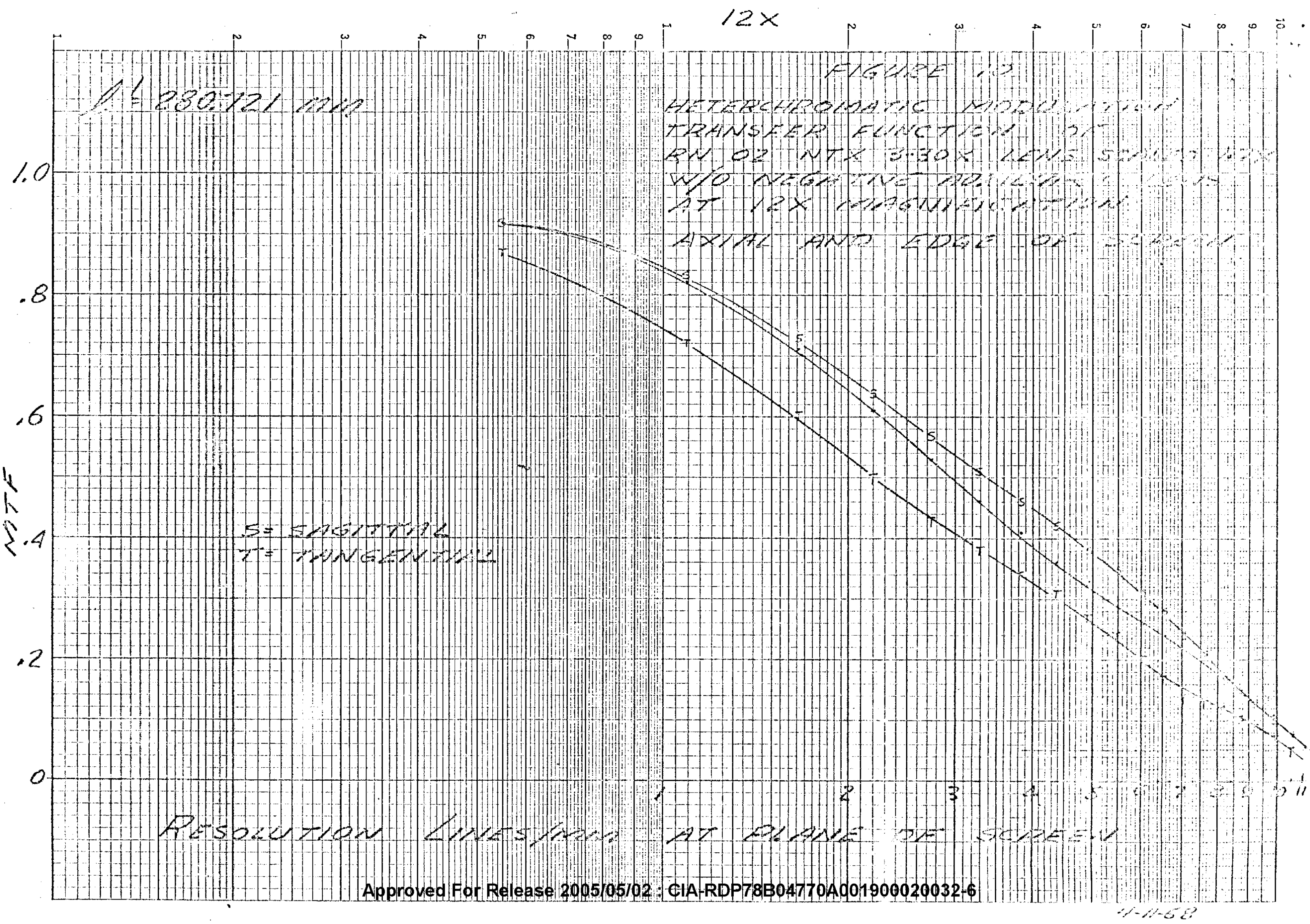

Approved For Release 2005/05/02 : CIA-RDP78B04770A001900020032-6

4-11-68

K&E SEMI-LOGARITHMIC 46 4973
2 CYCLES X 70 DIVISIONS MADE IN U.S.A.

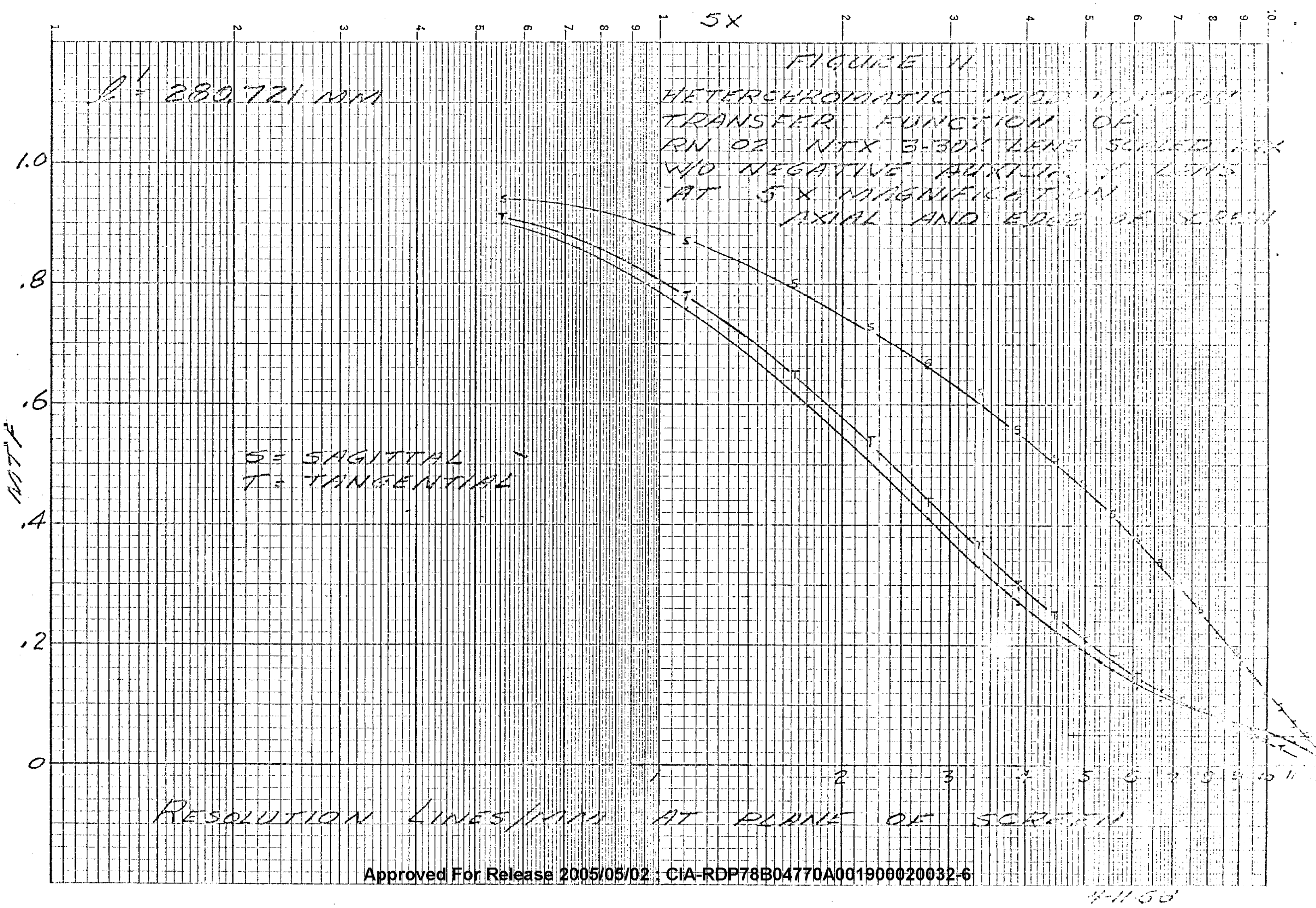

4-11-68

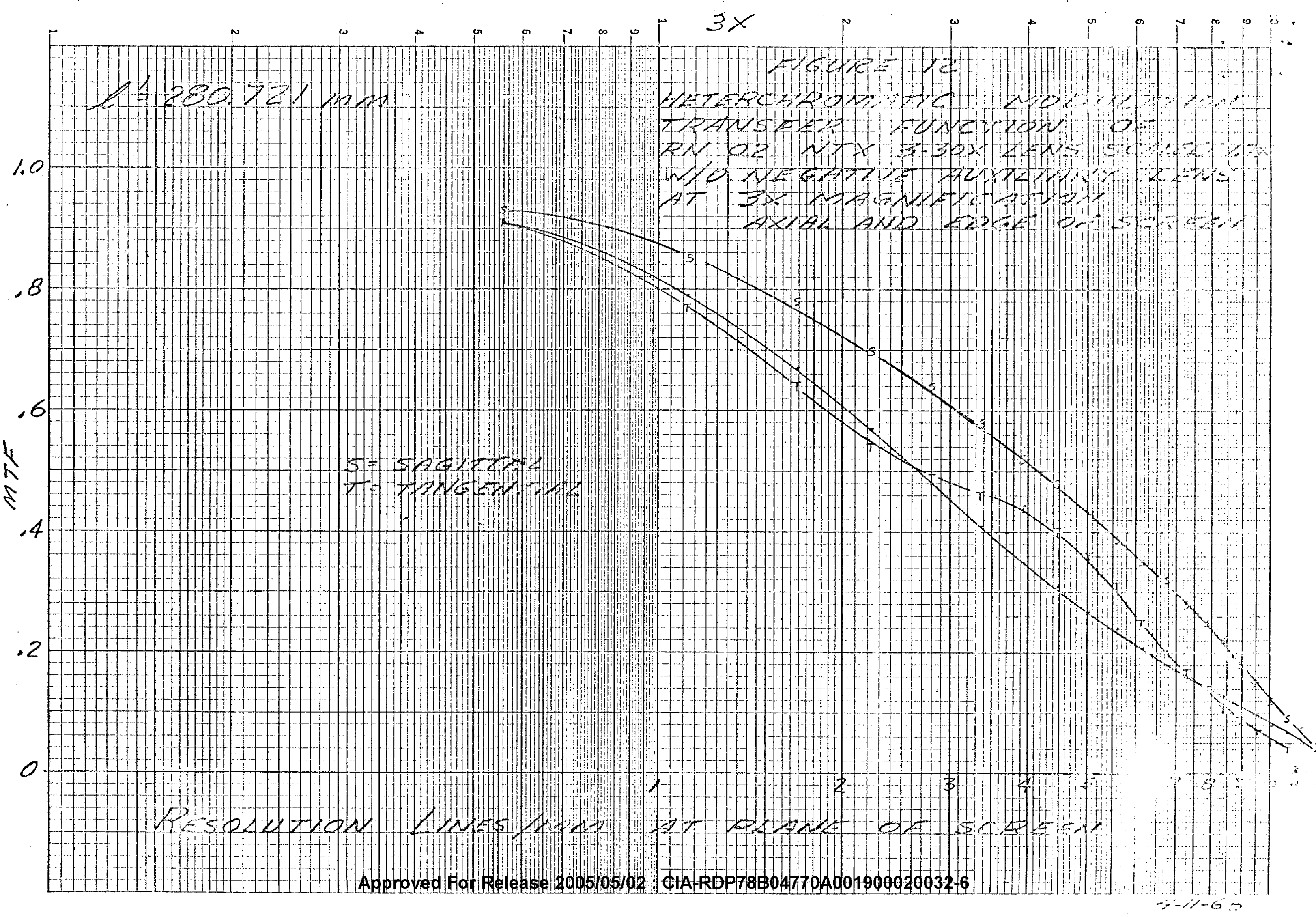

Approved For Release 2005/05/02 : CIA-RDP78B04770A001900020032-6

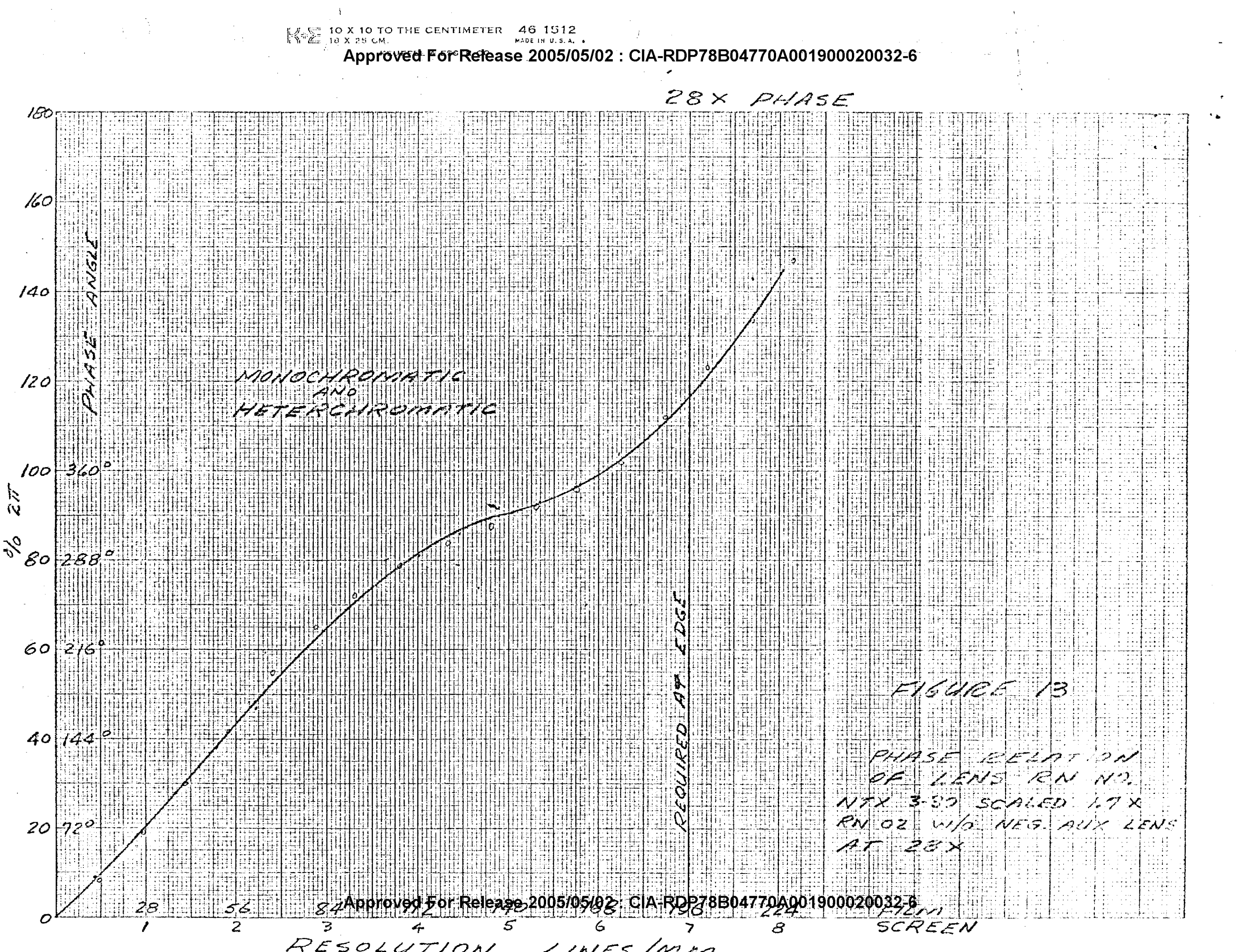
K+E 10 X 10 TO THE CENTIMETER 46 1512
18 X 25 CM.
MADE IN U.S.A.
28X PHASE
PHASE ANGLE
% 2π
MONOCHROMATIC
AND
HETERCHROMATIC
REQUIRED AT EDGE
FIGURE 13
PHASE RELATION
OF LENS RN NO.
NTX 3-37 SCALED 1.7X
RN 02 W/O NEG. AUX LENS
AT 28X
FILM
SCREEN
RESOLUTION LINES/MM

K+E 10 X 10 TO THE CENTIMETER 46 1512
18 X 25 CM.
MADE IN U.S.A.

20X PHASE

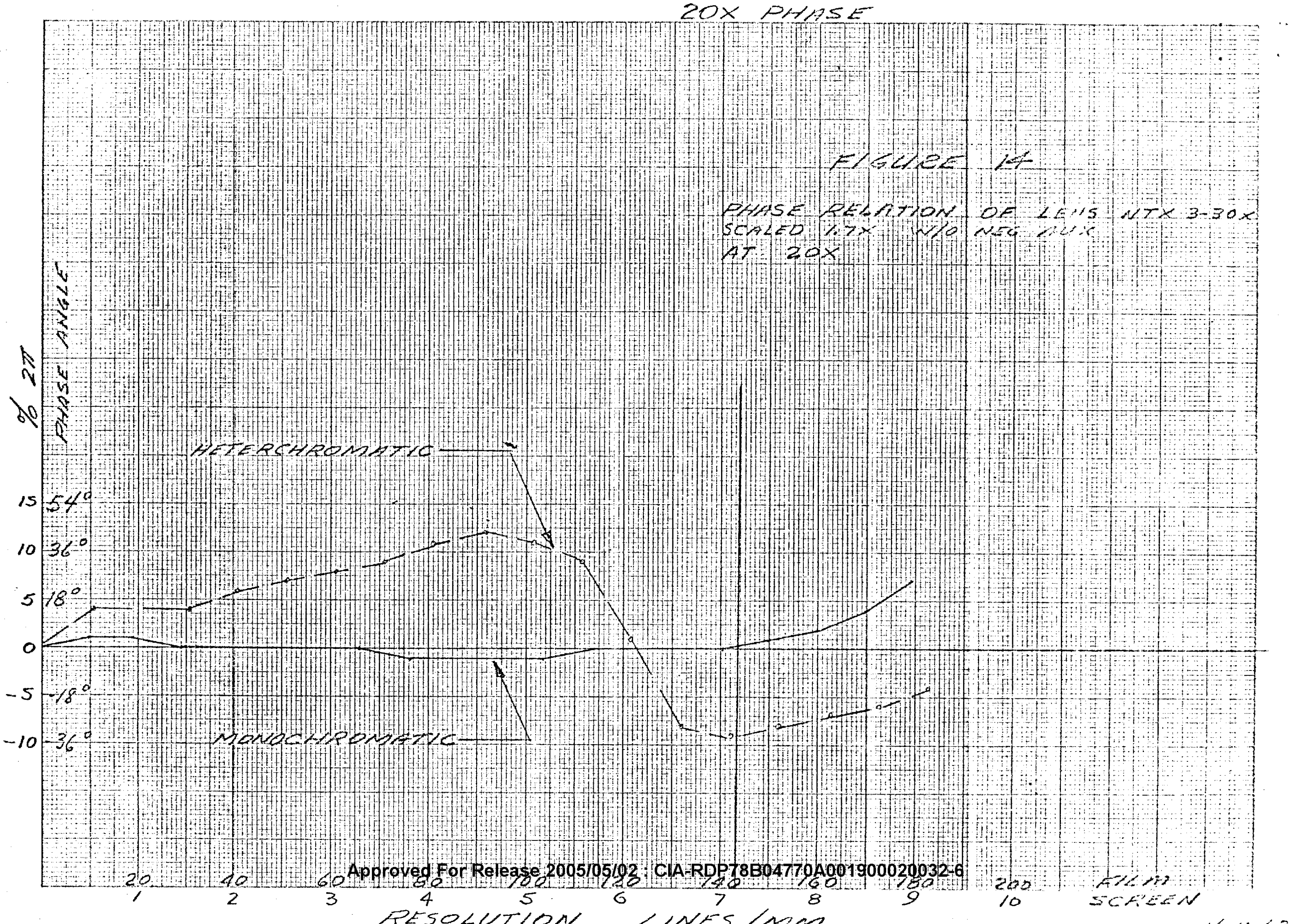

Approved For Release 2005/05/02 : CIA-RDP78B04770A001900020032-6

12X PHASE

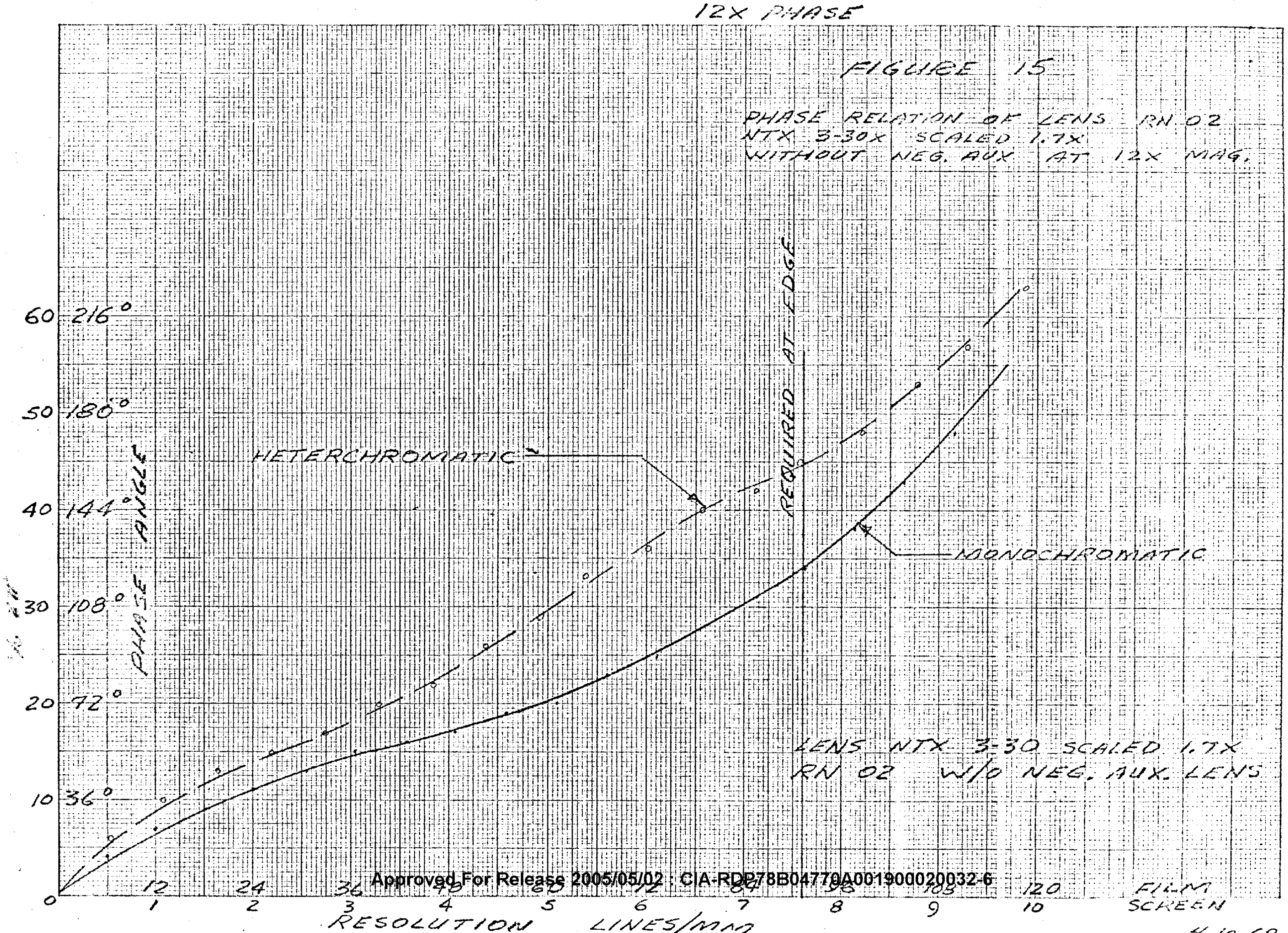
FIGURE 15
PHASE RELATION OF LENS RN 02
NTX 3-30X SCALED 1.7X
WITHOUT NEG. AUX AT 12X MAG.
REQUIRED AT EDGE
HETERCHROMATIC
MONOCHROMATIC
PHASE ANGLE
60 216°
50 180°
40 144°
30 108°
20 72°
10 36°
0
LENS NTX 3-30 SCALED 1.7X
RN 02 W/O NEG. AUX. LENS
12 24 36 48 60 72 84 96 108 120
1 2 3 4 5 6 7 8 9 10
FILM
SCREEN
RESOLUTION LINES/MM

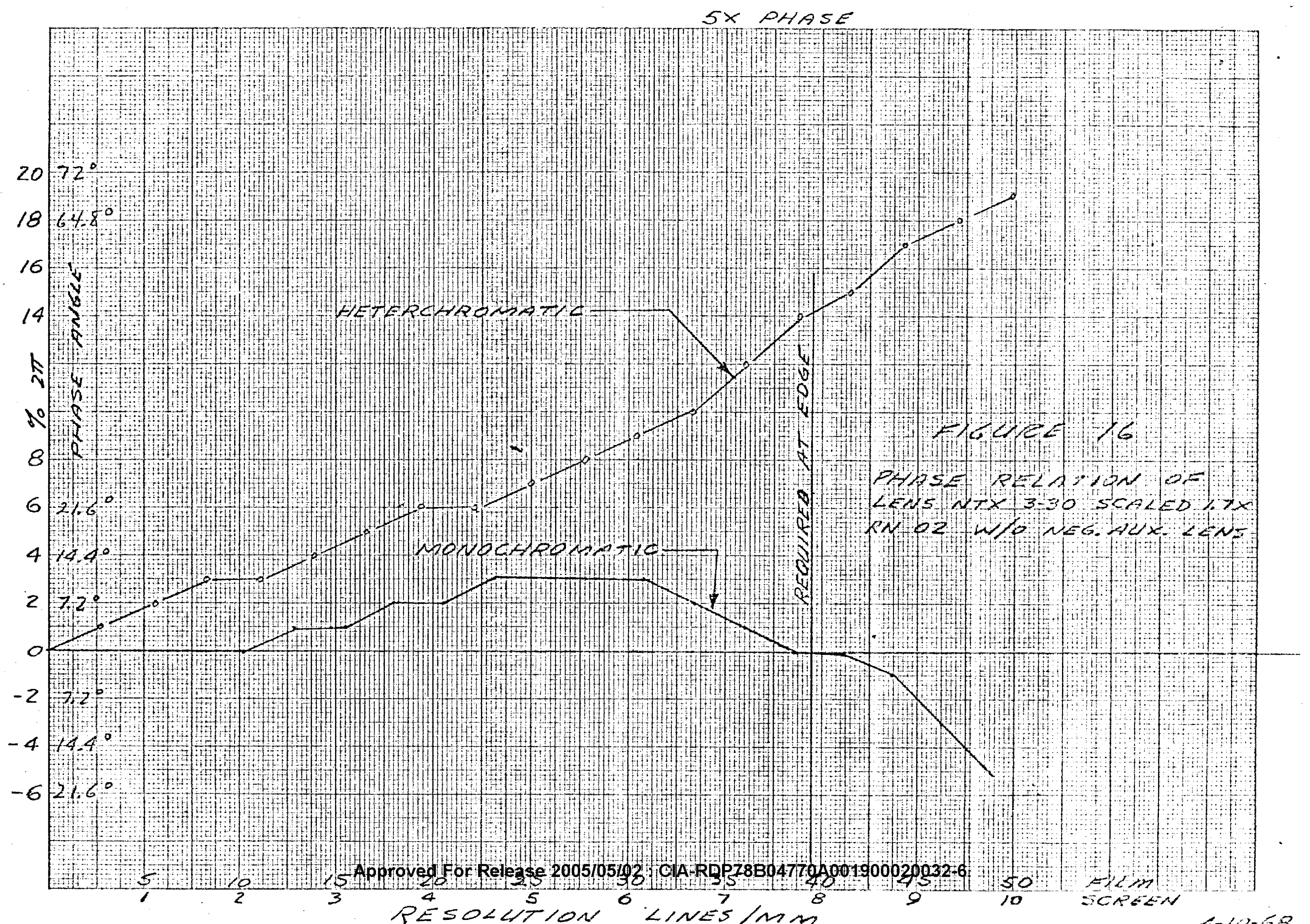
5X PHASE
% 2π PHASE ANGLE
20 72°
18 64.8°
16
14
8
6 21.6°
4 14.4°
2 7.2°
0
-2 7.2°
-4 14.4°
-6 21.6°
HETERCHROMATIC
MONOCHROMATIC
REQUIRED AT EDGE
FIGURE 16
PHASE RELATION OF
LENS NTX 3-30 SCALED 1.7X
RN-02 W/O NEG. AUX. LENS
5 10 15 20 25 30 35 40 45 50 FILM
1 2 3 4 5 6 7 8 9 10 SCREEN
RESOLUTION LINES/MM

3X PHASE

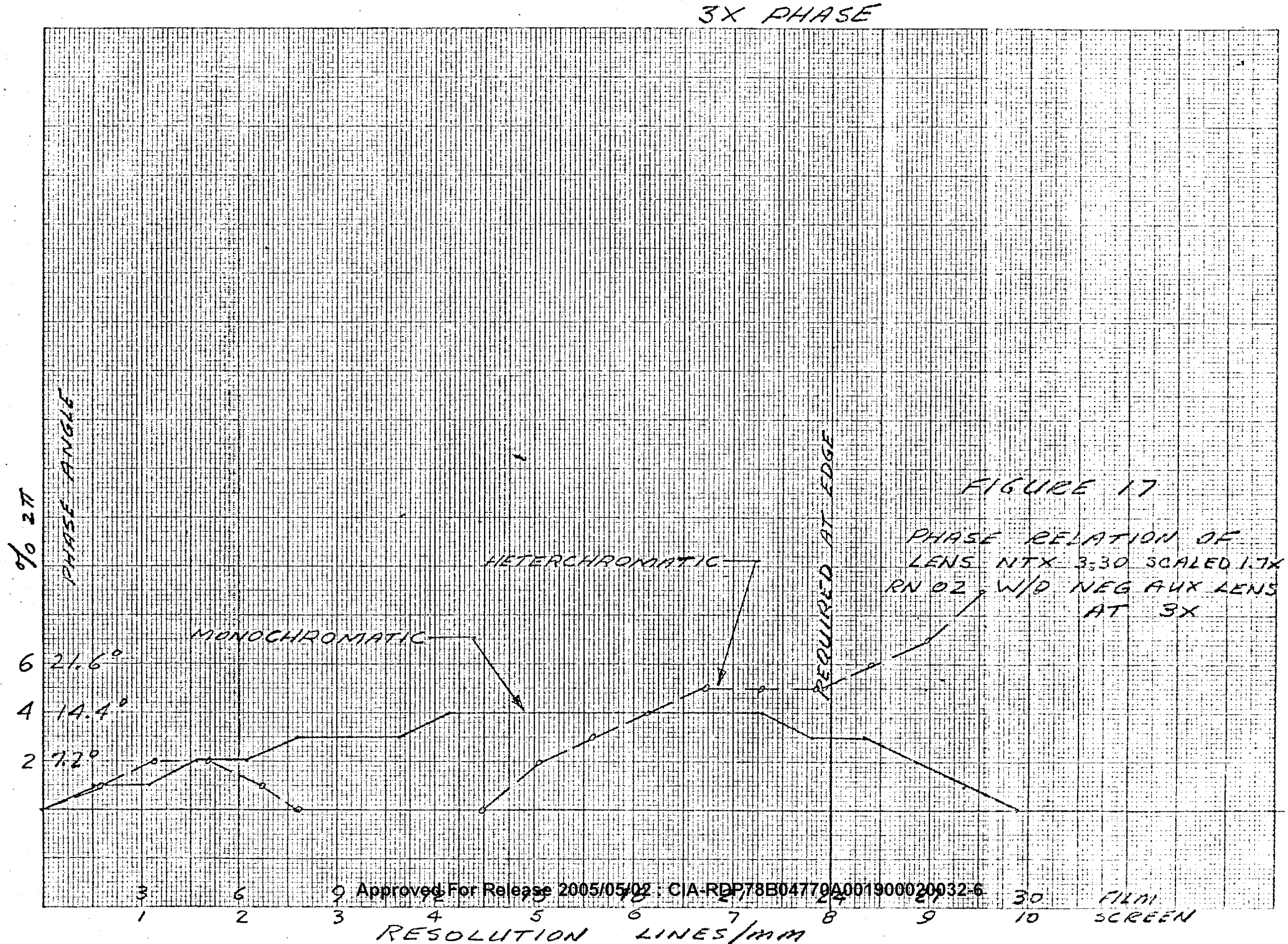

FIGURE 17
PHASE RELATION OF LENS NTX 3:30 SCALED 1.7X RN 02 W/O NEG AUX LENS AT 3X

ZOOM LENS PRESCRIPTION
FOR RUN 02 OF NTX 3-30X
LENS SCALED 1.7X (AT 28X SETTING)

RADIUS MM	THICKNESS MM	INDEX n_e	$n_F - n_C$
.00	1103.35	1.00000	.00000
2577.11	18.58	1.61127	.01033
- 1666.84	.84	1.00000	.00000
362.65	34.97	1.61127	.01033
- 213.20	8.64	1.72734	.02467
- 758.13	20.33	1.00000	.00000
- 144.85	7.12	1.69976	.01240
- 800.08	7.25	1.00000	.00000
1132.63	12.21	1.72734	.02467
- 149.15	6.36	1.00000	.00000
- 252.17	7.12	1.69976	.01240
173.61	217.03	1.00000	.00000
- 353.11	8.11	1.72734	.02467
651.67	3.95	1.00000	.00000
414.63	12.72	1.57487	.00995
- 179.97	5.50	1.00000	.00000
306.25	12.72	1.57487	.00995
- 204.68	3.95	1.00000	.00000
- 193.98	8.11	1.72734	.02464
- 486.86	26.76	1.00000	.00000
- 673.28	7.12	1.69976	.01240
193.11	6.36	1.00000	.00000
132.50	12.21	1.72734	.02467
2472.50	7.25	1.00000	.00000
- 329.27	7.12	1.69976	.01240
188.41	225.80	1.00000	.00000
1029.34	8.64	1.72734	.02467
220.75	34.97	1.61127	.01033
- 384.89	.84	1.00000	.00000
1484.45	18.58	1.61127	.01033
- 1179.61	45.62	1.00000	.00000
257.86	32.36	1.61127	.01033
776.68	81.23	1.00000	.00000
- 1071.23	8.29	1.62408	.01705
259.57	87.87	1.00000	.00000
1225.28	33.98	1.61127	.01033
- 333.96	280.80	1.00000	.00000

MOVING SPACES

FIGURE 18

GRAPH OF PREDICTED SCREEN BRIGHTNESS (AXIAL) AT THE VARIOUS MAGNIFICATIONS WITH DIFFERENT DENSITY FILTERS NOD 110

SOURCE BRIGHTNESS = 13X10⁶ CDLS/FT²

SCREEN GAIN (∠S 60) = 2

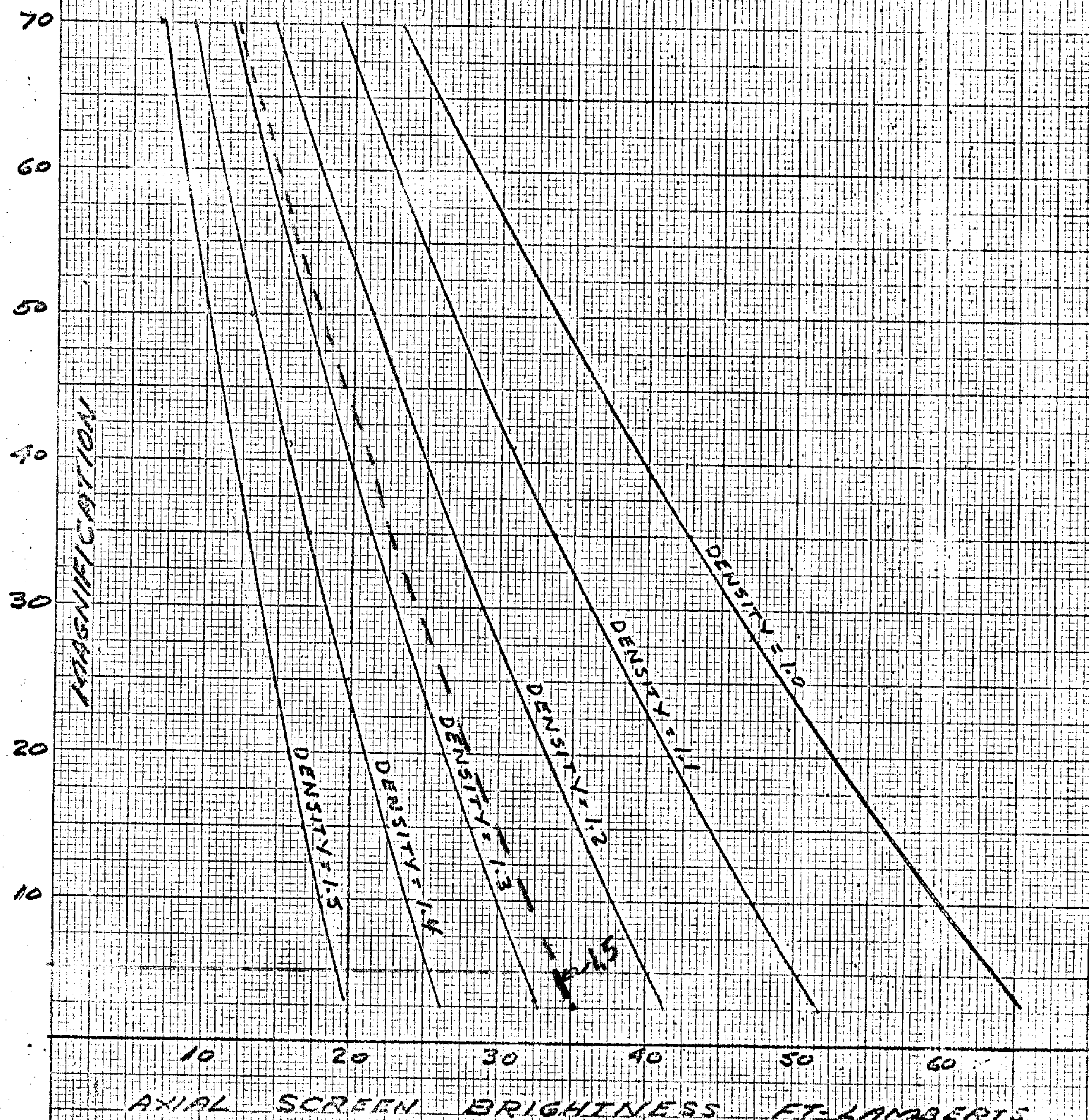

10 X 10 TO THE 1/2 INCH 359-11G
KEUFFEL & ESSER CO. MADE IN U.S.A.

SOURCE BRIGHTNESS REQUIRED TO PROVIDE 20 FT-LAMBERTS SCREEN BRIGHTNESS AT THE VARIOUS MAGNIFICATIONS NOD 110 (INCLUDES 1.5 NEUTRAL DENSITY FILTER)

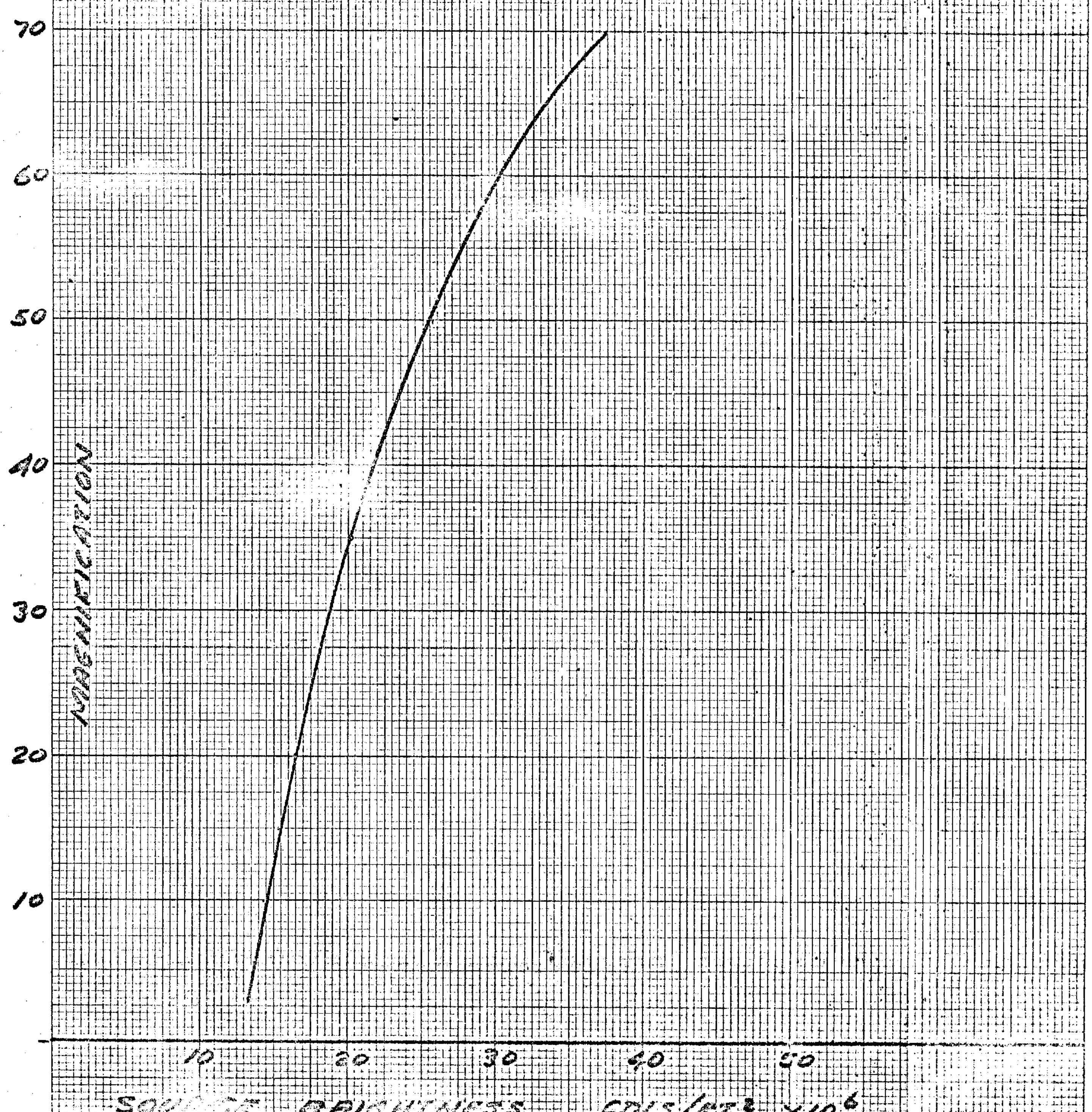

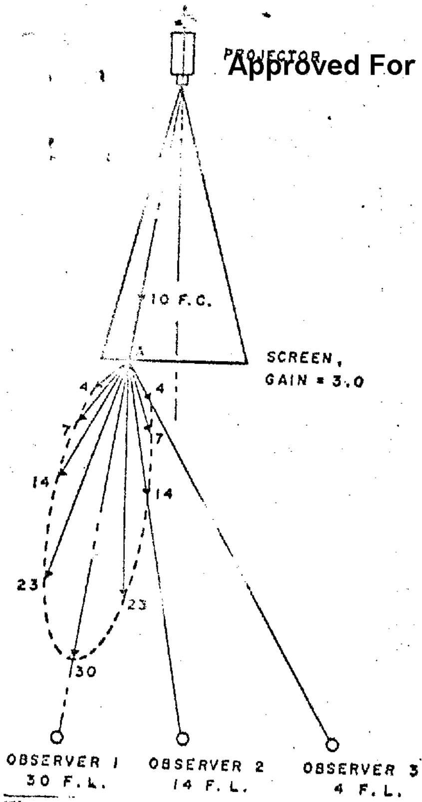

Fig. 1. Brightness distribution lobe for screen gain of 3.0.

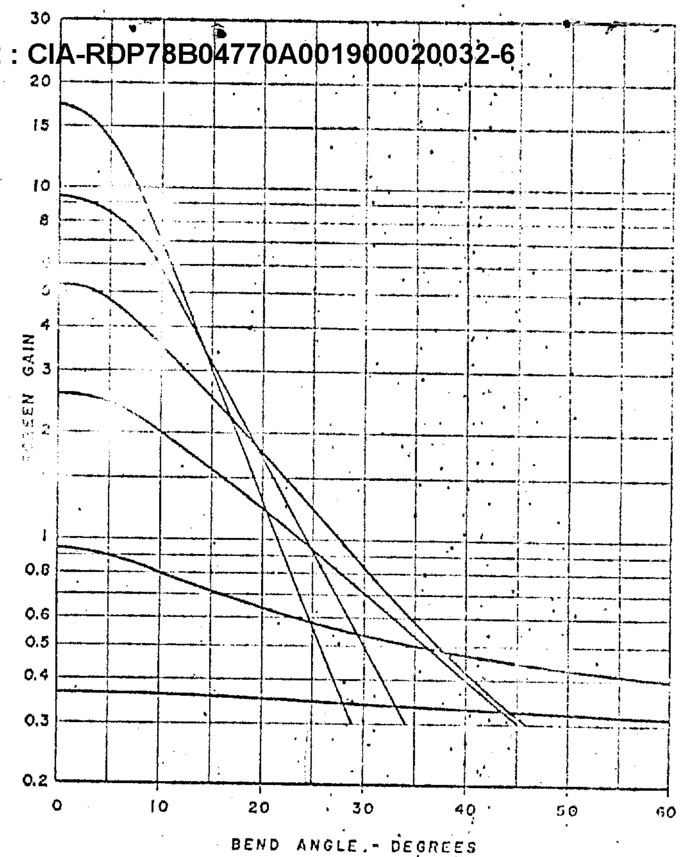

Fig. 2. Screen gain at various bend angles for several typical screens.

The behavior of a typical rear projection screen is illustrated in Fig. 1. This figure shows a projector, a screen and three observers. A light ray is shown incident upon the screen at point *A*. Continuation of the line representing the incident ray establishes the "principal axis" of the diffusion lobe. The incident light ray, partially diffused by the screen, spreads symmetrically about the principal axis. The incident light was arbitrarily adjusted to 10 ft-c to obtain the measured data in Fig. 1. The observed brightness of point *A* from any direction is indicated by the length of the arrow. Arrows are shown 10° apart. Observer 1, located on the principal axis, will perceive point *A* to have a brightness of 30 ft-L. Peak screen gain is therefore 3.0, the ratio of footlamberts to incident foot-candles. The brightness for observers 2 and 3 will be less than the peak since they are located off the principal axis. Any light reaching observers 2 and 3 must deviate from the principal axis by an angle determined by the position of the observer with respect to the principal axis. This angle is the "bend angle." The bend angle, therefore, depends upon the position of the observer with respect to the principal axis in question. The diffusion characteristics of several screens are shown in Fig. 2. Gain is plotted as a function of bend angle. The curves were obtained by measurement of actual practical screens.

Transmission, Diffusion and Reflection

One of the objectives in screen manufacturing is to select materials with a good light transmission capability to hold absorption losses to a minimum. Transmission has been used for many years to specify rear-projection screens; however, it is not a good index of performance, nor does it provide reliable information regarding the gain of the screen or its brightness distribution.

One method of manufacturing a rear-projection screen consists of spraying a clear ethyl cellulose or similar material onto a flat backing until the thickness is adequate for mechanical strength. After the coating has set, it is pealed off the backing, trimmed to size, and reinforced at the edges with tape and grommets. While the plastic material is clear, the two surfaces are rough (as a glass which is ground on both faces). The roughened surfaces provide a moderate diffusion of light with high transmission (85 – 90%). The degree of diffusion produced by this technique is limited, and for most purposes greater diffusion is required. The addition of white or other diffusing pigment to the liquid ethyl cellulose results in greater diffusion of the light, and also increases reflection.

It is important to note that diffusion provided by a clear plastic material, with rough surfaces, is caused by a change of direction of a light ray at each surface due to the relative incident and exit angles, and the refraction index of the plastic. There are little or no internal reflections. This type of screen is, therefore, non-depolarizing and can be used with polarized light, as in three-dimensional projection. The addition of white pigment to increase diffusion causes depolarization and makes the screen impossible to use with polarized light.

As more pigment is used, the reflection factor and diffusion are increased and the transmission is correspondingly reduced. At one point, reflection and transmission are equal and the screen may be viewed equally well from either side. Further addition of white pigment results in a white screen for front projection.

Another technique of screen manufacture consists of coating one side of a clear substrate, such as glass, Plexiglas, or flexible plastic, with a suitable diffusing layer. The diffusing layer is a pigmented carrier consisting of resins and solvent. The pigment may be any finely ground material having a different (generally higher) index of refraction than the carrier. High-index ground glass, titanium dioxide and similar materials have been used. The technique of coating only one side of a transparent backing is particularly effective in obtaining the fine grain and high resolution required for very small screens.

Figure of Merit

The wide variety of materials and diffusion techniques employed in screen manufacture produces screens of varying quality. The question arises, "How can the quality of one screen be compared to the quality of another?" Since the primary purpose of a rear-projection screen is to cause diffusion with minimum light loss, the bend angle that can be attained before the gain has fallen to one-half its peak constitutes a measure of quality, or "figure of merit."

Approved For Release 2005/05/02 : CIA-RDP78B04770A001900020032-6

FILE
Drawing Section
02157
955

Optically Compensated Zoom Lens

25X1

Investigation of the thin lens theory of zoom lenses results in a general statement concerning conjugate points, a simple proof of the maximum number of crossing points, and an algorithm for computing component focal lengths of a five-component symmetrical zoom lens. The three-component optically compensated zoom lens is discussed in detail. Results of applying the algorithm are given. A prototype of the five-component zoom lens has been built and is briefly discussed.

INTRODUCTION

The thin lens treatment of the optically compensated zoom lens will be introduced by considering systems symmetrical about the mid-travel position, that is, systems of magnification range M bounded at $M^{-1/2}$ and $M^{1/2}$. Further, only components participating in the zoom effect are considered, since components redundant to the effect transform fixed conjugates and may be separately treated by conventional means. Such exclusion leads additionally to a useful clarity of nomenclature and predictability of behavior.

The simplest zoom lens consists of a single component operating as shown in figure 1A. This system has two crossings; that is, the distance from object to image is the same at two magnifications. Also, there are two finite variable air spaces. Ignoring redundant components, it is clear that the next system in order of complexity (figure 1B) contains three components and four finite variable air spaces. In general, any zoom system as defined will have an odd number of components and even number of variable air spaces.

NUMBER OF CROSSING POINTS

It is next of interest to determine the maximum number of crossings possible, to extend consideration to the non-symmetrical case including infinite conjugates, and to include the case of linear compensation. The matrix method for paraxial rays is useful for this purpose.

The three-component zoom lens can be represented as in figure 2. The matrix method shows clearly that the number of possible crossing points is directly associated with the number of variable air spaces. The matrix for this system can be expressed as follows:

$$\begin{pmatrix} 1 & -t_0 \\ 0 & 1 \end{pmatrix} \begin{pmatrix} 1 & 0 \\ A_1 & 1 \end{pmatrix} \begin{pmatrix} 1 & -t_1 \\ 0 & 1 \end{pmatrix} \begin{pmatrix} 1 & 0 \\ A_2 & 1 \end{pmatrix} \begin{pmatrix} 1 & -t_2 \\ 0 & 1 \end{pmatrix} \begin{pmatrix} 1 & 0 \\ A_3 & 1 \end{pmatrix} \begin{pmatrix} 1 & -t_3 \\ 0 & 1 \end{pmatrix} = \begin{pmatrix} B & D \\ A & C \end{pmatrix}$$

where
$$A_1 = 1/f_1$$
$$A_2 = 1/f_2$$
$$A_3 = 1/f_3$$

When t_0 and t_3 are conjugate distances, then D in the matrix is equal to zero. Consider a movement of lenses f_1 and f_3 of an amount Δ. The spacings become $t_0 + \Delta$, $t_1 - \Delta$, $t_2 + \Delta$, and $t_3 - \Delta$. For how many values of Δ may $D = 0$? The algebra is greatly simplified if only the maximum power of Δ is retained in the matrix multiplication. Then the spacing matrix $\begin{pmatrix} 1 & -t + \Delta \\ 0 & 1 \end{pmatrix}$ can be written as $\begin{pmatrix} 1 & \Delta \\ 0 & 1 \end{pmatrix}$. The power matrix $\begin{pmatrix} 1 & 0 \\ A & 1 \end{pmatrix}$ can be written as

$\begin{pmatrix} 1 & 0 \\ 1 & 1 \end{pmatrix}$ when the powers of Δ are retained.[1] In multiplication only the maximum power of Δ is to be retained,

$$\text{so } \begin{pmatrix} 1 & \Delta \\ 0 & 1 \end{pmatrix}\begin{pmatrix} 1 & 0 \\ 1 & 1 \end{pmatrix} = \begin{pmatrix} 1+\Delta & \Delta \\ 1 & 1 \end{pmatrix} \longrightarrow \begin{pmatrix} \Delta & \Delta \\ 1 & 1 \end{pmatrix}$$

The three-component zoom then is represented by

$$\begin{pmatrix} 1 & \Delta \\ 0 & 1 \end{pmatrix}\begin{pmatrix} 1 & 0 \\ 1 & 1 \end{pmatrix}\begin{pmatrix} 1 & \Delta \\ 0 & 1 \end{pmatrix}\begin{pmatrix} 1 & 0 \\ 1 & 1 \end{pmatrix}\begin{pmatrix} 1 & \Delta \\ 0 & 1 \end{pmatrix}\begin{pmatrix} 1 & 0 \\ 1 & 1 \end{pmatrix}\begin{pmatrix} 1 & \Delta \\ 0 & 1 \end{pmatrix} \longrightarrow \begin{pmatrix} \Delta^3 & \Delta^4 \\ \Delta^2 & \Delta^3 \end{pmatrix}$$

The maximum power of Δ to appear in D is four, so there can be a maximum of four crossing points. Each factor Δ which appears in D arises from a variable air space. A five-component zoom lens will have two more variable air spaces and thus two more possible crossing points. The matrix method yields a similar result:

$$\begin{pmatrix} \Delta^3 & \Delta^4 \\ \Delta^2 & \Delta^3 \end{pmatrix}\begin{pmatrix} 1 & 0 \\ 1 & 1 \end{pmatrix}\begin{pmatrix} 1 & \Delta \\ 0 & 1 \end{pmatrix}\begin{pmatrix} 1 & 0 \\ 1 & 1 \end{pmatrix}\begin{pmatrix} 1 & \Delta \\ 0 & 1 \end{pmatrix} \longrightarrow \begin{pmatrix} \Delta^3 & \Delta^4 \\ \Delta^2 & \Delta^3 \end{pmatrix}\begin{pmatrix} \Delta & \Delta^2 \\ \Delta & \Delta^2 \end{pmatrix} \longrightarrow \begin{pmatrix} \Delta^5 & \Delta^6 \\ \Delta^4 & \Delta^5 \end{pmatrix}$$

A three-component zoom lens has only three possible crossing points when the object is at infinity. This comes about since a change in the position of the front component does not change the convergence or divergence of the light striking the component and thus the air space in front of the component is not a variable air space.

A slight extension to the above argument makes it possible to prove that linearly compensated zoom lenses may have the same number of crossing points as finite variable air spaces. The spaces in a three-component linearly compensated zoom lens can be represented as $t_0 + a\,\Delta$, $t_1 + b\,\Delta$, $t_2 + c\,\Delta$, $t_3 + d\,\Delta$; when a, b, c, and d are constants such as $a + b + c + d = 0$.

---

[1] The substitution of 1 for A is justified since we are interested in the highest powers of Δ resulting from multiplication. Multiplying some power of Δ by either 1 or A gives the same result as far as the highest power of Δ is involved.

Approved For Release 2005/05/02 : CIA-RDP78B04770A001900020032-6

In the matrix multiplication, the matrix for the first air space is $\begin{pmatrix} 1 & -t_0 - a\,\Delta \\ 0 & 1 \end{pmatrix}$.

Now if only the powers of Δ are retained, and all nonessential information is dropped, the matrix can be written $\begin{pmatrix} 1 & \Delta \\ 0 & 1 \end{pmatrix}$. This, however, is identical to the first term for the optically compensated lens and the remainder of the proof is identical.

LOCATION OF CONJUGATE POINTS

Another expression necessary to later development is one giving the object distance for a zoom system. Consider an optical system with a reference plane in the object space and a reference plane in the image space. The paraxial matrix is $\begin{pmatrix} B & D \\ A & C \end{pmatrix}$. If the light from the object is striking the first reference plane with a divergence of A_0, we can then write

$$\begin{pmatrix} 1 & 0 \\ A_0 & 1 \end{pmatrix} \begin{pmatrix} B & D \\ A & C \end{pmatrix} = \begin{pmatrix} B & D \\ A_0 B + A & A_0 D + C \end{pmatrix} .$$

The image will be formed at a distance $\dfrac{A_0 D + C}{A_0 B + C}$ from the reference plane in the image space.

Now consider the case when some component or components are shifted within the lens system. The new paraxial matrix can be represented as $\begin{pmatrix} B' & D' \\ A' & C' \end{pmatrix}$. The back conjugate for the same object location will be $\dfrac{A_0 D' + C'}{A_0 B' + A'}$.

For the system to work as a zoom lens in the two configurations, then

$$\frac{A_0 D' + C'}{A_0 B' + A'} = \frac{A_0 D + C}{A_0 B + A} ,$$

The equation is a quadratic in A_0. The system can have two different sets of conjugates and act as a zoom system in the two configurations. Nothing is implied about whether or not the same conjugates will apply for any other configuration of the lens system. Also, no limitation was placed on how the configuration of the lens system was changed. We can thus arrive at a general statement which applies to any type of zoom system.

Any lens system working in the zoom mode will function for two sets of conjugates at the most. More likely the system will work for only one set of conjugates.

THREE-COMPONENT ZOOM

The three-component zoom is one which can be investigated thoroughly. Consider again the system in figure 2. We will arbitrarily set $f_2 = -100$ and $t_1 = t_2 = 60$ for the nominal position. The motion of the outside elements will be ±50.

Since there may be four finite variable air spaces there can be four crossing points. One crossing point may lie outside the range of motion, or may disappear should the object distance or image distance become infinity. Systems with crossing points occurring at the end of travel and at the mid-position will be investigated, although another crossing point may exist. The solutions were found by trying values for f_1 and f_3, finding the conjugates for the ends of the travel, and then finding the error at the mid-position of travel. Either f_1 or f_3 was changed to reduce the error. Those solutions for no error in the mid-position are plotted in figure 3. Rather than plot according to f_1 and f_3, the diopter powers of the lenses are used. A number of solutions are shown which are not mentioned in any of the literature we searched. In the first quadrant two curves are shown. These are the two solutions for the quadratic in A_0. The closed loop is for the case when one conjugate is real. The other curve is for the case where both object and image are virtual. The closed loop is for the ordinary object and image, while the other curve is for the pupils. In the present case it is possible to find solutions where not only are the object and image relatively fixed, but the pupils are also relatively fixed.

The solutions of most interest lie on the closed loop in the first quadrant between the two indicated points. At one of these points the object is at infinity while at the other the image is at infinity. For portions of the curve between the indicated points, the system has a real object and a real image. The symmetrical case ($f_1 = f_3$) is of interest since it has the greatest magnification range, can have four useful crossing points, and has the smallest errors of focus between crossing points.

The solutions in the other quadrants are largely of academic interest. Those in the third quadrant consist of three negative components, and have small ranges of magnification.

The three-component zoom lens in which the fixed component is positive can be investigated in a similar fashion. The lens is shown in figure 4. In this case $f_2 = 133$, while $t_1 = t_2 = 60$ for the nominal case. The motion is again ±50. The solutions are plotted in figure 5. The useful solutions are in quadrant 3. No solution corresponding to the fixed pupils was found with the positive fixed component. Again the part of the curve of greatest interest lies between the two points where the curve is tangent to the two coordinate axes. At one point of tangency the object is at infinity while at the other point of tangency the image is at infinity.

The object and image are virtual for all values on the curve between the two tangent points. Again the symmetrical case ($f_1 = f_3$) is capable of four crossing points, has the maximum magnification range, and has the smallest focusing errors between crossing points.

FIVE-COMPONENT ZOOM

The investigation of the three-component zoom showed the superiority of the symmetrical case. By analogy it is to be expected that the symmetrical case in the five-component zoom would be desirable. The exact conjugates and magnifications required can be obtained by using auxiliary components. Should a good reason exist for desiring a five-component zoom lens which was not symmetrical, the best approach would probably be to find the symmetrical solution and modify it.

The notation used for the five-component, optically compensated zoom lens is shown in figure 6. In the illustrative examples $t_1 = t_2 = 60$ for the nominal, or one-to-one case. The range of motion is ±50. The system is capable of giving six crossing points. This is checked by finding the conjugates for ±10, ±30, and ±50 and comparing. If the matrix for a +10 motion is $\begin{pmatrix} B & D \\ A & C \end{pmatrix}$ then the matrix for -10 motion is $\begin{pmatrix} C & D \\ A & B \end{pmatrix}$, assuming the reference planes to be symmetrically placed.

The five-component, optically compensated zoom system can be determined by the following computational steps. Fix the values for f_1, t_1, and t_2. Assume values for f_2 and f_3. These will have to be of reasonable magnitude or the resulting solutions may be of little interest. Decide at which positions the system is to have crossing points. Suppose these are at ±a, ±b, and ±c. Call these position A, position B, and position C. Further specify $a < b < c$. Now the algorithm which will lead to a solution can be given in the following steps:

1. Put lens system in position A and find the conjugates for which system will work as a zoom system.

2. Put lens system in position C and compute error in focus.

3. Adjust focal length of f_3 to reduce focusing error for position C and return to step 1. Repeat until focusing error is sufficiently reduced, then go to step 4.

4. Put lens system in position B and compute error in focus.

5. Adjust focal length of f_2 to reduce focusing error in position B and return to step 1. When focusing error is sufficiently reduced in position B, the focal lengths for f_2 and f_3 have been found.

The algorithm has been programmed as an iterative routine for a digital computer. Examples of numerical solutions are given in tables 1 and 2. It is interesting to note that a large magnification range is obtainable in the optically compensated case, while focal shifts are relatively modest.

Table 1. FIVE-COMPONENT ZOOM - POSITIVE COMPONENTS MOVABLE

f_1	f_2	f_3	Object Distance	Magnification Range	Maximum Error
140	-123.6	217.7	599	6.0	0.003
120	-101.4	185.8	511	8.4	0.007
100	- 79.3	154.2	423	14.0	0.016
80	- 57.2	123.0	336	30.0	0.046
60	- 35.3	92.3	252	128.0	0.24
40	- 13.3	62.8	173	5300.0	2.86

Table 2. FIVE-COMPONENT ZOOM - NEGATIVE COMPONENTS MOVABLE

f_1	f_2	f_3	Object Distance	Magnification Range	Maximum Error
-120	165.7	-202.6	-584	5.3	0.004
-100	143.6	-170.8	-495	7.0	0.007
- 80	121.5	-139.1	-407	10.5	0.014
- 60	99.4	-107.6	-320	19.0	0.037
- 40	77.5	- 76.4	-234	56.0	0.13
- 20	55.8	- 46.1	-152	490.0	0.73

Clearly and optically compensated zoom lens with its single moving part is attractive from the standpoint of simplicity of construction. It should nevertheless be recognized that the linearly compensated zoom lens has certain merits tending to offset the additional mechanical complexity involved. In its most general form the elements of the linearly compensated zoom lens may all move independently, subject to the constraint that these movements are linearly related. An example where but two movements are allowed is shown in figure 7. Comparing figure 7 and 8, which have the same distance from object to image, it is seen that in this instance the linearly compensated example has a smaller focus error and a better distribution of power among the elements.

As a specific example of these studies a five-element optically compensated zoom projection lens has been designed and fabricated and is shown in figure 9. The application of the lens called for a magnification range of 10, with the upper and lower limits unspecified; that is 1-10, 3-30, etc. In this circumstance it was elected to develop a "module", ranging from $10^{-1/2}$ to $10^{1/2}$ in magnification, such that end elements could be added for later specified upper and lower limits. As has been noted, it is not possible to deviate excessively from a symmetrical construction (at mid-position travel) if the maximum number of crossings is to be obtained. Acceptance then, of such a symmetrical design eliminated coma, distortion, and lateral color in the mid-position.

Correction of aberrations at one extreme of travel resulted automatically in correction at the other extreme of travel. These considerations led to considerable simplification of the design task and reduced the number of tools and test plates by half, not an unimportant factor when small numbers of units are involved.

The basic module covers a 112-mm by 112-mm format at unit magnification. At one end of the travel the object format is 213-mm by 213-mm, and the image format is 67-mm by 67-mm. Focal shift throughout the range is well within the Rayleigh limit. At the 3.16 power setting axial resolution is better than 200 lines per millimeter in the object. Triplet end elements have been added, providing a 3 to 30 power range for projecting a 4 1/2-inch by 4 1/2-inch format on a 20-inch by 20-inch screen.

CONCLUSION

The algorithm described in this paper demonstrates a convenient means of exploring all arrangements of optically and linearly compensated zoom lenses. An upper limit to the number of crossings obtainable in terms of finite variable air spaces has been established.

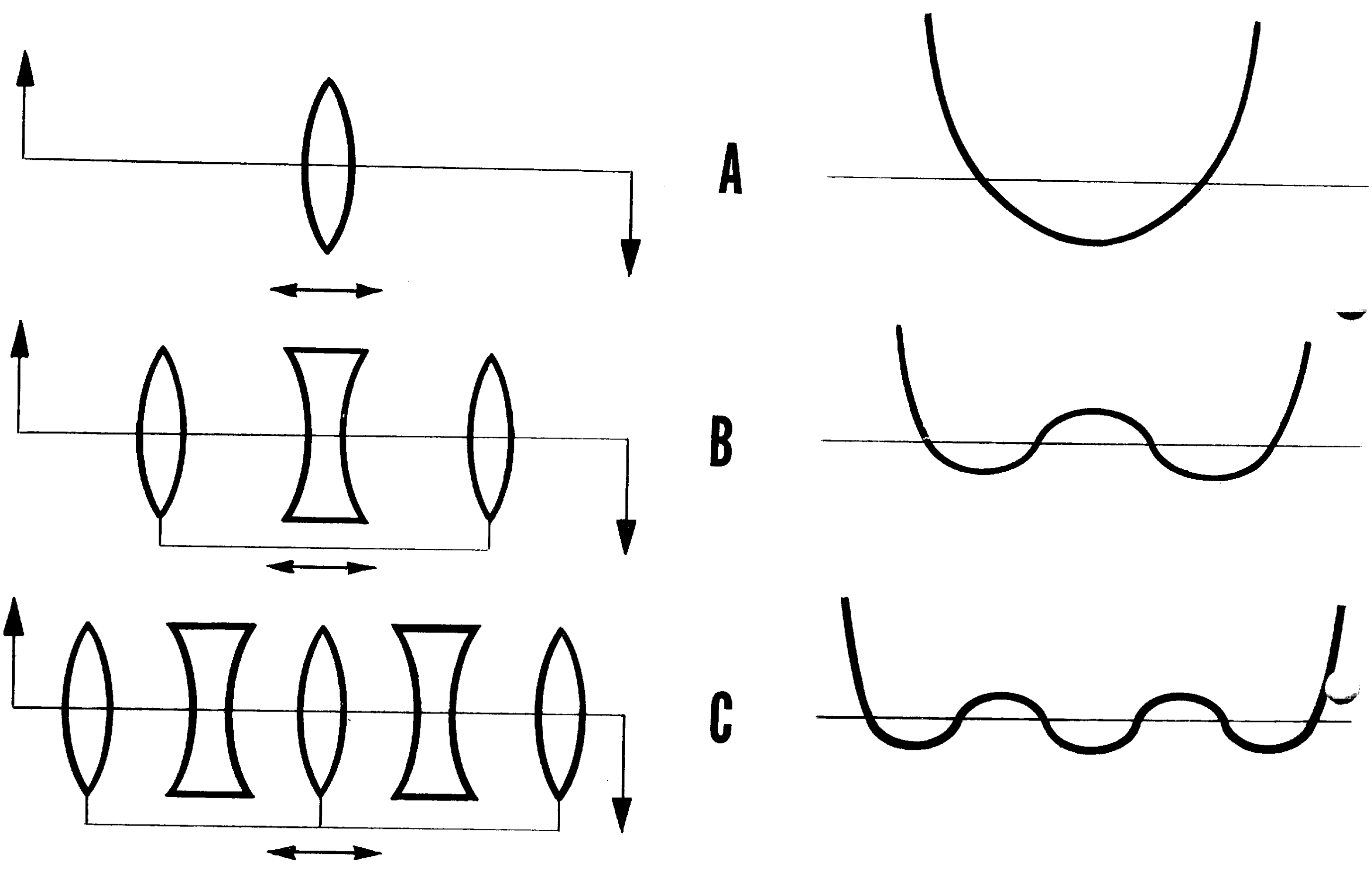

Figure 1. NUMBER OF POSSIBLE CROSSING POINTS WITH ONE, THREE AND FIVE-COMPONENT OPTICALLY COMPENSATED ZOOM LENSES

Approved For Release 2005/05/02 : CIA-RDP78B04770A001900020032-6

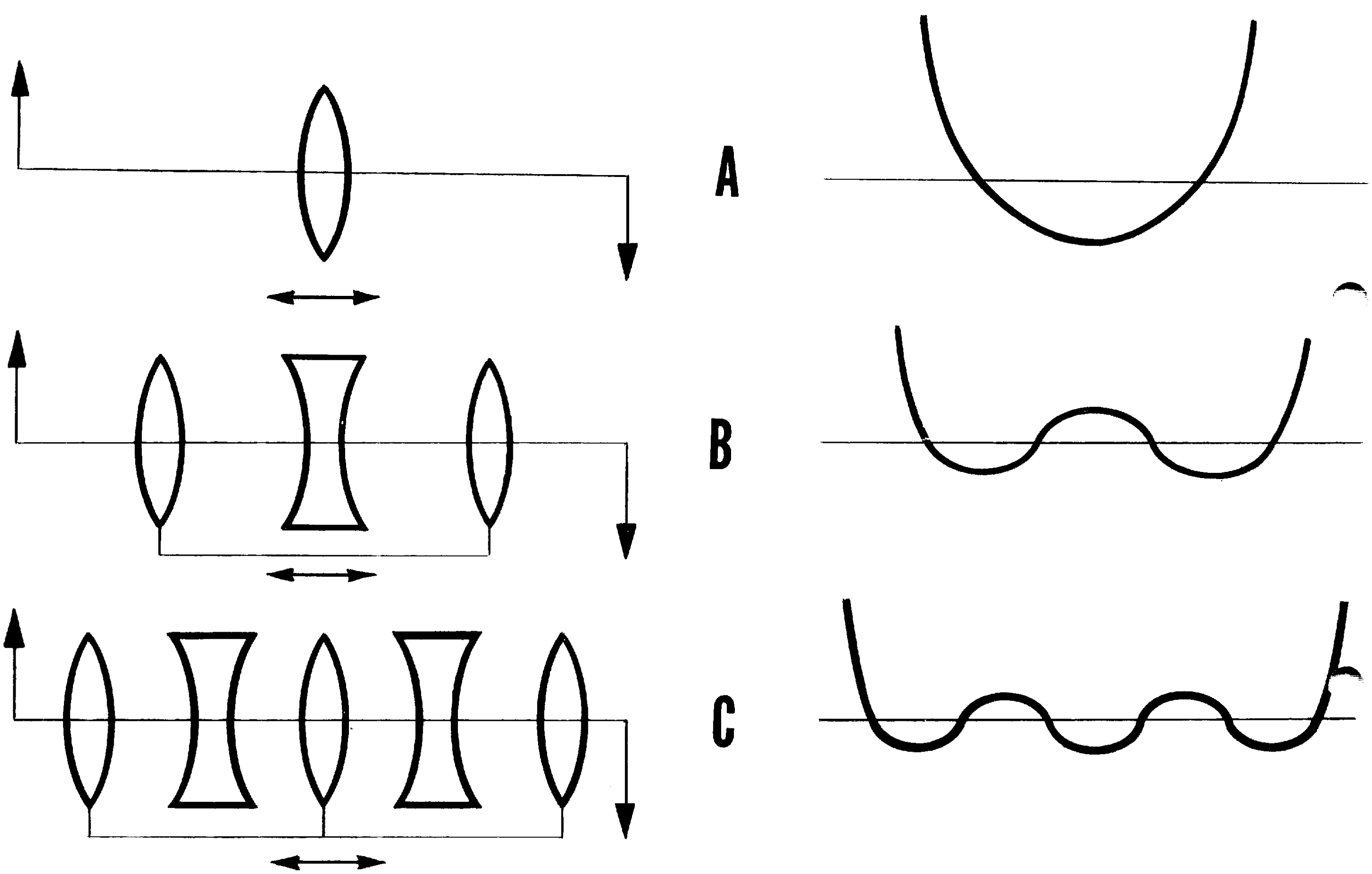

Figure 1. NUMBER OF POSSIBLE CROSSING POINTS WITH ONE, THREE AND FIVE-COMPONENT OPTICALLY COMPENSATED ZOOM LENSES

Approved For Release 2005/05/02 : CIA-RDP78B04770A001900020032-6

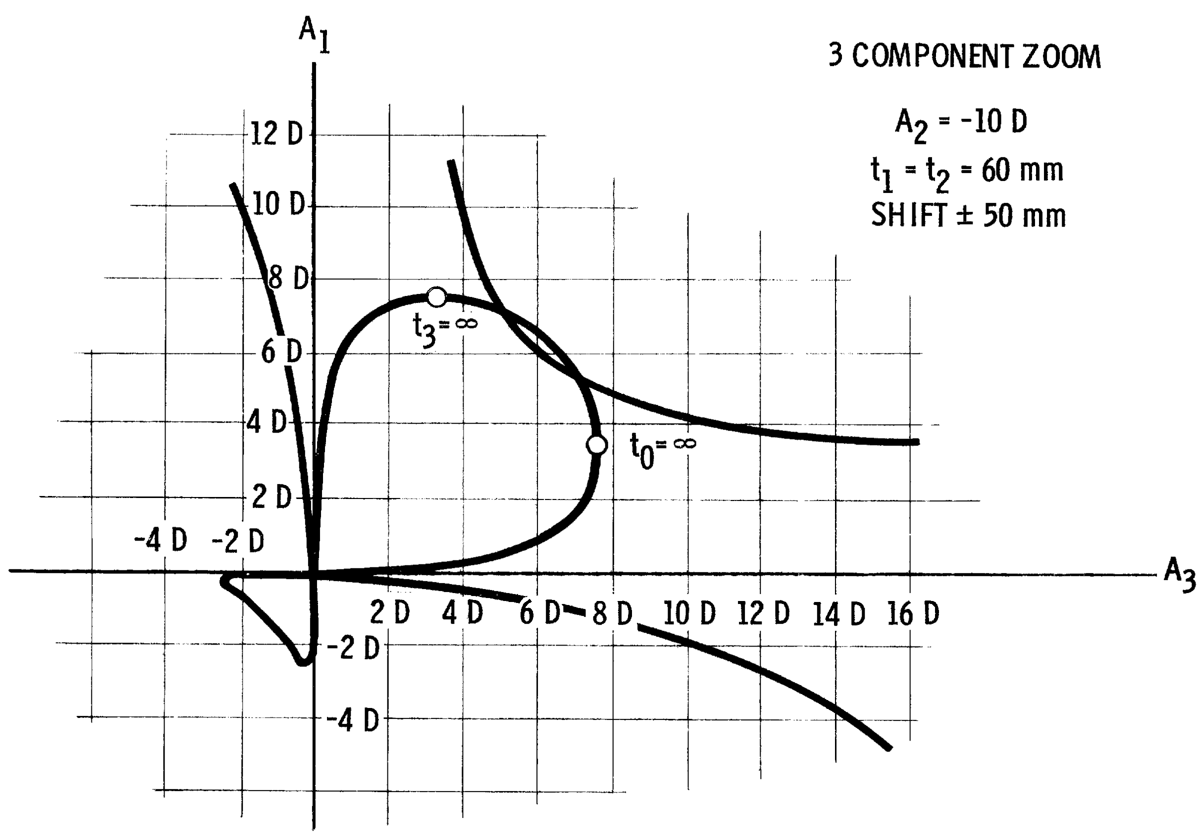

Figure 3. SOLUTIONS FOR A THREE-COMPONENT ZOOM LENS WITH CROSSING POINTS OCCURRING AT THE MID-POSITION AND AT THE TWO ENDS OF TRAVEL (NEGATIVE FIXED COMPONENT)

Approved For Release 2005/05/02 : CIA-RDP78B04770A001900020032-6

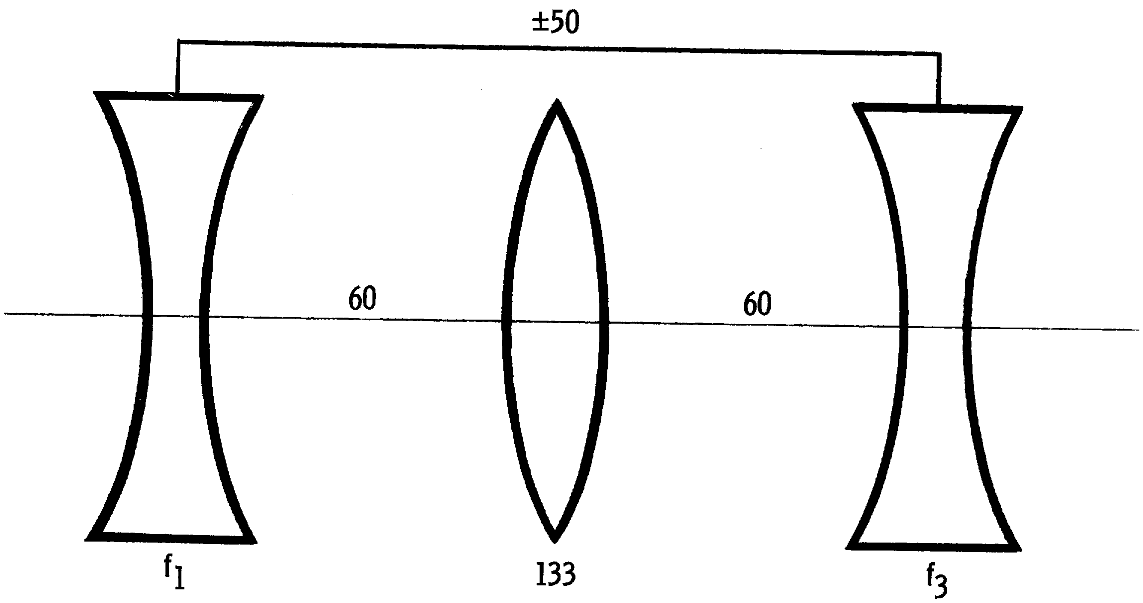

Figure 4. THREE-COMPONENT ZOOM LENS WITH POSITIVE FIXED COMPONENT

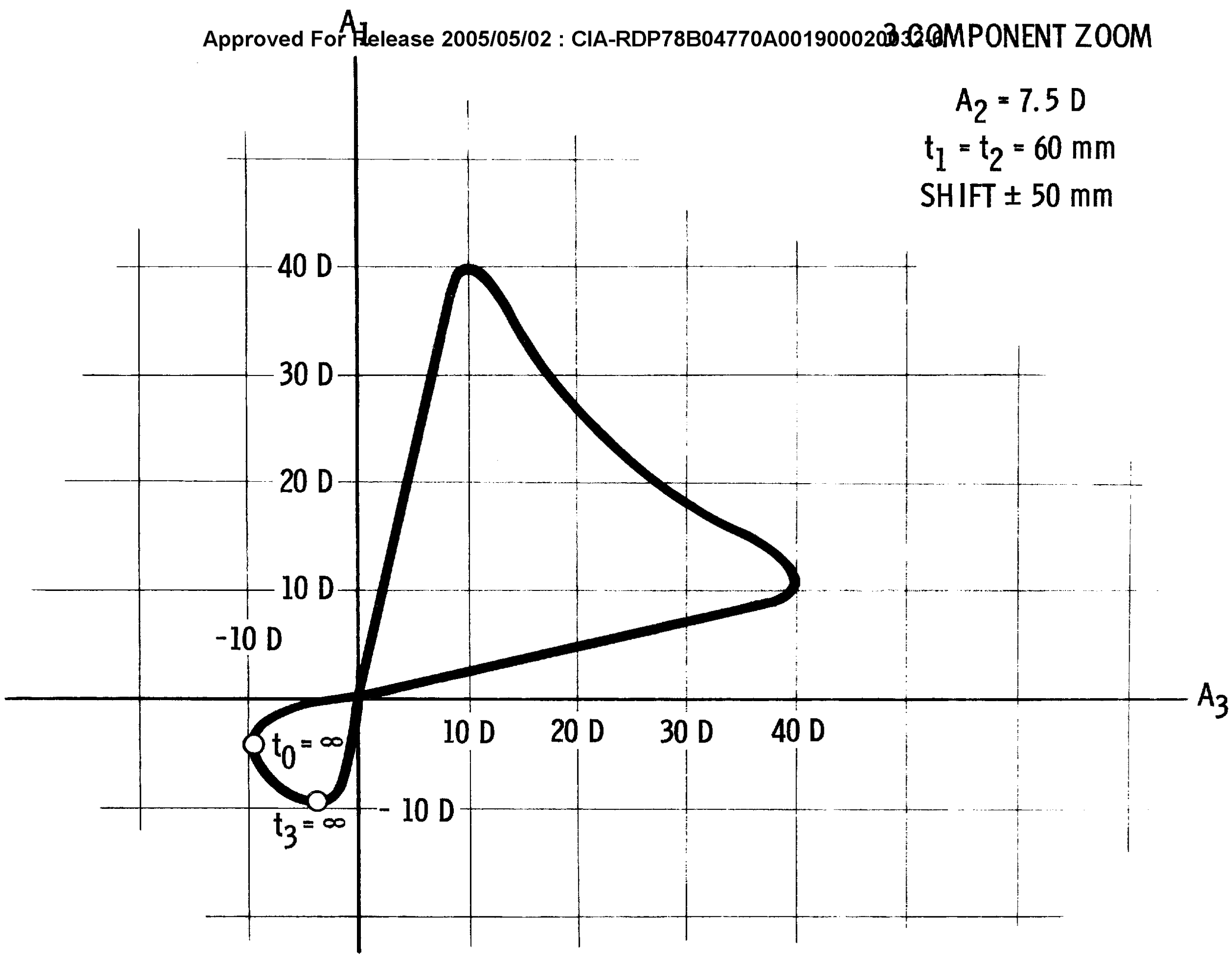

Figure 5. SOLUTIONS FOR A THREE-COMPONENT ZOOM LENS WITH CROSSING POINTS OCCURRING AT THE MID-POSITION AND AT THE TWO ENDS OF TRAVEL (POSITIVE FIXED COMPONENT)

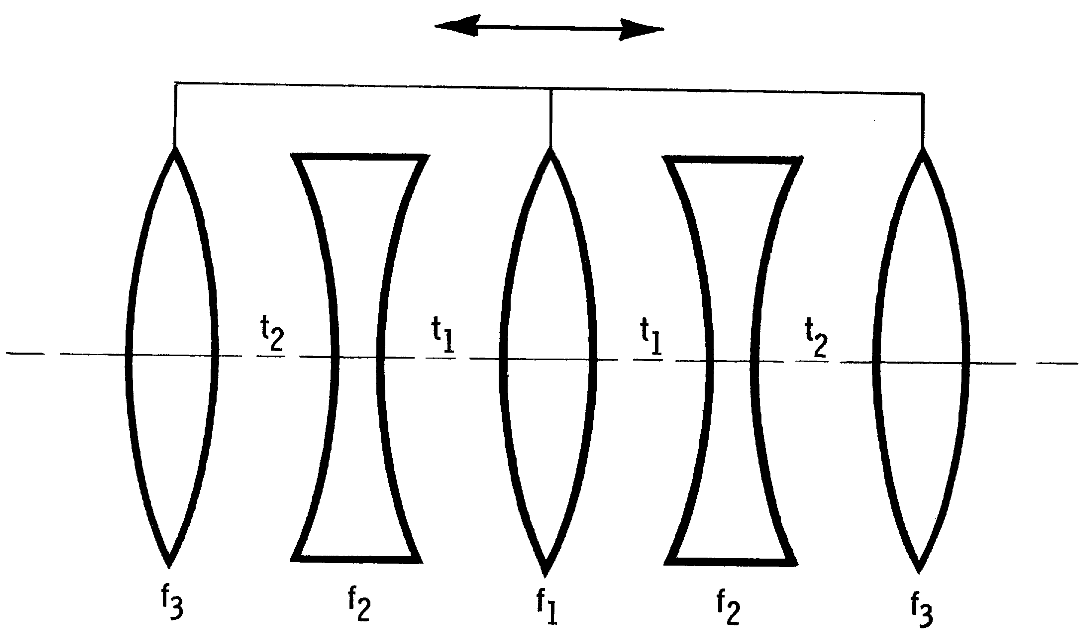

Figure 6. SYMMETRICAL FIVE-COMPONENT ZOOM LENS WITH NEGATIVE FIXED COMPONENTS

Approved For Release 2005/05/02 : CIA-RDP78B04770A001900020032-6

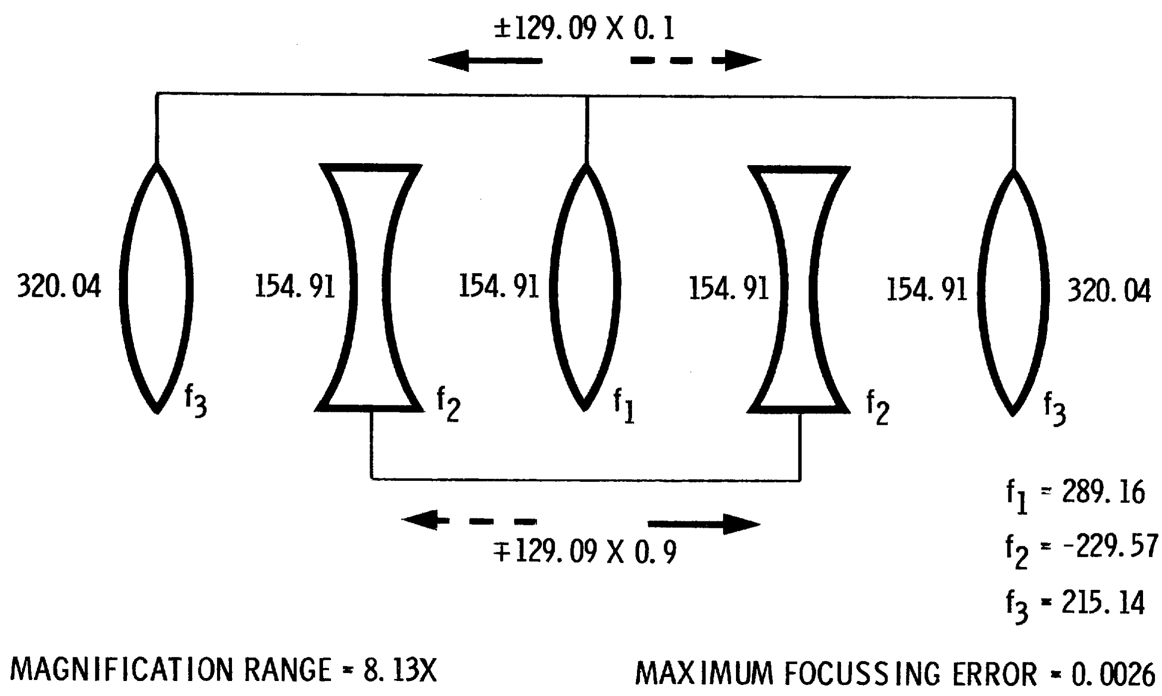

Figure 7. FIVE-COMPONENT SYSTEM WITH TWO MOTIONS LINEARLY RELATED - 8.13 TIMES MAGNIFICATION RANGE

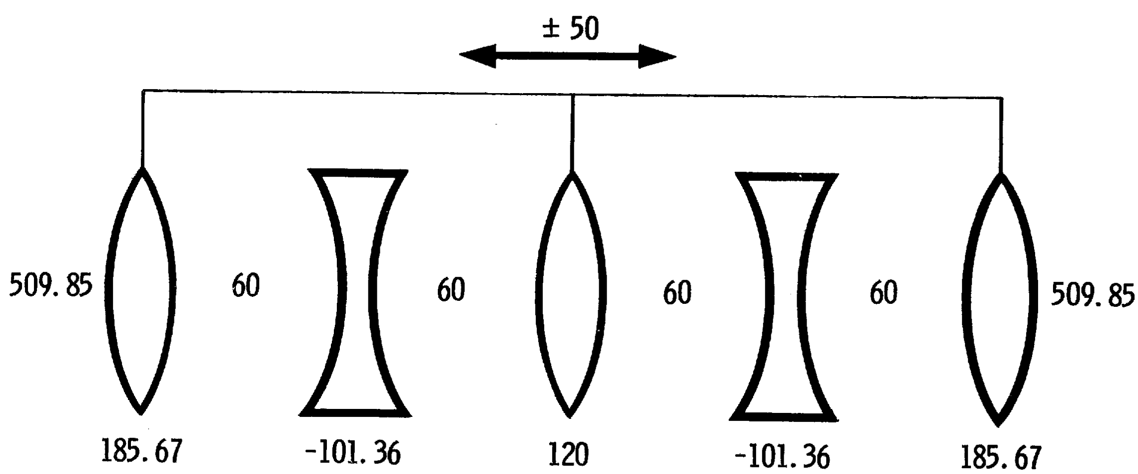

MAGNIFICATION RANGE = 8.39X MAXIMUM FOCUSSING ERROR = 0.0081

Figure 8. OPTICALLY COMPENSATED ZOOM LENS WITH SAME OVERALL LENGTH FROM OBJECT TO IMAGE AS SYSTEM IN FIGURE 7 - 8.39 TIMES MAGNIFICATION RANGE

Approved For Release 2005/05/02 : CIA-RDP78B04770A001900020032-6

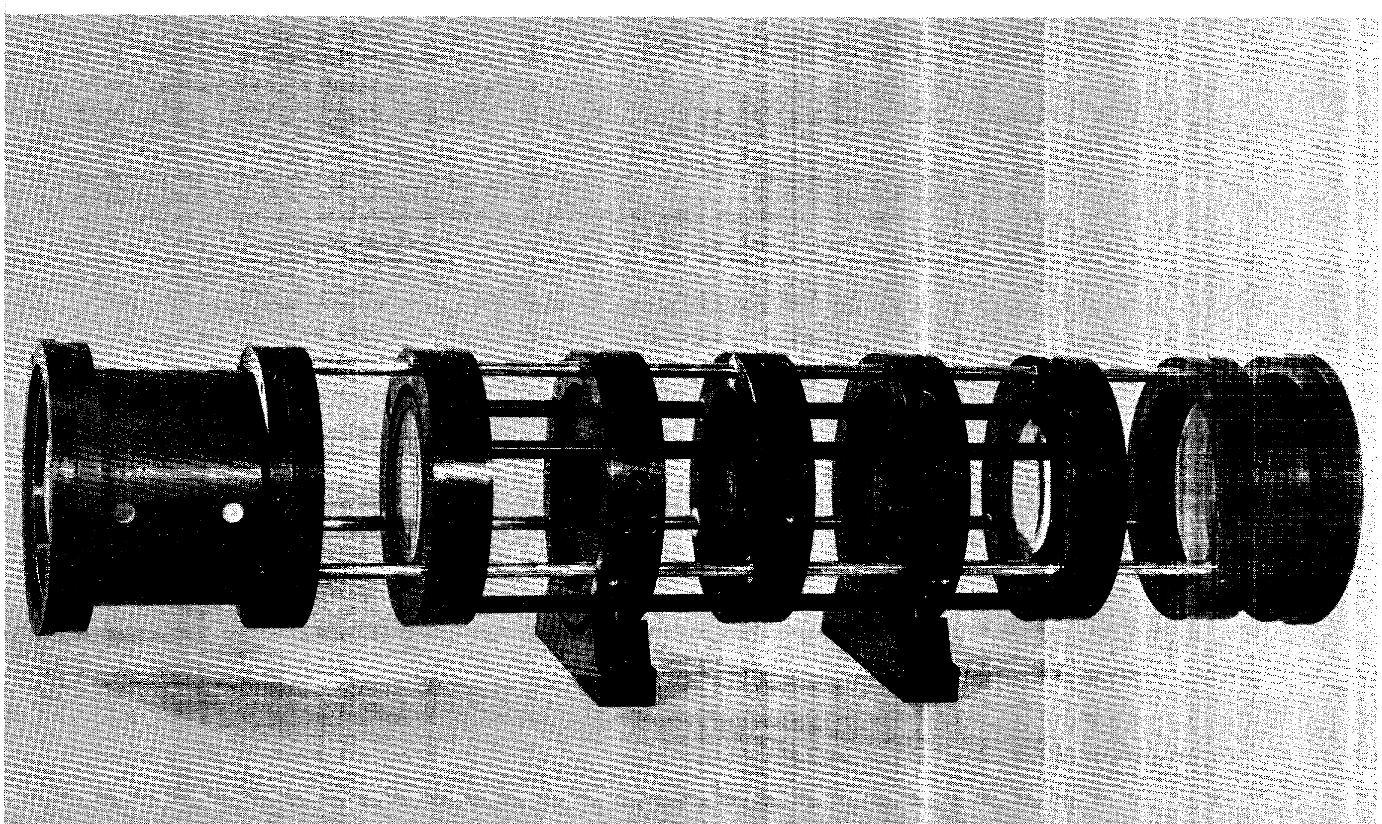

Figure 9. PROTOTYPE OF FIVE-COMPONENT OPTICALLY COMPENSATED ZOOM LENS WITH AUXILIARY END COMPONENTS (HOUSING REMOVED)

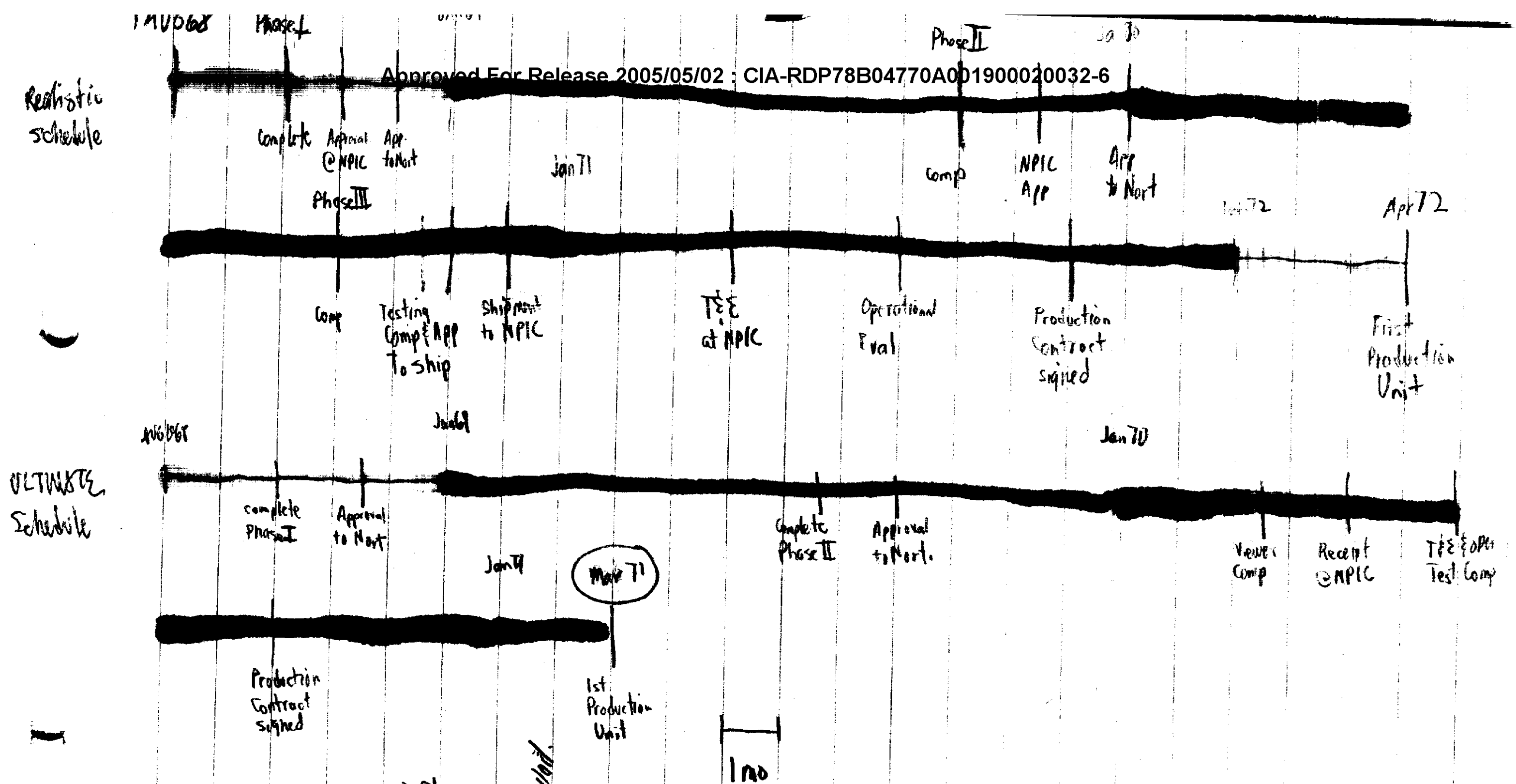

ORIGINAL OSL

31MAY → 30NOV68

PHASE I 31MAY1967 15 SEPT 67

PHASE II 15 MAY 68 8mo

III 30 NOV 68 6 1/2

Comp Production of 1st Unit

 02157

DEVELOPMENT BRANCH ROUTING SLIP

25X1

____ Take appropriate action
____ For your approval
____ Note and return to me
____ Investigate and report
____ See me about this
✓ Read and pass on

____ For your information
____ File
____ Route
____ Expedite
____ Prepare answer
____ Type (smooth) (rough)

From P Date 19 Nov 65

Comments:

This is a Air Force check out sheet for VIEWERS. PLEASE REVIEW AND COMMENT. CAN WE USE IT? HOW SHOULD IT BE MODIFIED.

P

WHAT ABOUT A LOW CONTRAST RESOLUTION TEST ALSO. I think we should have a standard check off guide such as this.

AGREE WITH LOW CONTRAST TEST

1. FILM HEATING IN STATIC TEST
2. LOADING OF FILM (EASE OF)

I agree that there might be a space for comments concerning loading and unloading film

How about a [illegible] for [illegible] measurement [illegible]? [illegible]

~~Chem~~ Do the platens accumulate dirt? degradation?

EQUIPMENT PERFORMANCE TEST

Manufacturer	Model & Type

Serial Nr	Site of Test	Date

I. GENERAL INSPECTION:

Test personnel shall be thoroughly familiar with applicable specifications, and items not specifically noted in this schedule shall be checked and discrepancies noted. Make a general inspection of the unit paying particular attention to workmanship and general appearance. Check interior and exterior surfaces, electrical wiring, transports, control panel, etc., for compliance with specifications. Make comments below:

II. PROJECTION SYSTEM TEST:

For the following tests, measure and record the test conditions at the time of the test:

Line voltage (at lamp) ______________ VAC

Temperature ______________ oF

Relative Humidity ______________ %

A. Light Test

1. With an open film gate and the brilliance control at maximum, take light intensity readings with a calibrated Photometer at the points indicated by the sketch below (points 1 thru 9) for each of the magnification ranges:

What type photometer?

Under what placement circumst[illegible]? [illegible]

[illegible]

2	3	4
1	9	5
8	7	6

	______X	______X	______X	______X
1	______	______	______	______
2	______	______	______	______
3	______	______	______	______
4	______	______	______	______
5	______	______	______	______
6	______	______	______	______
7	______	______	______	______
8	______	______	______	______
9	______	______	______	______

2. In all magnification ranges, traverse to both extremes and check for evidence of color fringing over the entire screen. Make comments below as to the degree of color fringing, if any, and in which magnification range(s).

There is/is not evidence of color fringing on the screen.

3. In all magnification ranges, check for evidence of "hot spots" over the entire screen. Make comments below as to the degree of hot spotting and in which magnification range, if any.

There is/is not evidence of "hot spotting" on the screen.

Isodensitrace excellent technique for this

BB. MAGNIFICATION & DISTORTION TEST

1. Place a calibrated grid of approximately 0.2" spacing in the film gate and clamp. Determine the length that each side of the projected grids should be by multiplying the actual grid spacing by the magnification range as engraved on the selector buttons, and record in the space below. Make 16 random measurements of the projected grid lines, 4 in each quadrant, in each magnification range. Half of these measurements should be in the X direction and half in the Y directipn; record measurements below.

Calibrated grid of ________________spacing.

Grid lines at____X ____________

Grid lines at____X ____________

Grid lines at____X ____________

Grid lines at____X ____________

IV	I
III	II

2. Measurements:

	___X	___X	___X	___X
Quad I				
Quad II				

Approved For Release 2005/05/02 : CIA-RDP78B04770A001900020032-6

Quad III

QUAD IV

3. **Magnification:** Compare the average of the projected grid line measurements with the "Grid lines at_____X" length (determined in B.1. above) to determine conformance with magnification specifications.

Does/Does not conform with magnification specifications in______X, ____X, ____X, ____X.

4. **Distortion:** Compare the projected grid line measurements with the "Grid lines at ____X" length (determined in B.1. above) to determine conformance with distortion specifications.

Does/Does not conform with distortion specifications in____X, ____X, ____X, ____X.

5. As a final distortion test, make a visual check of the entire screen to determine the presence of any distortions not discovered in performing the above tests, i. e., curved grid lines, wavy grid lines, etc. Make comments below:

2. Time the movement of a known length of film (15' or so) scanning at the slowest possible speed and at the highest magnification. Record the speed below. Repeat the test for the fastest scan speed and record the speed below. While in the slow scan speed, check for noticeable jerking or sporadic movements of the projected image. Slew an entire roll of film from one side to the other and record elapsed time below.

Slowest scan ___________inches per second

Fastest scan ___________inches per second

Slew____' film ___________minutes/seconds

There is/is not noticeable jerking or sporadic movement of the projected image at the highest magnification. Comments:

3. Repeat the test in paragraph 1 above using $9\frac{1}{2}$" Thin Base film.

4. Repeat the test in paragraph 1 above using 70mm St'd film.

IV. GENERAL OPERATION: While performing the above tests, all controls and operations should be thoroughly exercised and controls should be placed in every conceivable combination to check safety interlocks in the equipment. Make statements below as to proper operation of all functions.

A. Lateral Drive. (Extreme to opposite extreme, ____________seconds)

B. Film Motion Control.

C. Magnification Selection. (Elapsed time for worse change,_______secs)

D. Illumination Control.

6a

B. RESOLUTION TEST

1. Place a Standard High Contrast Air Force Resolution Target in the film gate and apply clamping. Make 5 readings of the minimum readable targets at each magnification setting, one in each quadrant and one at screen center, record readings below:

	Cntr	I	II	III	IV
______X					
______X					
______X					
______X					

This needs expanded considerably as to how readings will be interpreted

2. The brilliance control should be left in the maximum position throughout the entire test - preferably for at least 8 hours without shut-off during breaks in the test schedule. Test should start with a new lamp and should burn-out occur, record the time on the lamps used for the test. At the end of the test, check all optical elements for heat damage - check lamps for bulges and swelling.

III. FILM TRANSPORT TEST

A. <u>Film Degradation Test</u>: Load a roll of $9\frac{1}{2}$" standard base film which is free from any scratches or gouges, i. e., straight from the photo lab and in new condition. Scan and slew in both directions 60 times (30 times each way) with frequent stops and starts within a 10 to 20 foot marked segment of the film. Check this segment of film at the highest magnification for evidence of degradation.

Repeate for at least one other size, preferably 70 mm

The film is/is not appreciably degraded - make statement below as to seriousness of degradation, if any.

B. <u>Film Drive Test</u>

Load a full 8" diameter reel of <u>standard</u>/<u>or thin base</u> film and scan or slew throughout the entire length. Also, scan and slew back and forth several times at <u>or near each end of the film</u> to determine that operation of the film drive is in accordance with Film Drive Specifications.

The unit will/will not satisfactorily "handle" full reels of film throughout the entire length. Make comments below:

E. Fine Focus.

F. Scan/Slew Mode Selection.

G. Other, (List controls tested and make comments)

V. GENERAL: Personnel conducting tests should note below any comments regarding opinions on workmanship, machine suitability to the mission, machine strengths, machine weaknesses, etc. Make a lamp change and comment on the ease/difficulty of this operation.

Tests performed by: ______________________ ______________________

Name Title

______________________ ______________________

Mailing Address Telephone

HUMAN FACTORS STUDY

ADVANCED REAR PROJECTION VIEWER

OBJECTIVE

The objective of this report is to present the results of a study conducted to produce a configuration, based solely on human factors considerations, for the advanced, rear projection viewer.

METHOD

The study consisted of three major phases:

1. Preparation of a description of the interpreter's functions and tasks when using the advanced rear-projection viewer.
2. Establishment of a set of human factors design goals aimed at providing optimum man/machine interfaces for the performance of the identified functions and tasks.
3. Development of a configuration based on the design goals.

RESULTS

Description of Interpreter Tasks and Functions

It is important to note that with respect to the viewing equipment, the term "scan" means a specific, formalized operation. The results of this operation are principally to catalogue the quality of coverage for known targets located on the film and secondly, to report new targets. The cataloguing (which is called "indexing") is by far the most time consuming of the two activities even though the finding of the new targets is probably the most important. It is not unusual for a given mission to have the new targets number only a fraction of one percent of the old targets.

From the standpoint of the viewing equipment's acceptability by the operational personnel, the equipment must facilitate the "indexing" portion of the "scan." It should be noted that the "indexing" task is almost universally disliked and the operational personnel will be very sensitive to any equipment feature which makes the task more difficult; however, they will be equally sensitive and appreciative of any equipment which takes the drudgery from the task. Further, decreasing the effort required for indexing increases the time permitted for locating new targets.

In the Design Goals Section and the Flow Chart which follow, the term "collateral material" has been used to cover material used for indexing as well as for finding new targets.

Figure 1 is a generalized functional flow diagram of the scan function performed on the advanced rear projection viewer. The purpose of the flow is to identify, in a systematic way, those functions which have particular significance for design of the interpreter/machine interface.

Design Goals

The design goals presented below are identified with the function from the flow chart which generated them. Only those goals peculiar to the advanced rear projection viewer have been considered. Items having to do with normally sound human engineering practice, such as the layout of controls and displays and the rounding of corners to prevent injury to the operator, have not been detailed in this report.

FUNCTION 1.5—Place image in desired position on screen

1. Masking should be provided along edges of film to prevent excessive illumination on portions of the screen when areas near the edges are positioned in the center of the screen for viewing.

FUNCTION 1.6—Scan full screen

1. Viewing angles obtainable for entire screen should be as near normal to the screen as possible to reduce brightness loss to a minimum.
2. Viewing distances for the entire screen should be as near 14 inches minimum as possible for comfortable viewing.
3. Viewing angle for any portion of the screen should not impose awkward or uncomfortable postures or head positions.

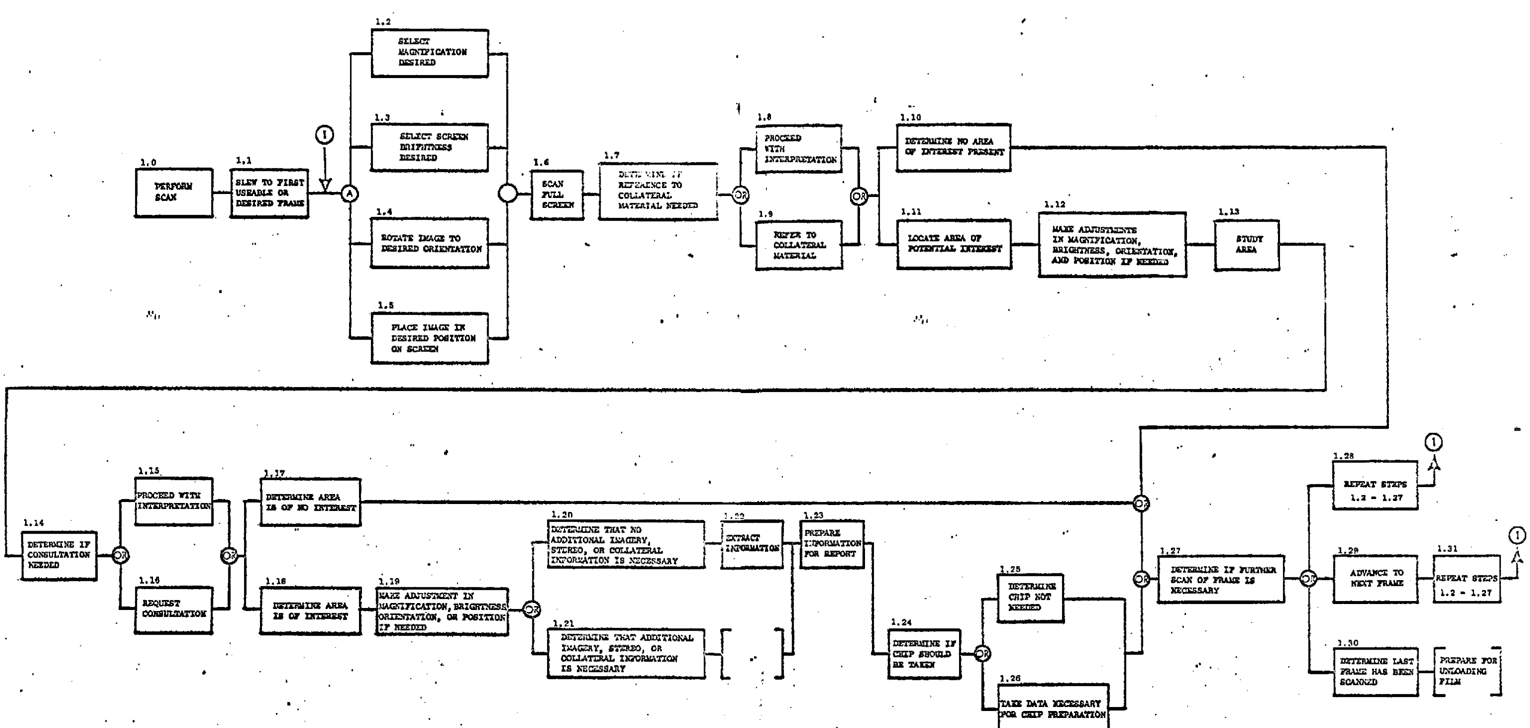

FIGURE 1. FUNCTIONAL FLOW DIAGRAM

FUNCTION 1.9—Refer to collateral material

1. Reference to collateral material should not require major shift of position.
2. Area provided for collateral material should be large enough to allow systematic viewing of material.
3. Area provided for collateral material should allow for convenient viewing of maps without restriction on map orientation.
4. Area provide for collateral material should allow for convenient, organized storage of material not in immediate use.
5. Viewing screen material and orientation should allow placement of collateral material on the screen for side-by-side comparison with projected image.

FUNCTION 1.11—Locate area of potential interest
and 1.22—Extract information

1. Viewing arrangement should allow interpreter to make use of all information on the imagery without placing film in a different piece of equipment.

FUNCTION 1.16—Request consultation

1. Work station design should allow convenient viewing of screen by at least two people simultaneously.
2. Collateral material area should allow convenient selection of material for viewing by any one of three people.
3. Work station design should not require major displacement of operator when consultant is present.

FUNCTION 1.23—Prepare information for report

1. Area provided for report preparation should be large enough to allow systematic arrangement of report materials.
2. Area provided for report preparation should be large enough to permit writing material to be oriented in a normal, comfortable manner.

3. Area provided for report preparation should be located so that no major shift of body position from viewing posture is required.
4. Area provided for report preparation should have convenient storage for report preparation materials such as pencils, paper clips, staplers, etc when they are not in use.

GENERAL

1. Viewing screen should not be damaged or broken by inadvertent bumping with operator's hands, elbows or with collateral material.
2. Work station should provide convenient place for ash trays, coffee cups, and operator's personal equipment such as scales, loupes, and glasses.
3. Work station should be designed to prevent damage to equipment or materials and spilling of ash trays, coffee and soft drinks.
4. Ease of film loading and unloading is critical. While provisions for long rolls of film must be made, it is normal in the scanning operation to have rolls which are quite short (as few as four frames in a roll). For this reason, frequent handling of rolls is required.
5. Provision for handling small film chips encased in plastic sleeves would greatly increase the flexibility of the viewer.

Configuration

The configuration which most nearly satisfies the design goals is one which will allow a sit-stand type of operation such as that performed at a drafting table. A sketch of the suggested configuration is shown in Figure 2. This configuration was chosen over one using standard office seating for several reasons.

1. In order to prevent awkward and uncomfortable viewing positions. For a 30 x 30 inch viewing screen, it is necessary to have the top sloping away from the interpreter (face of the screen tilted up). Figure 3 illustrates the angles of gaze for three screen orientations: (1) face of the screen tilted down 15° (top sloping toward the operator); (2) vertical; and (3) face of the screen tilted up 15°. For example if the operator can be positioned at a viewing distance of 14 inches so that his line of gaze is normal to the screen at the midpoint of the screen height, to see the top one third of the screen when it is tilted face downward 15°, he will have to direct his gaze upward between 50 degrees and 60 degrees. In the same situation, if the screen is tilted face upward 15°, his gaze will only be between 20 to 30 degrees upward. Since working for even short periods of time with the head tilted backwards is extremely likely to produce fatigue and accompanying discomfort symptoms in the back of the neck, the reduction obtainable by orienting the screen 15° face-up is very desirable.

2. In the 15° face-up configuration, if the height of the center of the screen is set for a normal viewing condition for a 50 percentile operator (line of gaze normal to the screen, viewing distance 14 inches) the bottom of the control panel, or writing surface will interfere with the thighs of the 95 percentile operator (assuming a 6-inch high control panel). If the screen is raised to accommodate the large man's thigh clearance, the viewing angles are significantly increased for the 5 percentile man. This has the undesirable effect of

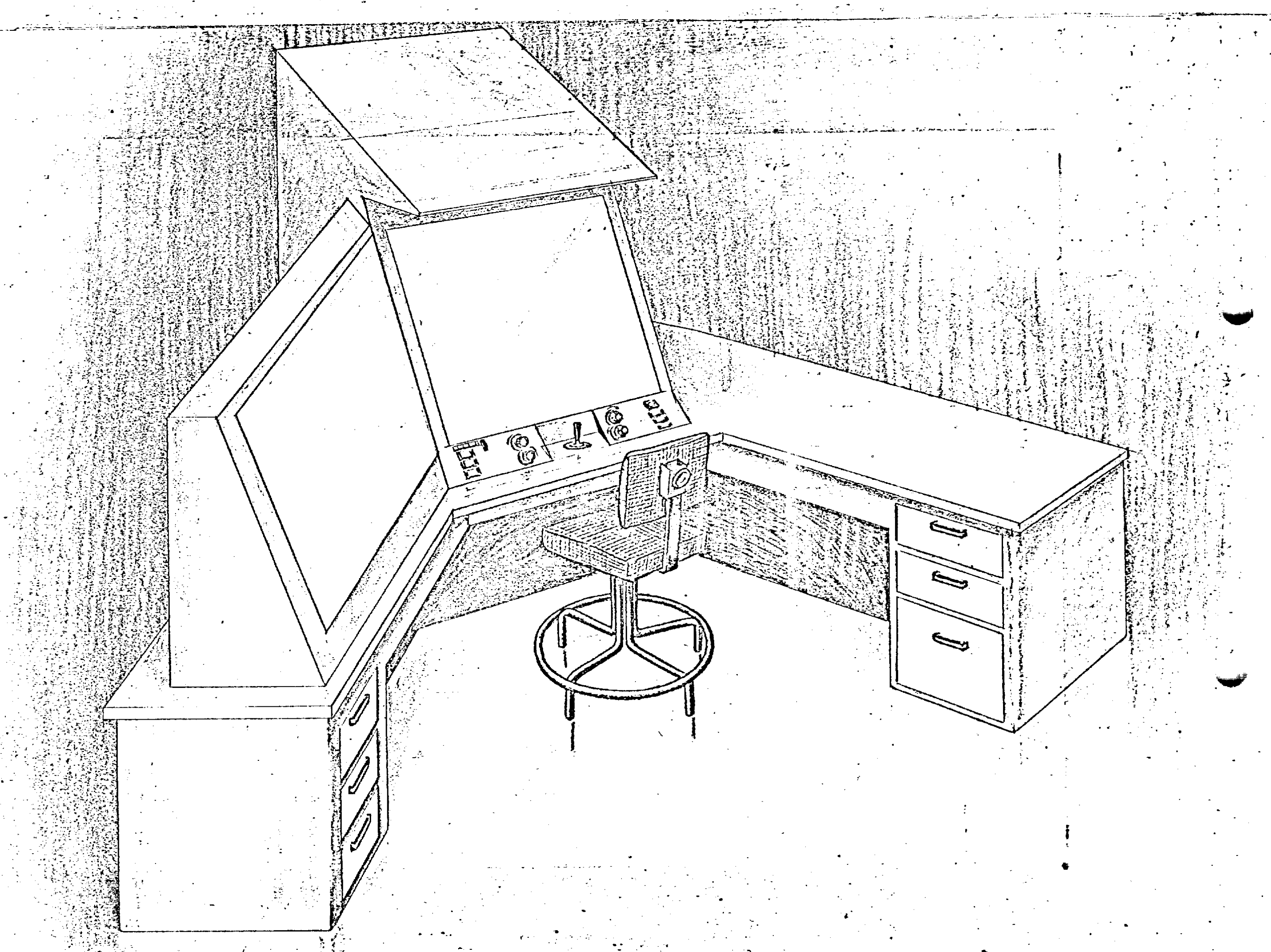

Approved For Release 2005/05/02 : CIA-RDP78B04770A001900020032-6

FIGURE 2.   REAR PROJECTION VIEWER WORK STATION

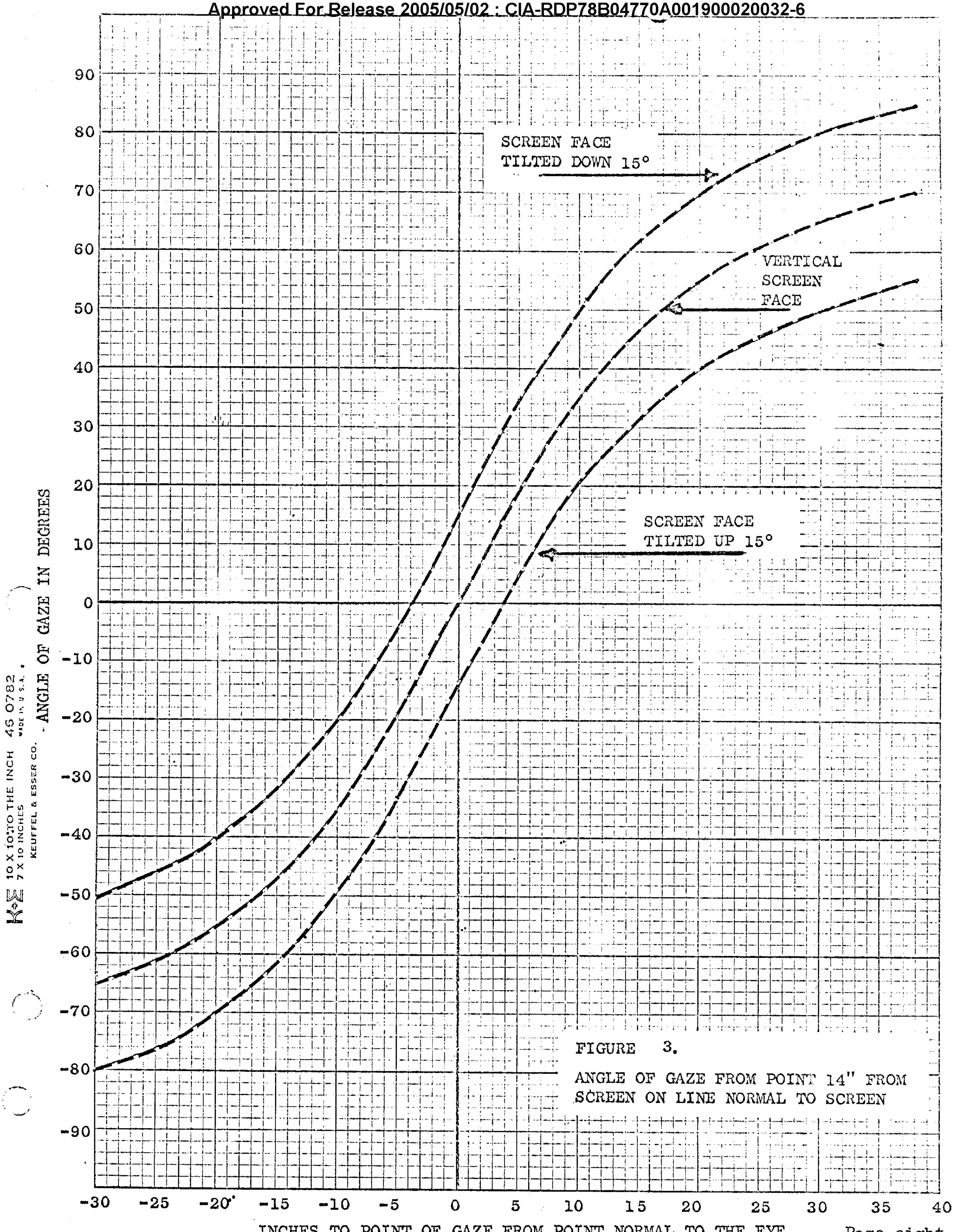

FIGURE 3.

ANGLE OF GAZE FROM POINT 14" FROM SCREEN ON LINE NORMAL TO SCREEN

Approved For Release 2005/05/02 : CIA-RDP78B04770A001900020032-6

increasing the angle of gaze above horizontal, which is itself, undesirable, and which has the additional drawback of reducing the brightness of the image reaching the interpreter's eye. Figure 4 illustrates the gain for Polacoat LS-60C at various viewing angles. These gains were converted into percentages, which are shown in Figure 5. Figure 6 shows this data plotted as a function of the location of the screen's surface with respect to the eye's position. Information is shown for two conditions; first, when the eye is fixed at a point 14 inches from the screen measured on a line normal to the screen, and second, when the eye moves at a constant height and maintains a viewing distance of 14 inches to the point to be observed on the screen. As can be seen from the curves, placement of the operator 4 inches below his optimum height (line of sight normal to the screen, passing through the midpoint of the screen) reduces the brightness at the center of the screen by 30 to 35 percent and for the top third of the screen by more than 50 percent.

3. The height for a sit-stand configuration with a screen in the 15° face-up configuration can be such that people standing and consulting with the interpreter can have a good view of the screen. Figure 7 shows a side view sketch of the viewer. The screen centerline height of 53.4 inches is based on a consideration of the following dimensions:

Seat height	27 inches
Thigh clearance	7 inches
Shelf thickness	1 inch
Control panel	4 inches
Height to screen	
Center	14.4 inches
TOTAL	53.4 inches

To arrive at the ideal operator's eye height from the 53.4 inches at the center of the screen, 3.6 inches must be added. This is the height above a point on the screen at which the eye must be in order to have a line of sight normal to the screen

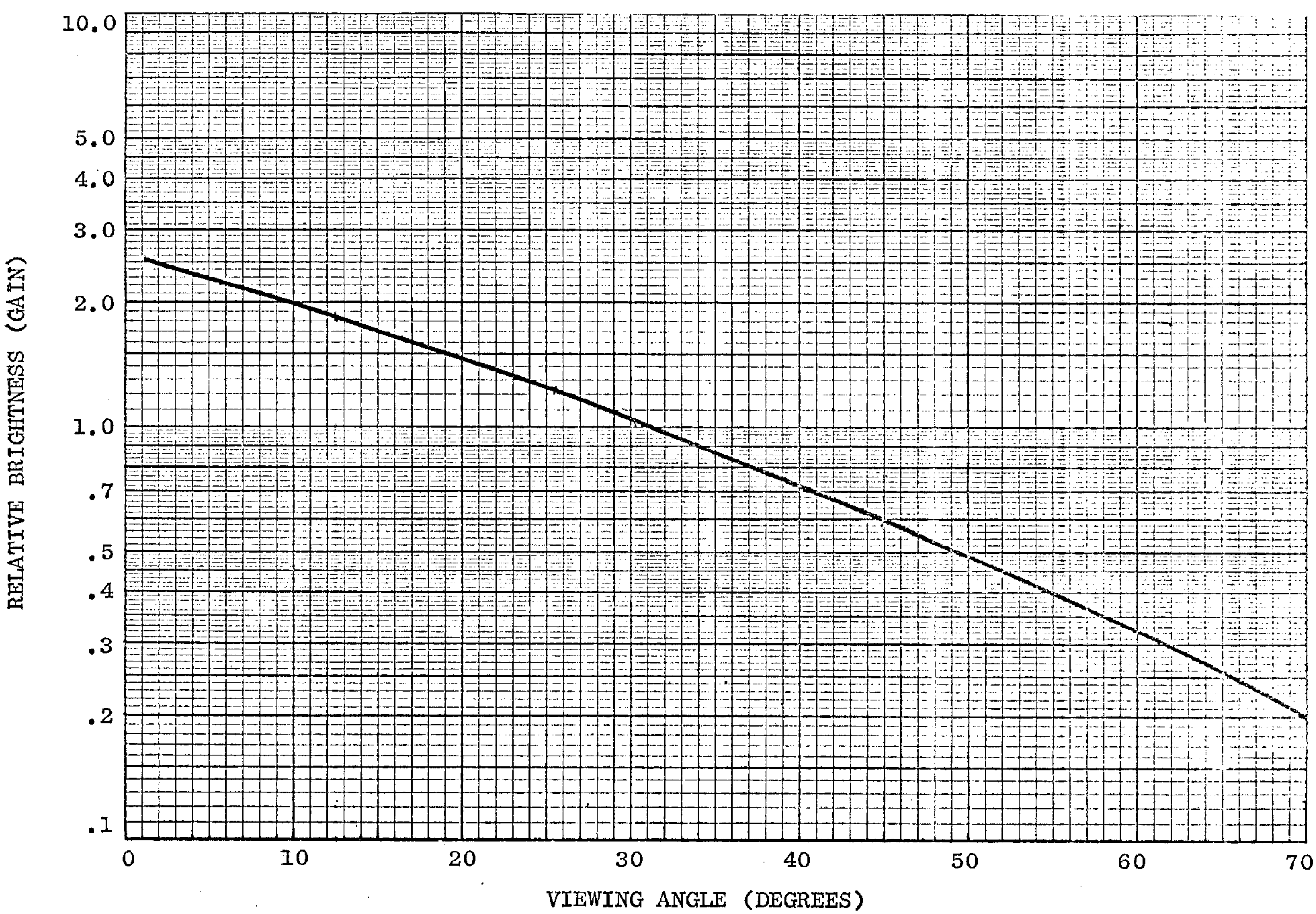

FIGURE 4. VIEWING ANGLE IN DEGREES FROM CENTRAL AXIS (FOR POLACOAT LS-60C)

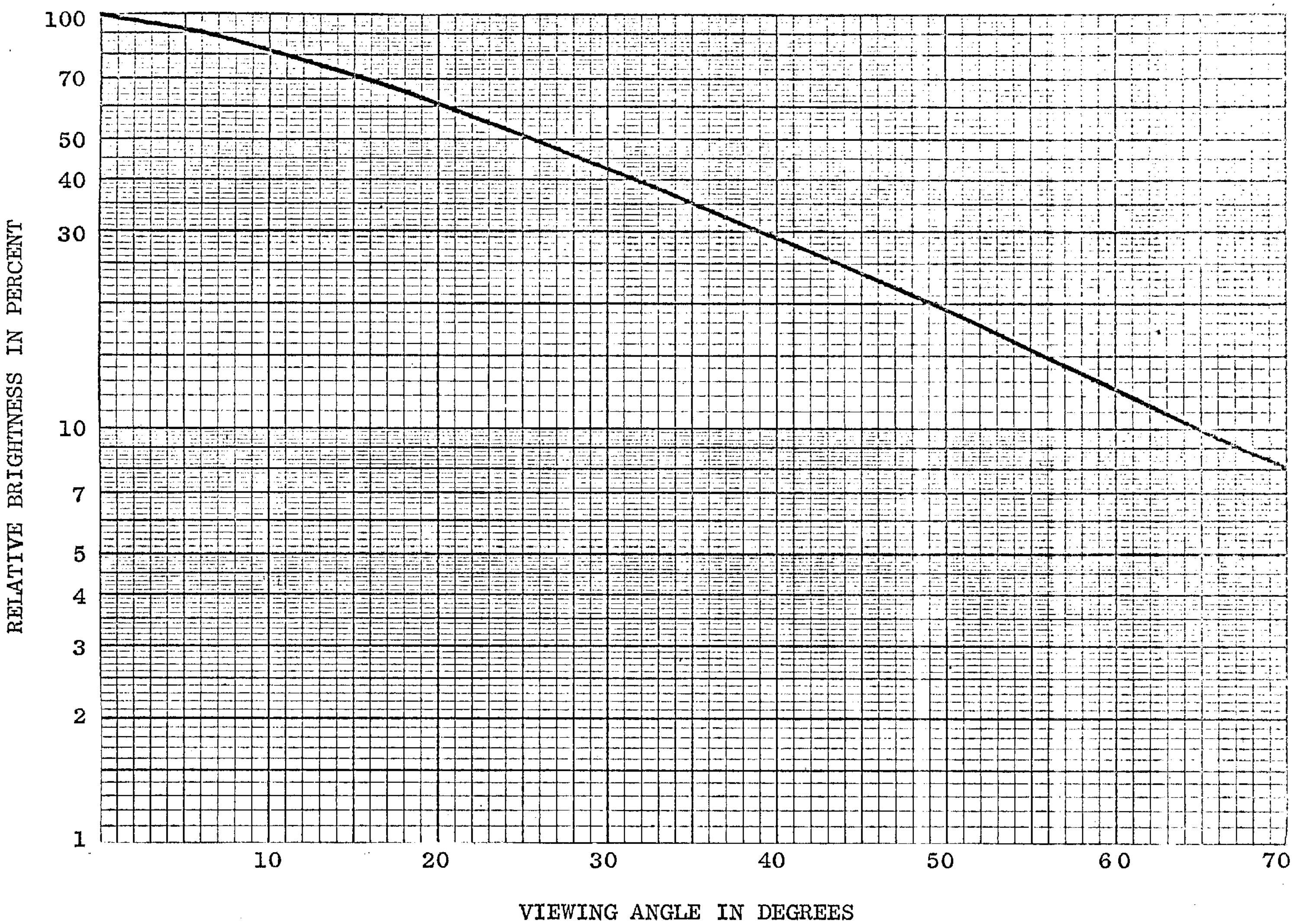

FIGURE 5. RELATIVE BRIGHTNESS IN PERCENT AS A FUNCTION OF VIEWING ANGLE FOR POLACOAT LS-60C

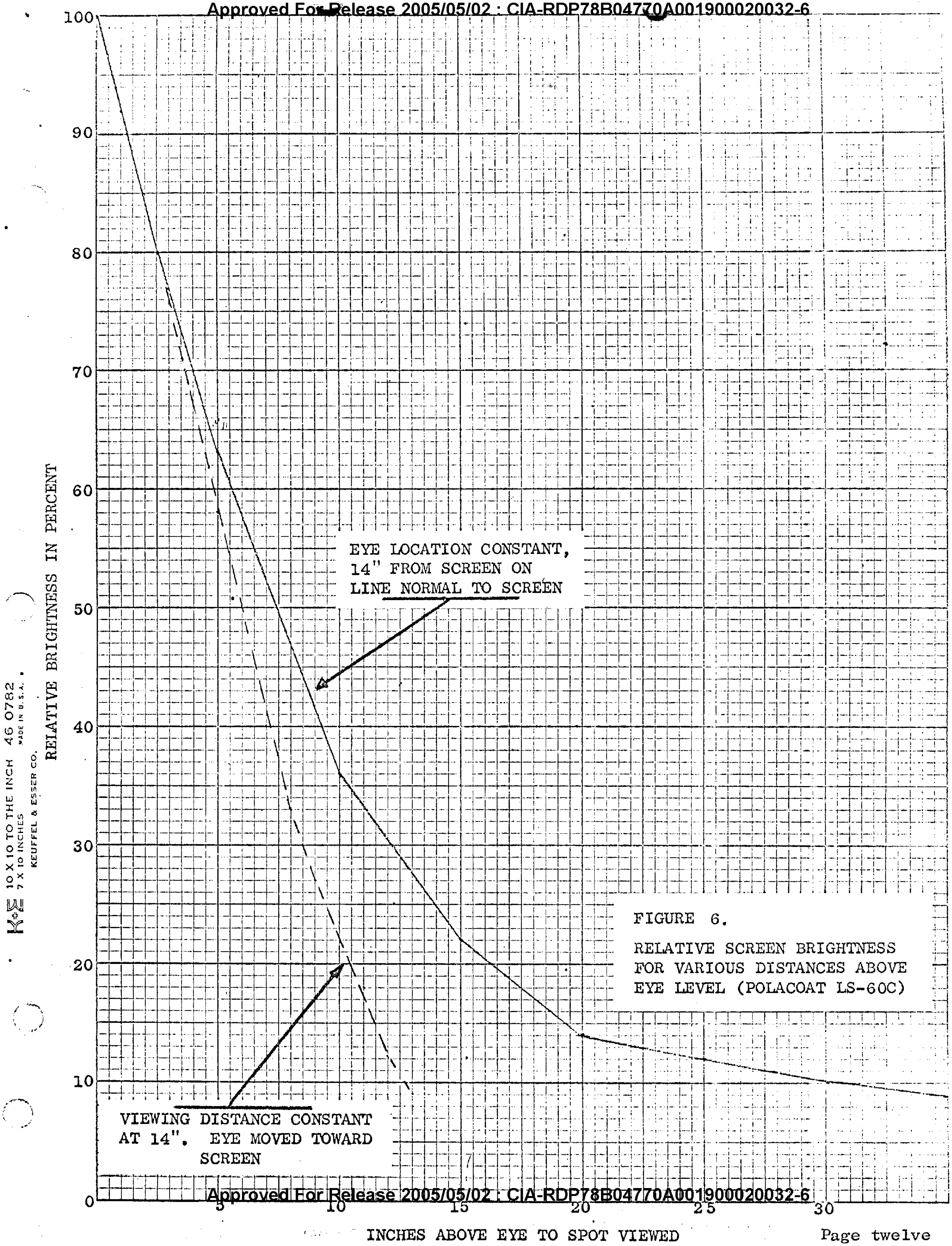

FIGURE 6.

RELATIVE SCREEN BRIGHTNESS FOR VARIOUS DISTANCES ABOVE EYE LEVEL (POLACOAT LS-60C)

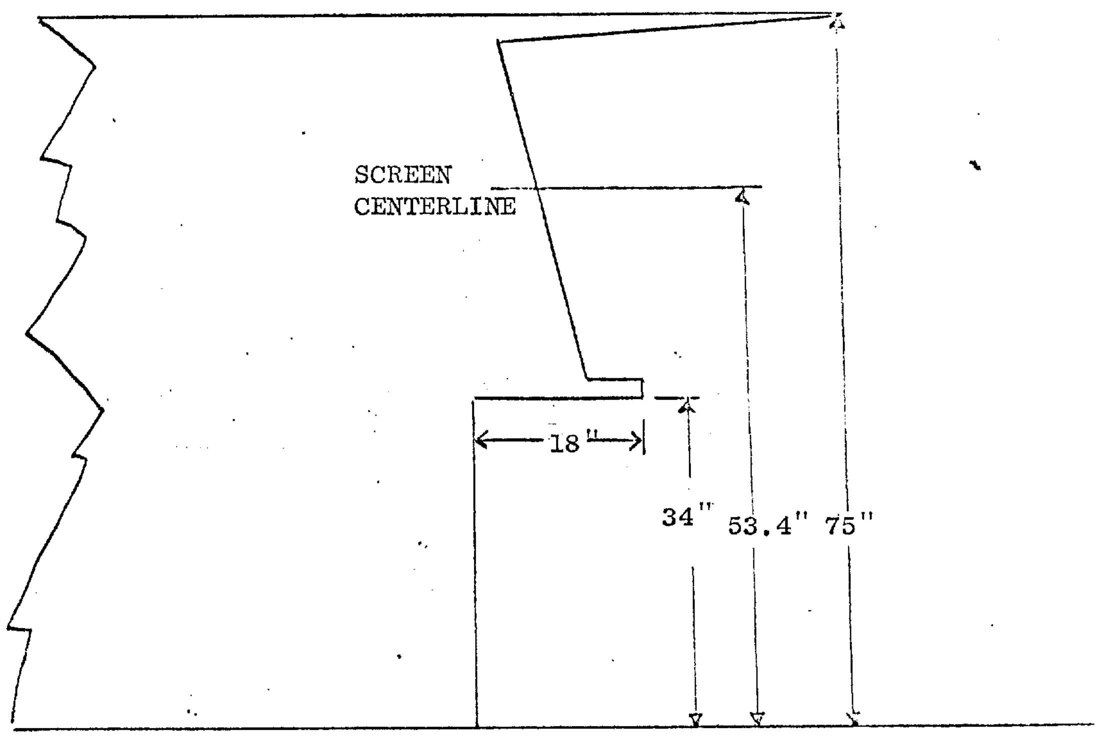

FIGURE 7. SIDE VIEW OF PROPOSED REAR PROJECTION VIEWER CONFIGURATION

at a 14 inch viewing distance. The ideal eye height for the 50 percentile operator should therefore be 57 inches. The actual eye height for a 50 percentile man seated on a 27-inch stool will be 56.5 inches, allowing for a normal 2 inch slump in sitting height. Figure 8 give the anthropometric data used in this study.

With a seat height of 27 inches, a foot rest must be provided which is adjustable through a range of 6 to 12 inches above the floor.

4. The 15 degree face-up configuration of the screen will allow the interpreter to place collateral material on the viewing surface to provide side-by-side comparisons with the information on the screen.

5. As shown in Figure 2, a large area is provided to the left of the operator for placement of collateral material at the same height and angle of the screen. This material will also be readily available to other interpreters during the consultation process.

6. A desk area is provided to the right of the screen (Figure 2) to provide a suitable writing surface and to allow viewing of collateral material that is not suited for the sloping board to the left of the screen. Desk-type storage space is provided on both extensions.

7. Consideration should be given to providing for direct viewing of the film through the optical system. An auxiliary lens system which could be mounted over a clear area of the screen would be the ideal way to provide for this from a human factors standpoint.

   Such a provision should greatly increase the flexibility of the viewer, allowing film viewing without the contrast or resolution loss of the screen. It should also significantly improve the interpreter's acceptance by providing him with nothing but "clear glass" between himself and the film.

STANDING EYE HEIGHT

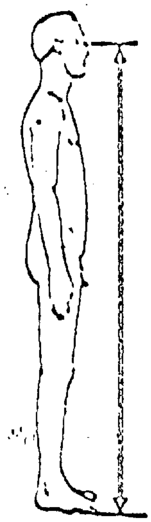

5%ile	60.8 inches
50%ile	64.7 inches
95%ile	68.6 inches

GLUTEAL FURROW HEIGHT

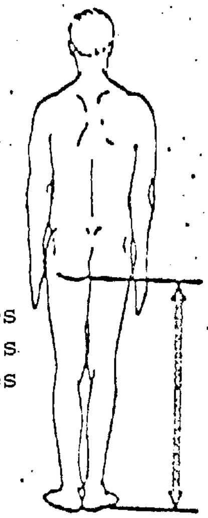

5%ile	29.8 inches
50%ile	31.6 inches
95%ile	34.3 inches

EYE HEIGHT ABOVE SEAT REFERENCE POINT

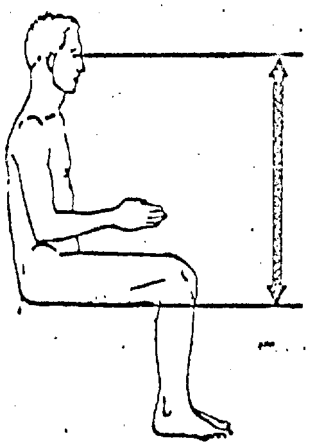

5%ile	29.4 inches
50%ile	31.5 inches
95%ile	33.5 inches

HEIGHT TO SEAT REFERENCE POINT

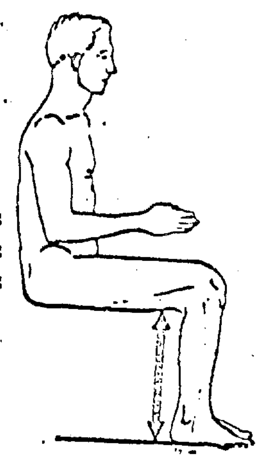

5%ile	15.7 inches
50%ile	17.1 inches
95%ile	18.2 inches

FIGURE 8. ANTHROMPOMETRIC DATA

(From Hertzberg et al., 1954)

 7-14-67

NOD 110/120 Optics

1. 2 Barrel System [redacted] 65-184 25X1

a) 3X → 30 X
25X → 70X
10:1 } 65-184
3:1 }

b) 3X → 15X
15X → 70X
5:1 } With overlap
5:1 }

2. Single Barrel - Omit Positive Auxiliary Lens-
Negative Lens Handles
Basic Magnification.

a) Cuts down the size of field angle therefore Zoom correction is reduced proportional to mag. in the omitted positive auxiliary.

b) May be incorporated into #1 above.

c) Glass size in the Zoom reduced.

3. Single Barrel Hybrid - Switch negative auxiliary lens.

a) 5:1 Basic Zoom System

Neg - Pos - 6X Low Range

" " -30X High Range

4. 2 Zoom Systems in Series

a) One continous Mag. - Switching not necessary

b)

5. Single Barrel

a) New Design - 48 Surface capability

b) Program written - being checked.

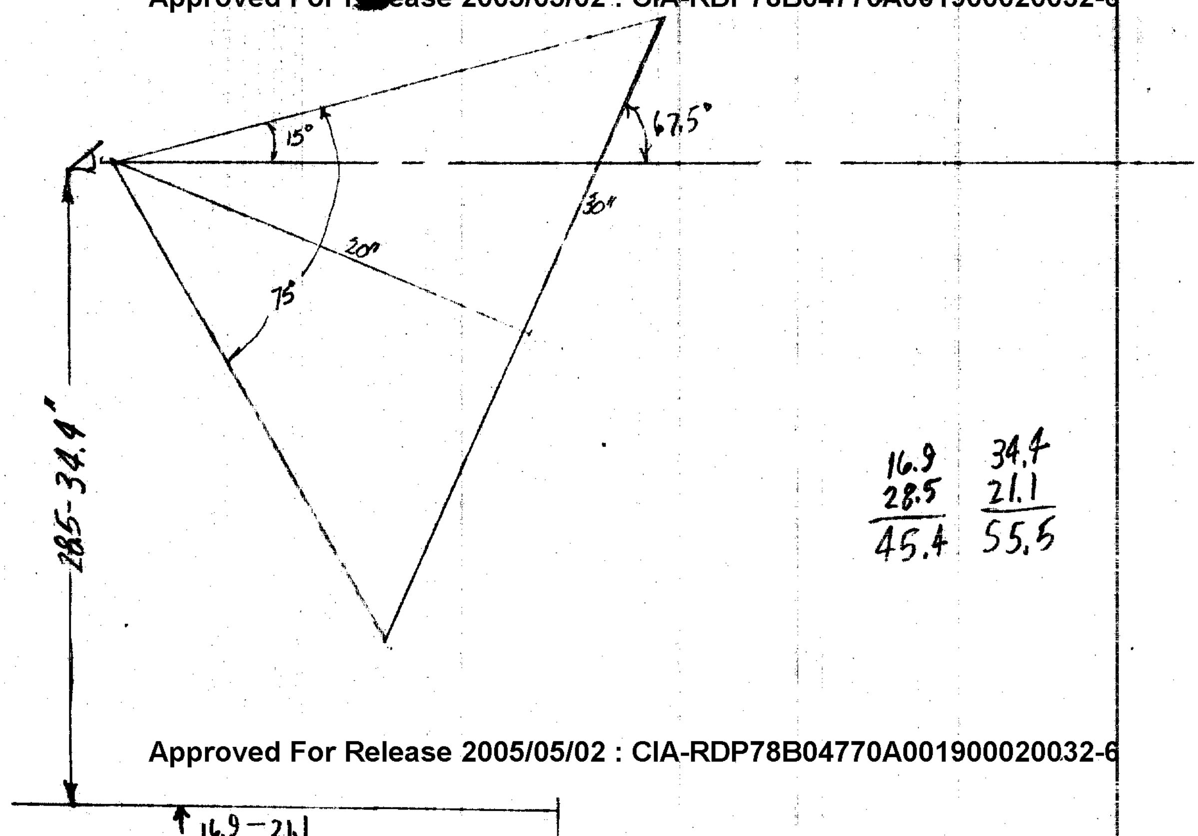
15°
67.5°
30"
20"
75°
28.5-34.4"
16.9-21.1
16.9
28.5
45.4
34.4
21.1
55.5

[redacted] 25X1

IN REPLY REFER TO

May 12, 1967

25X1 [redacted]
Post Office Box 8031
Southwest Station
Washington, D.C. 20024

Project #03016

Attention: Paul S.

Dear Paul,

Please excuse the delay but I ran into a priority problem with the final report.

Enclosed you will find copies of the references requested as well as others which seem relevant. I would be happy to talk with Ed. D. about placement of screens and other characteristics of rear-projection, P.I. equipment. It is not possible to make specific recommendations without more information; however, the following general comments may be of use:

CONVENTION

1. In general, the optimum location for a display is directly before the operator and from 0° to minus 30° from his horizontal line of sight. Thus, the screen should be located so that its center is about 15° below the horizontal sight line and its surface is normal to the direction of sight.

   When the screen subtends more than 30° at the preferred viewing distance, I suggest, as a rule of thumb, that the angle by which the screen's upper edge is higher than 0° should be one-half that by which its lower edge is below minus 30°. This rule recognizes that it is harder to look up than down.

   (With the exceptions I note below, all dimensions should be based on the 50th percentile anthropometric man.)

HORZ

IF LARGER SAY SUBTENDS 45°
THEN 5° ABOVE HORZ. & 10° BELOW

2. Glare, beyond that which can be controlled by choice of screen material must also be considered in screen placement. It is preferable to control the work area lighting so that recommendation 1., above, can be achieved without objectionable glare. If such control is not feasible, it may be necessary to change the screen angle -- the extent of the change dependent on the specifics of the glare source.

3. Many of the high resolution screen materials require that the interpreter look directly toward the light source to see the image. This directionality of the image forming characteristics of the screen material must also be considered in determining the screen's position. It follows that the screen should be placed so that a short man (5th percentile) can see an image in the upper edge of the display without getting out of his seat. The alternative is to provide an adjustable seat with suitable footrests, etc.

4. Some rear projection equipments have screen-mounted devices such as light pens, plotters and sights for mensuration and coordinate determination. In such instances, the screen may be positioned flatter and lower to both make it easier to reach the devices and also, if very precise manipulation is required, to provide a surface to steady the hand.

I note the requested references contained information on the general topic of screen resolution and, in particular, on methods of reducing the effect of screen grain. When at [redacted] I was involved in an 25X1
experiment, sponsored by Frankford Arsenal, to investigate the effects of different amplitudes, frequencies and types of movement on image quality of dynamically scanned fiber optics. As a side light of this study, some rear projection screen materials were also tested. I called
25X1 a friend at [redacted] for any information he had; 25X1
the resulting letter is attached. The [redacted] preliminary data is 25X1
not in agreement with the conclusion reached by the authors of the requested article regarding the necessity for two moving screen surfaces.

I would also like to make some general observations on screen resolution and graininess. It seems to me that these screen characteristics are relatively unimportant in the design of rear projection equipment. There are many screen materials, including certain vellums, that can give all the resolution a man can see at the recommended minimum viewing distance of 14" -- namely, about 5 to 7 lines/mm. If the images formed on the screen have greater detail than above, a person will require a supplementary optical aid to see it. As one of the main justifications for rear projection viewing is to get away from the requirement for viewing images through tubes and glass, it does not make much sense to provide resolution which requires supplementary devices.

If the image resolution is limited to less than 5 to 7 lines by the screen resolution, then the image can be further magnified, using a larger screen and moving the operator farther away. For example, even though a motion picture theater screen's resolution is lousy by any standard, it is not a significant factor in limiting apparent resolution to the theater-goer. The obvious limitation to following the "theater philosophy" is the lamp source heat and power problem which increases with large screen projections.

I think that the problem of image directionality is probably more critical than screen resolution, particularly when the operator has a sufficient magnification range to allow his placement far enough away from the screen to not see the grain. (Incidentally, reports of "screen graininess" by viewers are quite often due to film graininess -- you may have observed that such reports occur more frequently with high magnification.) The operator will find it particularly poor if, because of directional screen, he has to move his head and body "all over" to see the image.

Finally, I wish to emphasize another aspect of rear projection equipment use. Because viewing an image on such equipment appears natural and straightforward, little attention has been paid to the simple but necessary training or experience which is required to effectively use or to fairly evaluate the equipment. If the equipment is correctly designed, it will have the capability of displaying at high magnification nearly all the information in the film for viewing at a comfortable viewing distance (minimum 14 inches); however, the normal individual is so conditioned to "see more, get closer" he will inevitably move closer and be disappointed because there is simply no more detail to be seen. (This phenomena is related to the observation one can make in any TV store where people will marvel and rave over the high resolution of the 3" Sony TV viewed at two feet which actually presents much less information than the ignored large size TV set standing next to it viewed at 20 feet.) This natural tendency often leads to unjustified criticism of rear projection equipment. Unless one has a rear projection screen evaluated by a person with sufficient experience that he no longer feels the need to "get closer", evaluation should be done on an objective basis. The set of checkerboard targets varying in size and contrast which I have spoken about would be useful in making such an objective evaluation (PLUG).

I hope that the foregoing will be of use.

Very truly yours,

25X1

SJB:mg

REVISIONS				
SYM	ZONE	DESCRIPTION	DATE	APPROVED

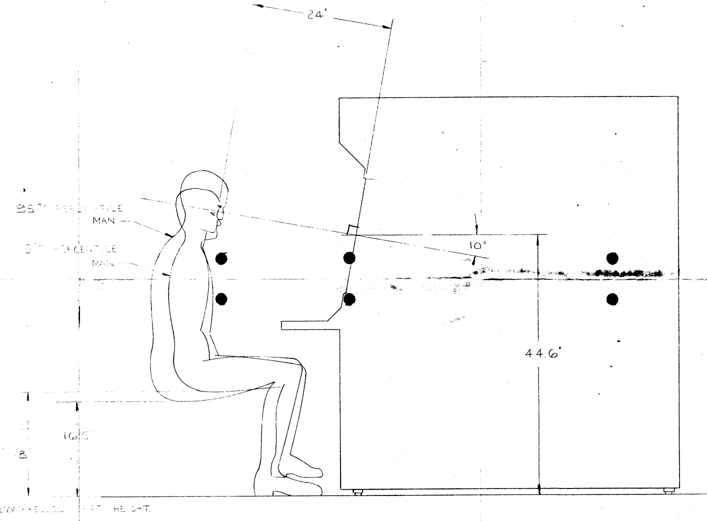

QTY REQ'D	SYM	NOMENCLATURE OR DESCRIPTION	CODE IDENT.	PART OR IDENTIFYING NO.	SPECIFICATION	MATERIAL OR NOTE	ZONE	ITEM NO.

LIST OF MATERIAL

UNLESS OTHERWISE SPECIFIED
DIMENSIONS ARE IN INCHES
TOLERANCES:
LINEAR .XX ±
.XXX ±
ANGULAR ±
DO NOT SCALE DRAWING

CONTRACT NO.
DRAWN
DESIGN APPR.
CHECKED
APPROVED
APPROVED

VIEWER
ANTHROPOMETRIC STUDY

CODE IDENT. 98453 | SIZE D | SK 3001600
SCALE 1/8 | WT | SHEET 2 OF 2

PART DASH NO.	NEXT ASSY	QTY
APPLICATION		

NOTES - UNLESS OTHERWISE SPECIFIED.

SBD FORM 709A (1-64)

25X1
25X1

KNEE HEIGHT (SITTING)

This is the vertical distance from the floor to the uppermost point on the knee. The subject sits erect with his knees and ankles at right angles (see Fig. 11-54). The data are given in Tables 11-58 and 11-59.

For men, 24.2 in. will accommodate all but the largest 1%, and 23.5 in. will accommodate all but the largest 5%, of Air Force personnel. Corresponding values for Army personnel are 24.5 in. (99th percentile) and 23.7 in. (95th percentile). For civilians, the corresponding values are 24.4 and 23.7 in. These values represent nude percentiles plus the arbitrary 0.2-in. safety factor.

For women, subtract 2.0 in. from the above values. Add 1.0 in. for men's shoes and light clothing, 1.5 in. or more for military boots and heavy clothing, and up to 3.0 in. for women's shoes and light clothing.

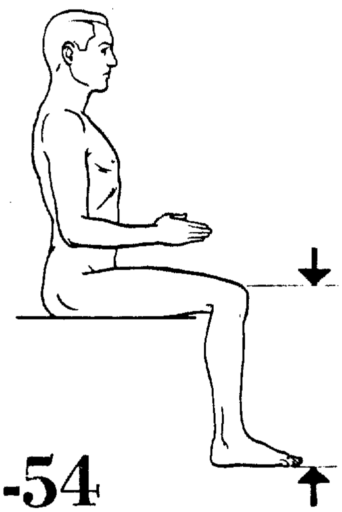

11-54

KNEE-TO-KNEE BREADTH

For this dimension, measurement is made of the maximum horizontal distance across the lateral surfaces of the knees. The subject sits erect with his knees at right angles and pressed together (see Fig. 11-55). The data are given in Tables 11-60 and 11-61.

For men, 9.6 in. will accommodate all but the largest 1% and 9.0 in. all but the largest 5% of all groups. These values represent nude percentiles plus the arbitrary 0.2-in. safety factor.

For women, the same values hold. Add 0.5 in. for light clothing, 2.0 in. for heavy clothing, and 9.5 in. for partial-pressure suits.

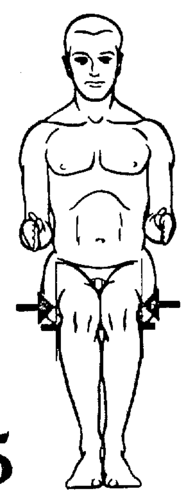

11-55

POPLITEAL HEIGHT (SITTING)

This is the vertical distance from the floor to the underside of the thigh immediately behind the knee. The subject sits erect with his knees and ankles at right angles and the bottom of his thighs and the back of his knees barely touching the sitting surface (see Fig. 11-56). The data are given in Table 11-62.

For men, 15.1 in. will accommodate all but

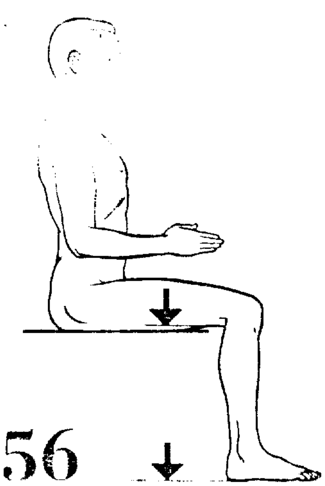

11-56

Approved For Release 2005/05/02 : CIA-RDP78B04770A001900020032-6

Table 11-59 Knee Height (Sitting) of Female Military Personnel

Population	Percentiles (in.) 1st	5th	50th	95th	99th	S.D.
Air Force personnel [1]						
Pilots	18.3	18.7	20.1	21.5	22.2	
Flight nurses	17.7	18.1	19.5	20.8	21.5	
Army personnel [2]	16.6	17.2	18.8	20.3	21.1	0.95

[1] Randall, et al., 1946. [2] Randall and Munro, 1949.

Table 11-60 Knee-to-Knee Breadth of Male Military and Civilian Populations

Population	Percentiles (in.) 1st	5th	50th	95th	99th	S.D.
Air Force personnel [1]	7.0	7.2	7.9	8.8	9.4	0.52
Cadets [2]	6.8	7.1	7.7	8.4	8.7	
Gunners [2]	6.7	6.9	7.6	8.2	8.5	
Truck and bus drivers [3]	6.8	7.3	8.1	9.2	9.5	

[1] Hertzberg, et al., 1954. [2] Randall, et al., 1946. [3] McFarland, et al., 1958.

Table 11-61 Knee-to-Knee Breadth of Female Air Force Personnel *

Population	Percentiles (in.) 1st	5th	50th	95th	99th
Pilots	6.5	6.7	7.6	8.6	9.6
Flight nurses	6.6	6.8	7.5	8.4	9.6

* Randall, et al., 1946.

Table 11-62 Popliteal Height (Sitting) of Male and Female Military and Civilian Populations

Population	Percentiles (in.) 1st	5th	50th	95th	99th	S.D.
Male Air Force personnel [1]	15.3	15.7	17.0	18.2	18.8	0.77
Male railroad travelers [2]	16.9 *	17.6 *	19.0 *	20.6 *	21.1 *	
Female railroad travelers [2]	16.2 *	16.7 *	18.1 *	19.5 *	20.1 *	

[1] Hertzberg, et al., 1954. [2] Hooton, 1945.

* Including shoes and light clothing (subtract 2 in. for nude dimension).

INTERPUPILLARY DISTANCE

This is the horizontal distance between the centers of the pupils with the subject looking straight ahead (see Fig. 11-27). The data are given in Table 11-24.

For men, 2.5 in. will accommodate average Air Force personnel, 2.3–2.8 in. will accommodate the 90% between the 5th and 95th percentiles, and 2.2–3.0 in. will accommodate the middle 98%. No other groups have been measured.

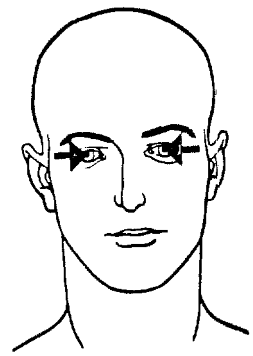

EYE HEIGHT (STANDING)

This is the vertical distance from the floor to the inner corner of the eye. The subject stands erect and looks straight ahead (see Fig. 11-28). The data are given in Table 11-24.

For men, 64.7 in. will accommodate average or 50th-percentile Air Force personnel. A range of 60.8 in. (5th percentile) to 68.6 in. (95th percentile) will accommodate the middle 90%, and a range of 59.2 in. (1st percentile) to 70.3 in. (99th percentile) will accommodate the middle 98%. There are no data for any other groups.

For women, subtract 4.5 in. from the above values. For clothing, add 1.0 in. for men's shoes, 1.3 in. for military boots, and up to 3.0 in. for women's shoes.

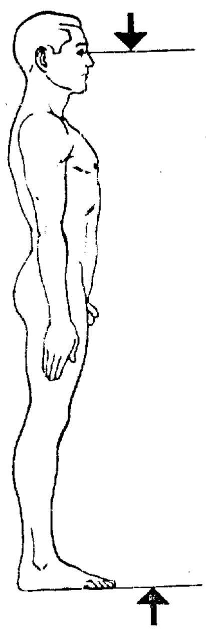

EYE HEIGHT (SITTING)

This is the vertical distance from the sitting surface to the inner corner of the eye. The subject sits erect and looks straight ahead (see Fig. 11-29). The data are given in Table 11-25.

For men, 31.5 in. will accommodate average or 50th-percentile Air Force personnel. A range of 29.4 in. (5th percentile) to 33.5 in. (95th percentile) will accommodate the middle 90%, and a range of 28.5 in. (1st percentile) to 34.4 in. (99th percentile) will accommodate the middle 98%. For civilians, 31.2 in. will accommodate the 50th percentile, 29.3–33.2 in. the middle 90%, and 28.6–33.9 in. the middle 98%.

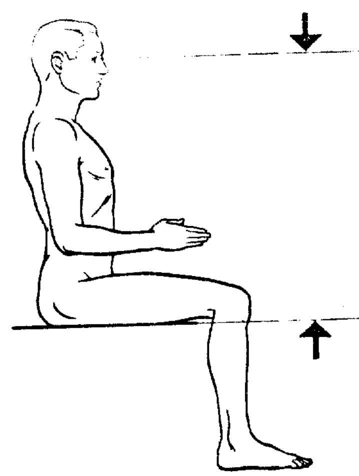

Table 11-24 Interpupillary Distance and Eye Height (Standing) of Male Air Force Personnel *

Dimension	Percentiles (in.) 1st	5th	50th	95th	99th	S.D.
Interpupillary distance	2.19 [illegible]	2.27	2.49	2.84	3.04 77MM	0.14
Eye height (standing)	59.2	60.8	64.7	68.6	70.3	2.38

* Hertzberg, et al., 1954.

Table 11-25 Eye Height (Sitting) of Male and Female Air Force Personnel

Population	Percentiles (in.) 1st	5th	50th	95th	99th	S.D.
Male flight personnel [1]	28.5	29.4	31.5	33.5	34.4	1.27
Female pilots [2]	27.9	28.5	30.0	31.6	32.4	
Female flight nurses [2]	26.3	27.3	29.3	31.1	32.2	

[1] Hertzberg, et al., 1954. [2] Randall, et al., 1946.

Table 11-26 Shoulder Height (Standing) of Male and Female Air Force Personnel

Population	Percentiles (in.) 1st	5th	50th	95th	99th	S.D.
Male flight personnel [1]	51.2	52.8	56.6	60.2	61.9	2.28
Male basic trainees [2]	50.3	52.0	55.9	59.9	61.8	2.41
Female basic trainees [3]	46.9	48.2	51.9	55.4	57.3	2.18

[1] Hertzberg, et al., 1954. [2] Daniels, et al., 1953a. [3] Daniels, et al., 1953b.

Table 11-27 Shoulder Height (Sitting) of Male and Female Air Force Personnel

Population	Percentiles (in.) 1st	5th	50th	95th	99th	S.D.
Male flight personnel [1]	20.6	21.3	23.3	25.1	25.8	1.14
Female pilots [2]	21.8	22.4	23.8	25.2	25.9	
Female flight nurses [2]	20.4	21.1	23.1	24.8	25.9	

[1] Hertzberg, et al., 1954. [2] Randall, et al., 1946.

§ 11.2.3

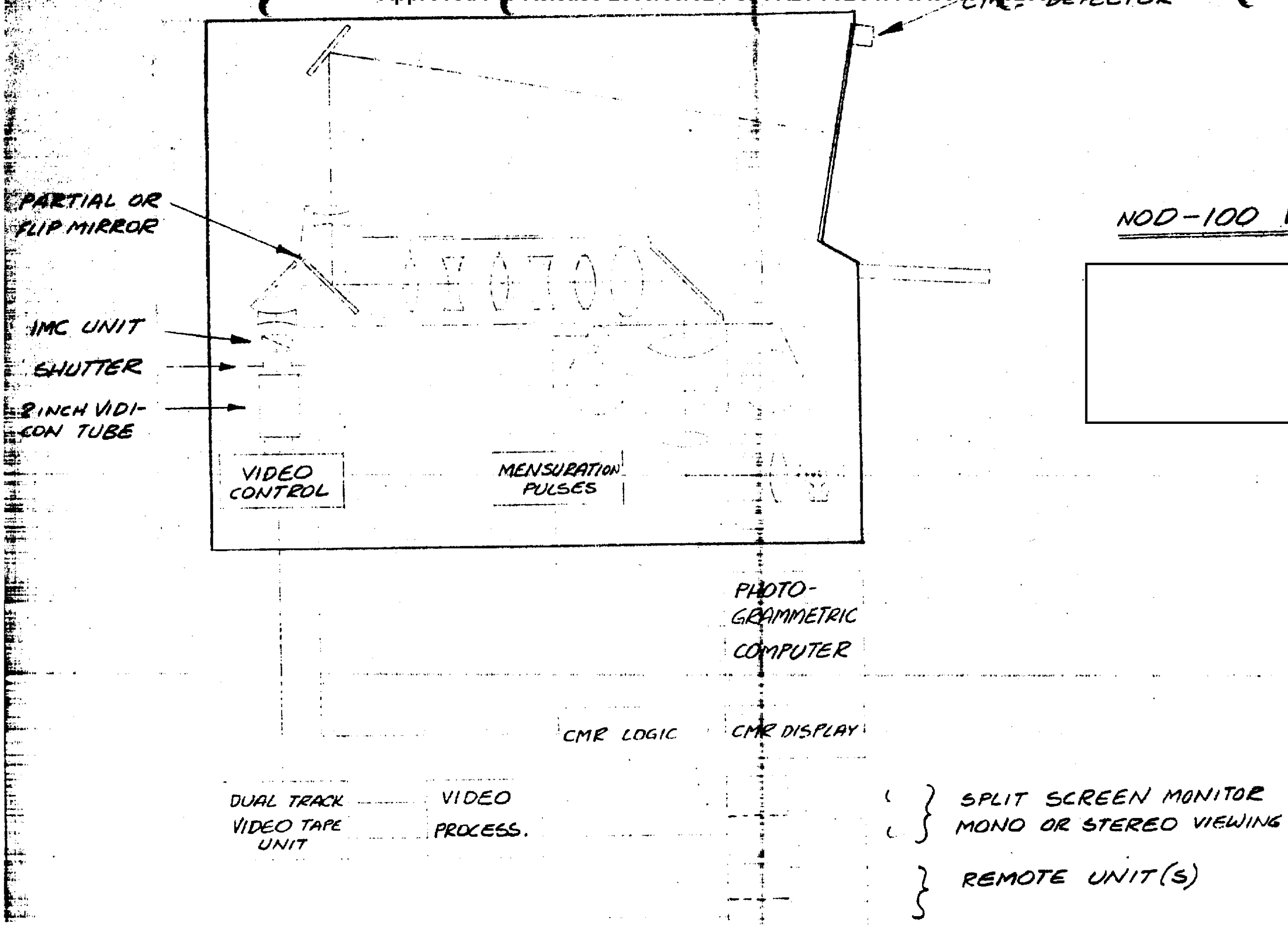

NOD-100 VIEWER

25X1

02151

12 Oct 66

QUESTIONS REGARDING [redacted]OOM LENS SYSTEM

25X1

1. What is the magnification range?

2. Are transparencies projected?

3. What is the light level on the screen with an open film gate?

4. How hot does the transparency get? Does the heat filter work properly?

5. Is the image brightness uniform over the entire screen? What screen size?

6. What is the amount of geometrical image distortion permitted?

 3/26/66

FILM TEMP

(WITH IR FILTER INSTALLED)

MAX (200X) 210°F
MIN (4X) 104°F

THE BULB OF THE THERMOMETER WAS PAINTED BLACK.

200X	210°F
130X	158°F
78X	140°F ←
47X	113°F
29X	104°F
4X	104°F

FILM TEMP

(WITH IR FILTER INSTALLED)

MAX (200X) 210 °F
MIN (4X) 104°F

THE BULB OF THE THERMOMETER WAS PAINTED BLACK.

200X	210°F
130 X	158°F
78X	140°F
47X	113°F
29X	104°F
4X	104°F